10-7-2016

Allosteric Modulation of the Cannabinoid Receptor One: Evaluation of Analogs of Indole-2-Carboxamide and Pyrimidinyl Biphenylurea

Leepakshi Khurana
University of Connecticut, Connecticut, leepakshi.khurana@uconn.edu

Allosteric Modulation of the Cannabinoid Receptor One: Evaluation of Analogs of Indole-2-Carboxamide and Pyrimidinyl Biphenylurea

Leepakshi Khurana, Ph.D.

University of Connecticut, 2016

G-protein coupled receptors (GPCRs) are one of the largest families of membrane proteins which play a fundamental role in the signaling cascades that maintain physiological homeostasis. In this research, we focused on an important member of the endocannabinoid system, the CB_1 receptor, which is primarily expressed in the neurons of the central and peripheral nervous system. Chapter 2 focuses on structure-activity relationships to identify chemical functionalities on the indole-2-carboxamides (the scaffold for ORG27569) that maintain allostery at the CB_1 receptor. These novel analogs were evaluated for their binding affinity at the allosteric site (K_B) and the impact of these analogs on orthosteric ligand binding (α). Paradoxically, these analogs activated CB_1 yet decreased G-protein coupling. Evaluation of the impact of these analogs on different pathways demonstrated that these analogs activate β-arrestin 1 mediated pathways. Chapter 3 focuses on optimizing another scaffold for allostery at the CB_1 receptor, pyrimidinyl biphenylureas. The scaffold was generated by replacing the pyridine ring of PSNCBAM-1 with pyrimidine and analogs of this scaffold were evaluated for allosteric parameters. Similar to indole-2-carboxamides, these positive allosteric modulators of CP55,940 binding, reduced G-protein coupling. These compounds hold promise to develop anti-obesity drugs. Chapter 4 focuses on identification of motifs on the CB_1 receptor which are key for binding allosteric

modulators ORG27569 and PSNCBAM-1. I leveraged the finding that these modulators bind CB_1 but not CB_2, and identified one extracellular region of CB_1 that impact ORG27569 binding. No impact on PSNCBAM-1 was seen, suggesting that this ligand may bind to a different site on the CB_1 receptor. These results will aid in the identification of amino acid residues that may play a key role in allosteric ligand binding.

Allosteric Modulation of the Cannabinoid Receptor One: Evaluation of Analogs of Indole-2-Carboxamide and Pyrimidinyl Biphenylurea

Leepakshi Khurana

B.Pharm. Delhi University-New Delhi, India, 2009

A Dissertation Submitted

in Partial Fulfillment of the

Requirements for the Degree of Doctor of Philosophy

at the

University of Connecticut,

2016

2016

APPROVAL PAGE

Doctor of Philosophy Dissertation

Allosteric Modulation of the Cannabinoid Receptor One: Evaluation of Analogs of Indole-2-Carboxamide and Pyrimidinyl Biphenylurea

Presented by

Leepakshi Khurana, B.Pharm.

Major Advisor: _____
Dr. Debra Kendall

Associate Advisor: _____
Dr. Kyle Hadden

Associate Advisor: _____
Dr. Charles Giardina

University of Connecticut,
2016

ACKNOWLEDGEMENTS

First and above all, I want to thank God for giving me this opportunity and capability to successfully complete my thesis.

I want to thank all the people who made this research possible; my major advisor Dr. Debra Kendall for accepting me as her student in her lab and constantly mentoring me all these years. Without her support and guidance, this dissertation would not have been possible. I would like to thank my committee members and examiners, Dr. Kyle Hadden, Dr. Charles Giardina, Dr. Andrew Wiemer and Dr. Olga Vinogradova for their constant inputs throughout my graduate career and agreeing to evaluate my work.

I would especially like to thank Dr. Kwang H. Ahn who taught me all the experimentation involved in my projects. His constant mentorship through all the years in this lab has made it possible for me to complete this work. To have worked with him and learn from him has truly been a blessing for me. I thank all my lab mates for making these tough years of graduate school a little easy with their science and humor; my friends Aditya Pote, Priya Katyal, Japneet Kaur, Komal Kedia and Shruti Sharma for bearing with me when I would vent out my stress about graduate school.

I would like to thank my family especially my mother Late Suman Khurana for encouraging me to dream big in life and my father Mr. Ashok Kumar Khurana, for his constant love and support. I want to thank my sister Jitika Khurana, my brothers Rohit Khurana and Tushar Batra and my brother-in-law Mudit Sharma for always being a phone call away when I needed them the most. And especially I want to thank my 7 month-old niece, Anaisha Sharma for coming into our lives and making this year of finishing my thesis truly beautiful.

TABLE OF CONTENTS

CHAPTER 1

Introduction

CHAPTER 2

Indole-2-carboxamides as allosteric modulators of the CB_1 receptor

CHAPTER 3

Pyrimidinyl biphenylureas as allosteric modulators of CB_1 receptor: establishing structure-activity relationships

List of Figures

List of Tables

Chapter 1

Introduction

1.1 The G protein-coupled receptor superfamily

G-protein coupled receptors (GPCRs) represent one of the largest families of proteins in the mammalian genome (Lander et al., 2001; Venter et al., 2001). Around 750 genes out of 35,000 human genes encode for GPCRs. Their tertiary structure is characterized by seven transmembrane α-helices connected by intracellular and extracellular loops. On the intracellular surface, these receptors are associated with a heterotrimeric G-protein. These receptors respond to various stimuli including ions, amines, proteins, peptides, lipids and even photons and transduce signals across the biological membrane (Fredriksson et al., 2003). GPCRs are involved in many fundamental physiological functions. The importance of GPCRs is evident as more than half of currently known therapeutic drugs target these receptors (Flower et al., 1999; Komatsu et al., 2015), yet only a minority of these receptors has been exploited therapeutically (Vassilatis et al.,2003). Therefore these receptors offer potential targets for drug discovery.

1.2 GPCR classification system

One of the first classifications of GPCRs was based on sequence homology and classified GPCRs into six classes as shown in Figure 1.1. These classes and their prototype members are as follows: Class A (rhodopsin-like), Class B (secretin receptor), Class C (metabotropic glutamate), Class D (fungal mating pheromone receptors), Class E (cyclic AMP receptors) and class F (frizzled/smoothened) receptors. This classification includes all the known GPCRs including those from vertebrates and invertebrates. The classes were further divided into subclans and were

assigned roman numbers. The family D and E which represents fungal pheromone receptors and cAMP receptors do not exist in humans. Also, in class A, the subclan IV includes invertebrate opsin receptors and (Attwood and Findlay 1994; Kolakowski, 1994) and class F which contains archebacterial opsins is not part of GPCRs found in humans.

Due to the large sequence differences between mammalian and invertebrate GPCRs, this classification was severely hampered. Fredrikkson et al., in 2003, introduced a different system which used large scale phylogenetic analyses of human GPCRs to establish five main families of GPCRs. The system is called the GRAFS system and includes glutamate (G, 22 members), rhodopsin (R, 672 members), adhesion (A, 33 members), frizzled/taste 2 (F, 36 members) and secretin (S, 15 members) families. The rhodopsin family with the highest number of members is further subdivided into 13 groups. Very few human receptors could not be classified into any of the groups according to the classification criteria and are called as "other 7TM receptors" (Fredrikkson et al., 2003). A key difference in this classification from the previous classifications of GPCRs is it separates the secretin and adhesion families which are not seen in Class A-F classification. Although the two families have high sequence identity in their transmembrane helices (TM), their N-terminus shows high sequence divergence (Scioth et al., 2005).

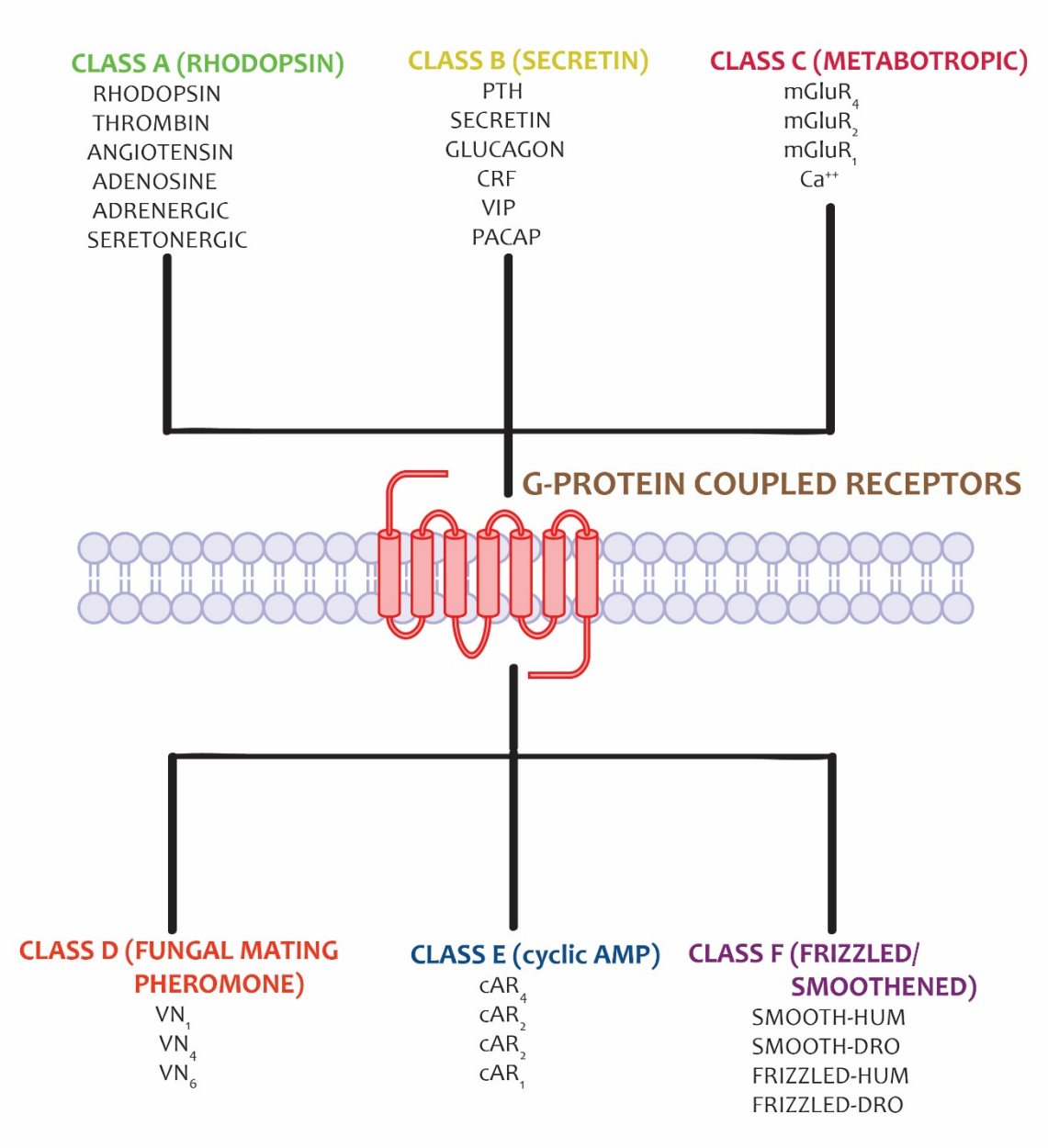

Figure 1.1 Classification of GPCRs. GPCRs have been traditionally classified into 6 classes based on sequence homology: class A (rhodopsin), class B (secretin), class C (metabotropic glutamate), class D (fungal mating pheromone (VR)), class E (cyclic AMP (cAR)) and class F (frizzled/smoothened). Examples of receptors belonging to these classes are written in black. The figure is modified from Bockaert et al., 1999.

1.3 GPCR ligands and activation states: from a two-state model to multiple-state model

In the past, many theories on GPCR activation have been proposed. Most of them are based on the theory proposed by Clark which states that a drug, upon binding to a receptor, can induce an intracellular signal depending upon what state it fixes the receptor in and it is this conformation that defines the transduced action (Clark et al., 1937).

1.3.1 Two-state equilibrium model

Traditionally, the process of ligand binding and signaling of GPCRs has been defined by a two-state equilibrium model which is based on the principle of change in equilibrium between two distinct conformations of the receptor (Leff et al., 1995; Freire et al., 1998; Park et al., 2008). The ternary complex model is the most commonly used two-state model to describe G-protein activity. The ternary complex involves three moieties: the receptor (R), agonist (A) and the G-protein (G). The activation of the receptor relies on its ability to couple to G-protein and thus, it is the receptor-G protein complex which defines the active state of the receptor as shown in Figure 1.2. Coupling of the receptor to G protein (RG) results in the active state of receptor which displays higher affinity for agonists. On the other hand, the uncoupled state is inactive and displays lower affinity for agonists (De lean et al., 1980).

The notion that conformations between the two states, i.e. the active state (R*) and the inactive state (R), exist came after the identification of constitutive active mutants (CAMs) for many GPCRs. The first CAM was identified for the β_2-adrenergic receptor where mutations in the third intracellular loop (IC3) resulted in a mutant with higher affinity for agonists and an increase in agonist potency in the absence of G-protein. This could not be accommodated by the classical ternary complex model. Therefore, an extended ternary complex model was defined,

where the receptor exists in two interconvertible states R and R*, which is an intrinsic property of the receptor itself. This model could accommodate the idea of constitutive activity of receptors where the mutations that increase the level of constitutive activity shifted the equilibrium favoring the R* state as shown in Figure 1.2 (Samama et al., 1993).

Based on this extended model, agonists were defined as ligands which shifted a larger proportion of receptor molecules towards the R* state. The definition of full and partial agonists depends on the proportion of receptor molecules shifted to the active state. Inverse agonists promote shifting the equilibrium towards the inactive R state. Antagonists are defined as ligands which have equal affinity for both R and R* state and have no effect on the basal activity of receptors (Park et al., 2008).

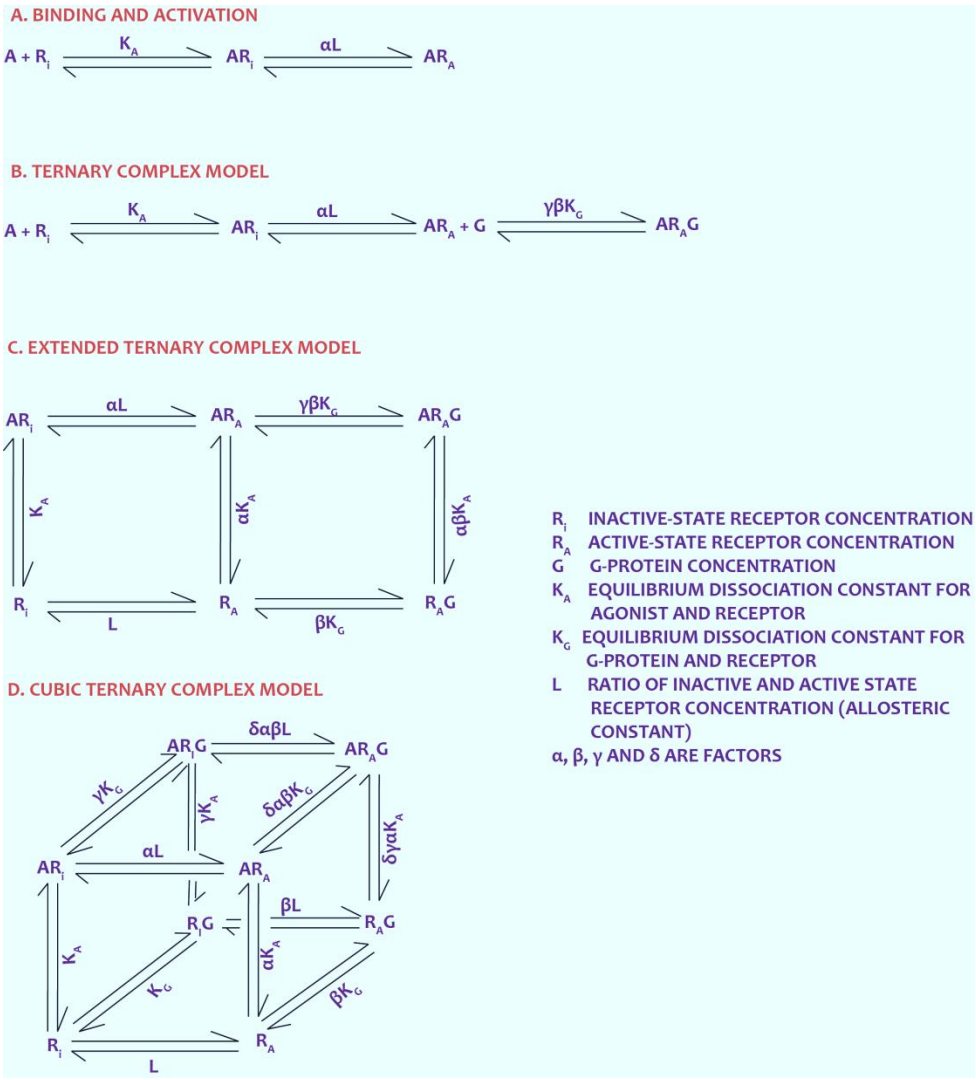

Figure 1.2 Different models of GPCR activation. (A) the classical model of GPCR activation where agonist (A) binds to the inactive receptor (R_i) and forms a complex (AR_i), which then isomerizes to an active form of receptor (R_A) due to the efficacy of agonist. (B) the ternary complex model of GPCRs where agonist binding to the inactive receptor causes conformational changes in the receptor and activates the receptor. The activated receptor then binds to G protein (G) to form a signaling complex (AR_AG). (C) The extended ternary complex model which incorporates the constitutive signaling from GPCRs. The inactive receptor R_i can isomerize to R_A independent from the presence of an agonist and interact with G protein. β and γ are factors by

which the affinity of the receptor for G-protein coupling is modified upon activation of the receptor either spontaneously or in the presence of an agonist, respectively. (D) the cubic ternary complex model, where the inactive receptor can also bind to G protein to form the R_iG complex which is non-signaling by nature. The factors δ, β and γ define the modification in the affinity of receptor for G-protein. Modified from Kenakin et al., 2002.

1.3.2 Alternative model describing multiple states of the receptor

Recent evidence of agonist-directed trafficking of receptor stimulus has led to the notion that receptors can exist in multiple conformations between the R and R* state. Different agonists induce a spectrum of different conformations of the receptor and it is these conformations that define the signaling downstream. They promote binding of different G-proteins or β-arrestins which in turn impact downstream signaling. This suggests that theoretically, a receptor can exist in a limitless number of conformations, Rn*.

An example for the existence of multiple signaling states is seen in the dopamine receptor D2L. When co-expressed with different G-protein subunits in SF9 cells and analyzing the effect of different agonists on membrane preparations, it was seen that different agonists could differentially activate different G-protein subunits (Gazi et al., 2003, Perez et. al, 2005). This suggests that different agonists may adopt different conformations which can have a varying degree of selectivity for the different G-proteins.

Another example of multiple signaling states can be seen with differences in efficacy of ligands for different signaling pathways. In the 5-HT_{2A} receptor, for example, structurally diverse ligands from three families, the tryptamine, ergoline and phenethylamine family displayed differential efficacy for PLC or PLA_2-mediated pathways. This further supports the hypothesis that different agonists can display different conformations of GPCRs, thus differing in their selective activation of different pathways (Kurrasch-Orbaugh et al., 2003, Perez et al., 2005).

An alternate model for GPCR activation called cubic ternary complex model exists which includes the ideas of extended ternary complex but differs from it in that G-proteins can also bind to the inactive receptor in this model as shown in Figure 1.2. This introduced the existence

of a complex formed between an inactive receptor and G-protein which does not evoke a response and ligand binding to this complex would act as an antagonist or inverse agonist for the receptor (Weiss et al., 1996). An example that supports this notion is tiotidine, an inverse agonist for the H2 histamine receptor which binds to the receptor coupled to G_s that does not evoke a response (Perez et al., 2005).

1.4 Structural features of GPCRs

The typical architecture of class A GPCRs includes seven transmembrane helices (TM) with three intracellular (IC) and three extracellular loops (EC), a cytoplasmic C-terminus with an α-helix (H8) parallel to the cell membrane and an extracellular N-terminus (Moreira et al., 2014). Many structure-function studies have identified key structural elements in this class of GPCRs and have validated the function of these elements. Some of these conserved motifs as shown in Figure 1.3 and are discussed below. The residues are numbered according to a numbering system by Ballesteros where the first number represents the helix the residue belongs to. The last two numbers following the period are denoted to an amino acid based on the number of residues it is away from the most conserved residue of the helix which is numbered .50. The residues down the helix are numbered as .51, .52 and so on and the residues up the helix are numbered as .49, .48 and so on.

(1) **The ionic lock**: this represents the strong intermolecular interactions between the residues $Glu^{3.49}$/$Arg^{3.50}$ of the conserved (D/E)RY motif in the TM3 region with residues $Glu^{6.30}$/$Thr^{6.34}$ in TM6. These molecular interactions constraint the movements of TM helices to maintain the receptor in the inactive state (Ballesteros et al., 1998; Moreira et al., 2014).

(2) **The hydrophobic arginine cage**: the conserved $Arg^{3.50}$ is restrained in its conformation by conserved hydrophobic amino acids at positions 3.46 and 6.37. When GPCRs are activated, the $Arg^{3.50}$ within the (D/E)RY motif adopts an extended conformation and points towards the center of the protein core, which results in disruption of its ionic interactions with $Glu^{3.49}$ and $Glu^{6.30}$. The conserved hydrophobic amino acids form a hydrophobic cage surrounding this $Arg^{3.50}$ so that the GPCR is maintained in its inactive state (Ballesteros et al. 1998, Caltabiano et al., 2013).

(3) **The NPxxYxF motif in the TM7 region:** This motif is present in the cytoplasmic end of TM7. The two most essential residues in this motif are the proline and the tyrosine. The proline in this motif forms a kink or distortion in the TM7 α-helical structure. As a result, the tyrosine in this motif faces into the pocket formed by TM2, TM3, TM6 and TM7, which allows for direct interaction of tyrosine with $Phe^{7.60}$ in H8 and with the side chain and backbone of $Arg^{2.40}$ in TM2 via water molecules. This aqueous pocket is presumed to stabilize the GPCRs in its inactive state. The solvent interactions are weak which allows for the ease of breaking of these interactions when an agonist binds and easy switch of GPCR to an active state (Edwards et al., 2004; Fujiyoshi et al., 2002; Rosenbaum et al., 2009).

(4) **The rotamer toggle switch**: Another molecular switch that operates during agonist activation of the receptor is the rotamer toggle switch. This refers to the coordinated change in the rotameric angles upon binding of a ligand among aromatic residues in TM6. The $Trp^{6.48}$ of the CWxP motif is surrounded by this cluster of aromatic amino acids which undergo a conformational change and point towards TM5 in the active state

as opposed to the inactive state where these residues point towards the TM7 (Visiers et al., 2002; Moreira et al., 2014).

These structural/functional motifs were earlier published based on computational modeling and were later validated by crystal structures (Palczewski et al., 2000; Schousboe et al., 2003).

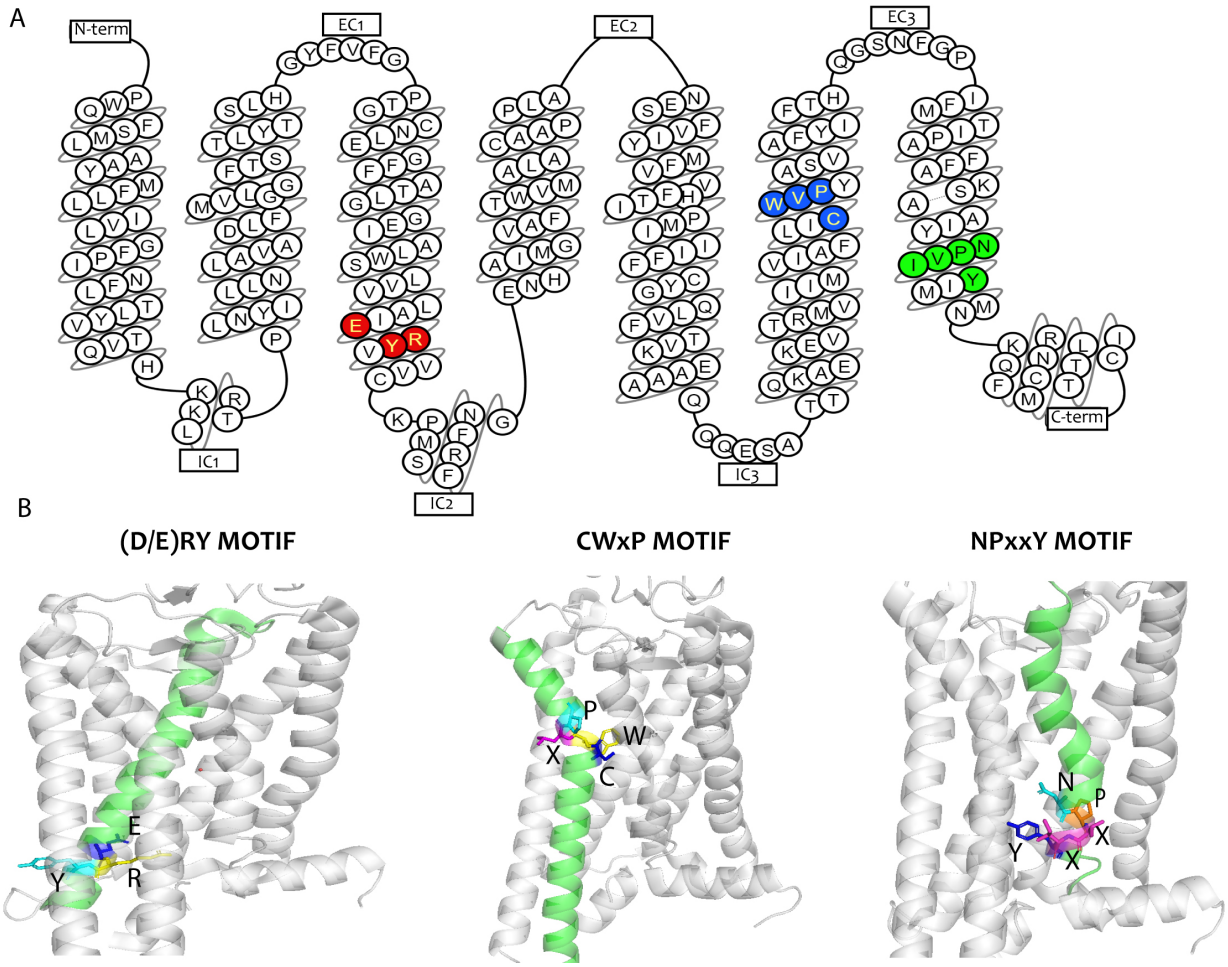

Figure 1.3 Common structural motifs in GPCRs. (A) 2-D diagram of human rhodopsin (gene OPN2) showing three important motifs, (D/E)RY, CWxP and NPxxY motif. Modified from Munk et al., 2016. The (D/E) RY motif carries the molecular switch called the ionic lock which maintains the receptor in the inactive switch. The CWxP motif carries the molecular switch called the rotamer toggle switch, which plays a key role in activation of receptors. (B) Crystal structure of rhodopsin (PDB ID: 2X72) highlighting the three motifs. The helix which contains the motif is highlighted in green color. Modified from Trzaskowski et al., 2012.

1.5 Lifecycle of a GPCR

In the past few decades, a wealth of information has been gained that reveals the complex life cycle a G-protein undergoes. The mechanism by which a GPCR is delivered to the cell surface to allow GPCR-ligand interactions and then salvaged from the cell membrane is of paramount importance. The main steps involved in the GPCR life cycle are shown in Figure 1.4.

1.5.1 Biosynthesis

Before a GPCR reaches the cell surface, a receptor undergoes a continuous process of maturation. Nascent GPCRs interact with accessory chaperone proteins in the endoplasmic reticulum (ER) (Ellgard et al., 2003). These chaperones ensure the proper folding of the GPCRs along with other cell machinery proteins which include:

(1) Protein disulphide isomerase: which allows disulphide bond formation between unpaired cysteines
(2) Heat shock protein Hsp-70: which masks the hydrophobic surfaces on the protein
(3) Calnexin and Calreticulin: which interact with immature *N*-glycosyl chains (Enna et al., 2011)

The properly folded proteins are then transported to the endoplasmic-golgi intermediate complex (ERGIC) and golgi by packing them into COPII-coated vesicles. The proteins, in the golgi, undergo additional modifications including maturation of the glycosylated chains. Strict-quality control checks in the Golgi apparatus ensure that the misfolded or immature proteins are degraded via the proteasome pathway. The properly folded and mature proteins are then delivered to the cell surface. (Ellgard et al., 2003; Lefkovitz et al., 2006).

Oligomerization and heterodimerization are also believed to play a key role in the biosynthesis and trafficking of GPCRs from the ER. Proper targeting of the receptors to the cell surface may require heterodimerization of some GPCRs such as α_{1D}-AR which needs to dimerize with a closely related α_{1B}-AR for its transport and expression on the cell surface (Hague et al., 2004, Lefkovitz et al., 2006). Multiple GPCRs like vasopressin (Terrillon et al., 2003; Lefkovitz et al., 2006) and β_2-adrenergic receptors (Salahpour et al., 2004), undergo homodimerization in the early stages of synthesis, mostly in the ER. Thus, dimerization of receptors also plays a key role in synthesis and trafficking of receptor, atleast for some of the GPCRs.

1.5.2 Maintaining cell surface stability of receptors

Not only is the proper folding and transport of a receptor to the cell surface important, it is very vital to ensure the stability of the receptor once it resides in the cell membrane to ensure proper ligand interactions. Many proteins have been identified, which play a key role in stabilizing the receptors at the plasma membrane. These include muskelin, protein 4.1N, Homer, actin binding protein 280/filamin A, postsynaptic density-95 (PSD-95) and sphinophilin (Tan et al., 2004). PSD-95, for example interacts with the C-terminus of the β_1-adrenergic receptor and maintain its stability at the cell surface, as is evident from decreased receptor internalization on overexpression of PSD-95 (Xiang et al., 2002).

1.5.3 GPCR signaling and the role of guanine exchange factors (GEFs)

A vast array of ligands such as photons, small molecules, hormones, proteins can activate GPCRs. For the GPCR to signal, a heterotrimeric G-protein has to dissociate into its α and $\beta\gamma$ subunits. GDP-bound α subunit tightly binds to the $\beta\gamma$ subunit. When a GPCR is bound to an agonist, the agonist GPCR complex acts as a GEF and causes exchange of GDP for GTP at the

G-protein, which promotes dissociation of G-protein into its subunits, which then couple to various effector molecules to stimulate downstream signaling pathways.

Other than the GPCR itself, there are many other reported GEFs that have been reported to trigger G-protein signaling pathways independent of the receptor. Dexras 1, for example, has been reported as a putative GEF for activation of Gαi subunits (McCudden et al., 2005).

Another group of proteins reported to play an important role in G-protein signaling independent of GPCRs are AGS (activators of G-proteins). These accessory proteins act as GEFs at the G-proteins and play a key role in regulation of GPCR signaling (Cismowski et al., 2005).

1.5.3 Endocytosis of GPCRs

Extensive information has been gathered in the past regarding the endocytotic trafficking of GPCRs. Proteins identified to play a key role in endocytosis are the G-protein receptor kinases (GRKs) and β-arrestins (non-visual arrestin). Additional accessory proteins work with the GRKs and arrestins for endocytosis to take place. Upon activation of a receptor by agonists, a GPCR becomes prone to phosphorylation by GRKs. β-arrestins bind to the phosphorylated receptors which terminate the G-protein signaling and the arrestin bound receptors move to endosomes for degradation or lysis (Hanyaloglu et al., 2008). Agonist-independent phosphorylation of receptors is also demonstrated by GPCRs, although the rate of internalization is slower. β_2-adrenergic receptors, for example, in the presence of agonist, are sequestered from the cell surface with a half-life of 10 mins but in the absence of an agonist, the receptors stay on the cell-surface for more than an hour (Zastrow et al., 1994).

Two isoforms of β-arrestins have been demonstrated to be important for desensitization and sequestration of heptahelical proteins. These are arrestin 2 (β-arrestin 1) and arrestin 3 (β-

arrestin 2). Although both β-arrestin 1 and β-arrestin 2 are involved in the endocytotic cycle, the two isoforms differ in their abilities to desensitize and sequester the receptors. In β_2-adrenergic receptor, for example, it was demonstrated using knockout mice for β-arrestin 1 or β-arrestin 2 that it is the β-arrestin 2 form that is 100-fold more potent than β-arrestin 1 for sequestration of receptors. However, both β1 KO mice and β2 KO mice displayed similar levels of impairment of agonist-stimulated desensitization. The role of the two isoforms of arrestin can be different for different GPCRs. For example, in angiotension I type 1A receptor (AT_{1A}-R), the two isoforms displayed equal levels of impairment of agonist-stimulated desensitization. However, for internalization, the β1 KO mice showed slight impairment whereas the β2 KO mice showed no change (Kohout et al., 2001).

The β-arrestin bound receptors may be endocytosed by formation of three types of vesicles: clathrin-coated, caveolin-coated or uncoated vesicles (Claing et al., 2002). Clathrin-coated endocytosis is implicated in endocytosis of many GPCRs. The process begins at the plasma membrane by the formation of a coated pit in the membrane. The arrestin-bound receptors form interactions with adaptor proteins (particularly AP2) and cluster in the growing coated pit. Adaptor protein-2 (AP2) interacts with binding sites for phosphatidylinositol-2-phosphate (PIP2) to interact with plasma membrane. PIP2 is a lipid that is highly concentrated in the plasma membrane (Robinson et al., 2004). AP2 recognizes short sequence motifs in the cytoplasmic domains of internalized proteins such as YXX-phi, where X can be a variable and phi represents a bulky hydrophobic amino acid (Ohno et al., 1995; Sorkin et al., 2004). The adaptor proteins link the membrane proteins and clathrin, which causes co-assembly of cargo proteins, adaptors and clathrin. The protein amphiphysin, then dimerizes at the neck of the coated-vesicle formed and the GTPase enzyme binds to amphiphysin and drives cleavage of the neck of the vesicle and

the coated pit is released and moves to the endosomes (Robinson et al., 1994; Schmid et al., 1997).

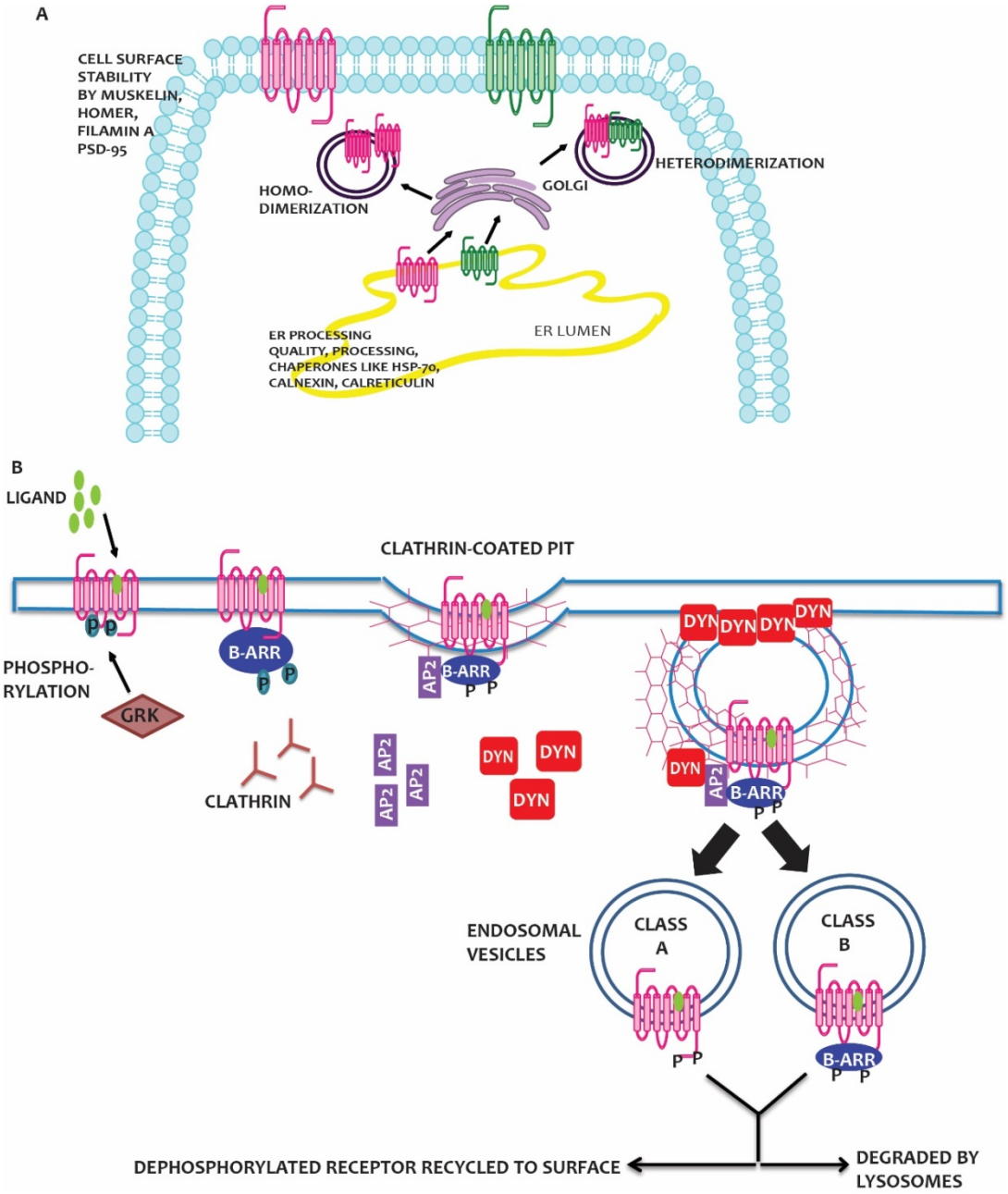

Figure 1.4 Different stages in the GPCR life cycle. (A) After synthesis of GPCRs, the receptors undergo processing and folding in the ER. Chaperone and quality-control proteins ensure proper folding and sending the unfolded proteins to a proteasome pathway. GPCRs also undergo homo- or hetero-dimerization while in the ER. The properly folded proteins are sent through the Golgi apparatus where GPCRs may undergo additional modifications and then are transported to the cell surface. Many proteins, as shown, ensure cell stability of GPCRs. B, GPCRs, upon persistent agonist activation are phosphorylated by GRKs and β-arrestin binds to the phosphorylated receptor. The internalization machinery proteins such as AP-2 and clathrin are recruited by β-arrestin and the receptors are transported to the clathrin-coated pits for endocytosis. The protein dynamin plays a key role to knick the clathrin pit, which causes endocytosis of the receptor. After endocytosis, the receptors are either de-phosphorylated and recycled to the cell surface or degraded by lysosomes. Two classes of GPCRs exist based on their interaction with β-arrestins. Class A GPCRs represent those GPCRs where the interaction with β-arrestins is transient and the GPCRs goes alone in the endocytotic vesicles without the arrestins. This includes receptors such as dopamine D1A, β_2AR, μ opioid receptor and endothelin 1A. Class B includes those GPCRs where the receptor bound to β-arrestin goes into the endocytotic vesicle thus representing a non-transient interaction (Shenoy et al., 2003). Modified from Lefkowitz et al., 2006.

1.6 Allosteric modulation of GPCRs

Recent research in GPCRs has shifted focus to identifying ligands which bind to a topographically distinct site than the one where the endogenous ligands bind (orthosteric site). These sites are called allosteric sites and the ligands which bind at these sites to modulate receptor activity are called allosteric modulators as shown in Figure 1.5. GPCRs are naturally allosteric because G-proteins allosterically modulate agonist binding.

1.6.1 Types of allosteric modulators

There are four types of allosteric modulators:

(1) Potentiators or positive allosteric modulators (PAMs): ligands that increase receptor function. The positive modulation can be seen by an increase in agonist affinity or efficacy. PAMs can also function by blocking desensitization of the receptor (Burford et al., 2012).

(2) Allosteric antagonists or negative allosteric modulators (NAMs): ligands that decrease receptor function through decrease in agonist affinity or efficacy.

(3) Allosteric agonists (Ago-allosterics or ago-agonists): allosteric compounds which display positive modulation in the absence of the orthosteric ligand.

(4) Silent allosteric modulators (SAMs): ligands that bind at the allosteric site but do not modulate the receptor function.

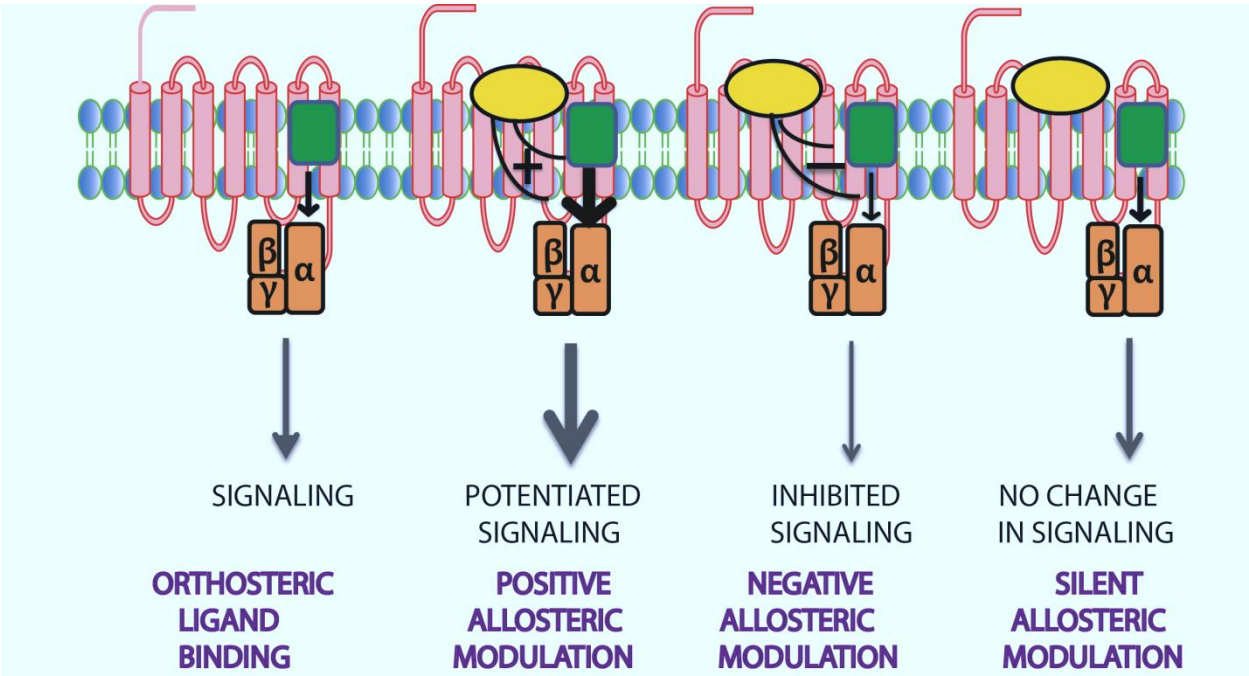

Figure 1.5 Different types of allosteric interactions. Orthosteric ligands (shown in green) bind at the site, where the endogenous ligands bind and cause conformational changes which causes downstream signaling. PAMs (shown in yellow) bind at the allosteric site and may increase the binding affinity of orthosteric ligand or efficacy of the orthosteric ligand. NAMs decrease the binding affinity or efficacy of the orthosteric ligand. SAMs are ligands which bind at the allosteric site but have no impact on the binding affinity and efficacy of orthosteric ligand. The G-protein with its three subunits is shown in orange. Modified from Wootten et al., 2013.

1.6.2 Therapeutic benefits of allosteric modulators

Allosteric ligands have a number of advantages over their orthosteric counterparts as therapeutic agents. First, allosteric modulators show higher subtype specificity than orthosteric ligands. Since allosteric sites have not undergone a high evolutionary pressure, allosteric sites do not have a high sequence identity between subtypes and thus targeting these sites could help develop

subtype-specific drugs (Conn et al., 2009). Such subtype specificity with allosteric modulators has been reported for many GPCRs such as adenosine receptors (Goblyos et al., 2011) and metabotropic glutamate receptors (Lindsley et al., 2004). Second, allosteric sites offer an opportunity to develop therapeutics for receptors where targeting the orthosteric site has not yielded successful drugs. For example, for the GLP-1 receptor no orthosteric agonists have been identified yet but allosteric agonists have been reported (Knudsen et al., 2007; Burford et al., 2011). Third, unlike orthosteric drugs, allosteric modulators may have an effect only when the endogenous ligand is present and thus maintain the temporal and spatial characteristics of endogenous signaling. PAMs, for example, may amplify the endogenous signaling but the temporal regulation of signaling is not affected. This could be of great importance especially with neurotransmitters where the timing of signaling is very important. The spatial characteristics of endogenous signaling are also maintained because unlike orthosteric ligands which can potentially act on every tissue that expresses the receptor, allosteric modulators can impact signaling only where the endogenous ligand acts (Conn et al., 2009; Burford et al., 2011). Fourth, orthosteric ligands cause significant downregulation of receptors due to constant firing of the receptors. Since allosteric activity may not be constant as it may depend on the endogenous signaling, in some instances these modulators offer potential for lesser desensitization of receptors (May et al., 2007). Fifth, allosteric activity has a ceiling effect and thus can be used to develop ligands with better safety profiles than orthosteric ligands where there is an increase in modulation of the receptor with increasing concentrations and no ceiling effect (Wild et al., 2013).

The practical advantages of the allosteric modulators led to two marketed drugs that target the allosteric sites on GPCRs i.e. Cinacalcet and Maraviroc. Cinacalcet is a positive

allosteric modulator of the calcium sensing receptor (CaSR). It is approved for treatment of primary and secondary parathyroidism (Messa et al., 2008). Cinacalcet interacts with the allosteric pocket between the 6^{th} and 7^{th} TM (Miedlich et al., 2004). Maraviroc, on the other hand, is a negative allosteric modulator of CCR5 chemokine receptor, approved as an anti-HIV drug. It allosterically inhibits the binding of two CCR5 ligands, RANTES and MIP1a (Hughes et al., 2009). Both the drugs exhibit enhanced safety profiles which exemplify the advantages of developing allosteric modulators from a drug discovery point-of view (Burford et al., 2011).

1.6.3 Detection and quantification of allostery

Many different radioligand binding or functional assays can be used to detect and quantify allostery at GPCRs. The simplest method to validate allostery at GPCRs is to perform equilibrium binding assays. Such binding assays can define two important parameters for allostery: K_B, which is the equilibrium dissociation constant of the allosteric modulator which defines the affinity of the allosteric modulator for the receptor; and α, the cooperativity factor which defines the magnitude and direction of impact the allosteric modulator and orthosteric ligand have on each other when both occupy the receptor. When $\alpha>1$, the ligand is a positive allosteric modulator whereas when $\alpha<1$, the ligand is a negative allosteric modulator. $\alpha=1$ denotes no allosteric modulation. The two parameters are calculated based on allosteric ternary complex model (Christopoulos et al., 2002; Price et al., 2005) which is as follows:

$$Y= [A]/\{[A]+(K_A (1+[B]/K_B)/(1+\alpha [B]/K_B))\}$$

where Y represents the fractional specific binding; K_A and K_B are the equilibrium dissociation constants for the orthosteric and allosteric ligands respectively; [A] and [B] are the concentrations of the orthosteric and allosteric ligand, α is the cooperativity factor. Another

method to detect the above two parameters through radioligand binding assays is to perform kinetic assays to determine the impact of allosteric compounds on the association or dissociation of orthosteric ligands. PAMs increase the association kinetics or decrease the dissociation kinetics of the orthosteric agonists. NAMs, on the other hand, increase the dissociation kinetics or increase the association kinetics of the orthosteric agonists. Apart from radioligand binding assays, functional assays such cAMP assays, calcium assays can also be performed to identify allosteric interactions of ligands with the orthosteric ligand. Functional assays allow readouts which can easily be translated into therapeutic functions that the allosteric modulator may have by investigating the signaling pathway of interest (May et al., 2007)

Two important characteristics of allosteric modulators need to be considered while analyzing allosteric modulator curves. First, allosteric modulators may display probe dependence which means that the allosteric activity of a modulator may be biased for a given orthosteric probe. This means that a modulator can vary in nature and magnitude of allosteric activity depending on the orthosteric ligand (Kenakin et al., 2005). For example, LY2033298 is a positive modulator of binding affinity of Ach at the M_4 mAch receptor, but shows no modulation for two pharmacophorically different antagonists, N-methylscopolamine and quinuclidinyl benzilate (Leach et al., 2010; Keov et al., 2011).

Another important characteristic of allosteric modulation, which adds to the complexity of these ligands, is the possibility of functional selectivity or stimulus bias. In simplified terms, it means that a ligand can be a positive allosteric modulator for some pathways associated with a receptor and have a negative modulation or no impact on others. Such selectivity for modulation of certain pathways has been exhibited by some allosteric modulators (Urban et al., 2007). For example, the allosteric modulator of M_1 mAch receptor, VU0029767 positively modulates

intracellular calcium mobilization of acetylcholine but is neutral for phospholipase D-mediated pathways (Marlo et al., 2009). Another example of such selectivity is demonstrated by 1-(4-ethoxyphenyl)-5-methoxy-2-methylindole-3-carboxylic acid, which is an allosteric modulator for CRTH2 receptor. This modulator acts as an allosteric antagonist for β-arrestin mediated signaling of prostaglandin D2 but is neutral for prostaglandin D2-mediated signaling via G-protein pathways (Mathiesen et al., 2005). This functional selectivity for different pathways suggest that multiple functional endpoints need to be evaluated to screen allosteric modulators for GPCRs and clinical efficacy of such modulators may be determined by a mix of efficacy of these compounds for different pathways. Such functional selectivity also offers opportunities to develop pathway selective therapeutics from these allosteric modulators.

1.7 Crystal structures of GPCRs: what have we learned

GPCRs are the target for more than 40% of marketed drugs (Hopkins et al., 2006, Komatsu et al., 2015). Drug targeting of these receptors has focused on synthesizing ligands which are structurally related to the endogenous ligand and thus, can bind and activate the endogenous pathways or can bind and block the signaling of the receptors. However, drug discovery with GPCRs has been severely impeded by the lack of crystal structures of GPCRs, which hinder our understanding of the mechanisms of binding of these drugs.

Membrane proteins are particularly difficult to crystallize due to the highly hydrophobic surfaces of these proteins and the instability of flexibility of these proteins which make them difficult to solubilize, purify and crystallize (Carpenter et al., 2008). Due to the advancement in structural biology techniques, the last decade has seen a boom in the number of crystal structures

obtained for GPCRs which provide us with a wealth of information about the inactive and active states of GPCRs and the different interacting motifs of GPCRs.

In 1993, the first 2-D crystal structure of rhodopsin was obtained (Schertler et al., 1993) which was followed by a high resolution crystal structure in 2000 (Palczewski et al., 2000). Since then, many crystal structures of rhodopsin in inactive (Li et al., 2004; Okada et al., 2004; Standfuss et al., 2007) and active states (Salom et al., 2006; Park et al., 2008; Scheerer et al., 2008; Standfuss et al., 2011; Choe et al., 2011) have been determined. Rhodopsin is a visual pigment found in the photoreceptor cells of retina, which transduces signals from photons to allow perception of light (Hubbard et al., 1958). The structure of bovine rhodopsin bound to 11-*cis*-retinal as shown in Figure 6 revealed key features common to the GPCR family. The primary architecture showed seven transmembrane helices connected by three intracellular and extracellular loops, an extracellular N-terminus and an intracellular C-terminus. The EC2 loop was the longest of the extracellular loops and involved in ligand binding.

The ligand-binding pocket is highly hydrophobic and is located on the extracellular surface of the transmembrane helices. The key residues that stabilize the binding of retinal include the residues Met207, Phe208 and Phe212 from H5, and Trp265 and Trp268 from TM6 (Palczewski et al., 2000; Li et al., 2004; Okada et al., 2004; Standfuss et al., 2007). The receptor is maintained in its inactive state by an interaction between the Arg135 from TM3 and Glu246 from TM6, which is commonly referred to as the "ionic lock". In the inactive receptor, the TM6 shows a bend at 36° formed by Pro267 which keeps both the ends of the transmembrane away from the core of the transmembrane bundle. The C-terminus of the receptor shows a short amphipathic helix called H8, which is perpendicular to TM7 and anchors the receptor covalently to the membrane via palmitoylation of Cys322 and Cys323. The C-terminus includes important

sites of phosphorylation which includes Ser334, Ser338 and Ser343, which are recognized upon phosphorylation by arrestins to arrest G-protein signaling. The intracellular loop 3 (IC3) is highly flexible and disordered in the inactive state of rhodopsin (Zhou et al., 2012).

Upon activation, several conformational changes are seen in the motifs that were stabilizing the inactive state of the receptor as shown in Figure 1.6. Upon exposure to light, the *cis*-retinal undergoes a cis-trans transition that is responsible for activation of the receptor. Changes in the conformation of the receptor occur to allow binding of G-protein on the intracellular side. The TM6 at Pro267 bends further away from the TM core on the intracellular side and a crevice of 14Å diameter for G-protein binding is formed (Scheerer et al., 2008; Standfuss et al., 2011; Choe et al., 2011). As a result of bending of TM6, the ionic lock which constraints the receptor in an inactive state breaks. The NPXXY motif on TM7 shifts towards TM6 and orients Tyr306 towards the helix, which also aids in breaking the ionic lock. The C-terminus of TM5 is elongated due to addition of majority of IC3 loop into TM5 to provide interface to the G-protein for coupling to the receptor (Zhou et al., 2012).

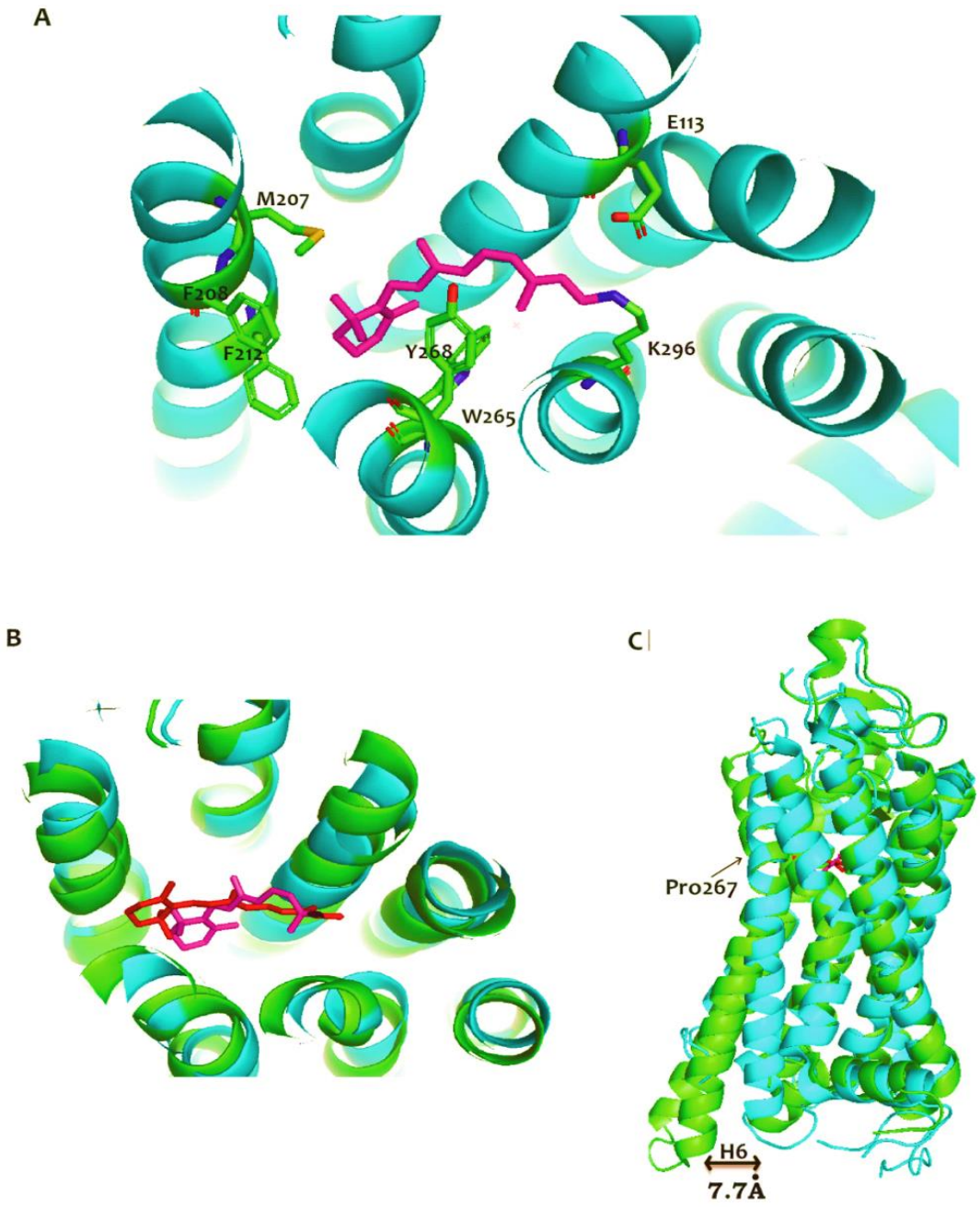

Figure 1.6 Comparison of inactive and active state crystal structures of rhodopsin (A) Inactive state crystal structure of rhodopsin (in cyan, PDB:1F88) with 11-cis retinal (in pink) showing some of the key residues that stabilize the ligand in the binding pocket (B) Superimposed inactive (in cyan, PDB:1F88) and active state (in green, PDB: 3PQR) crystal structure of rhodopsin revealing conformational changes in retinal upon photoactivation with all-trans retinal

shown in red and the ground state 11-cis retinal in pink. (C) Superimposed structures of inactive (in cyan) and active (in green) conformations of rhodopsin. The H6 shows an outward movement on the cytoplasmic end (as shown by a horizontal arrow) by bending at Pro 267 which creates a crevice for G-protein to bind. The H5 elongates on the cytoplasmic end and creates a larger interface for G-protein interaction. Adopted and modified from Zhou et al., 2012.

The structure of rhodopsin established the basis of our understanding of GPCRs, however this receptor is unusually very stable with cis-retinal keeping it in a non-signaling conformation. However, most of the GPCRs are highly flexible and equilibrate between multiple conformational states upon ligand binding (Kobilka et al., 2007). The crystal structure of the β_2-adrenergic receptor helped to gain insight into the key interactions that stabilize such GPCRs due to the high basal activity exhibited by this receptor. The inactive state crystal structure shown in Figure 1.7 was obtained with antagonist carazolol bound to the receptor and a T4L fusion protein was inserted at EC3 to stabilize the protein. The crystal structure revealed that the extracellular loops of the receptor allow entry of the ligand into the binding pocket which is formed by TM3, TM5, TM6, TM7 and the EC2 loop. The ionic lock which maintains GPCRs in an inactive state was in open conformation which suggests the high basal activity of this receptor (Moukhametzianov et al., 2011). Some of the key interactions which stabilized the binding of carazolol in the binding pocket included a salt bridge between the ammonium moiety and $Asp^{3.32}$, hydrogen bonding of the hydroxyl group with $Asn^{7.39}$ and between aromatic groups of carazolol and $Ser^{5.42}$ (Rosenbaum et al., 2007; Warne et al., 2008; Shonberg et al., 2015). In 2011, an agonist-bound β_2-AR crystal structure was solved in complex with a covalent ligand FAUC50. They key interactions that stabilized the agonist-bound structure were hydrogen bonds between catechol-replacing ring of FAUC50 and $Ser^{5.42}$ and $Ser^{5.46}$ (Rosenbaum et al., 2011). Crystal structures of the receptor with partial agonists lacked hydrogen bonding with Ser5.46 suggesting weaker binding interactions in the orthosteric pocket. These crystal structures revealed structural differences between agonists and partial agonists that correlate with their efficacy at the receptor (Warne et al., 2011).

Overall, around 20 different receptors from the class1A rhodopsin-like family have been solved in complex with different ligands. These crystal structures have been the basis of structure-based drug design, homology modeling of receptors with unknown structures and virtual ligand docking. It has allowed a better appreciation of the structural understanding of GPCRs and laid the basis for a more refined and targeted drug design (Shonberg et al., 2015).

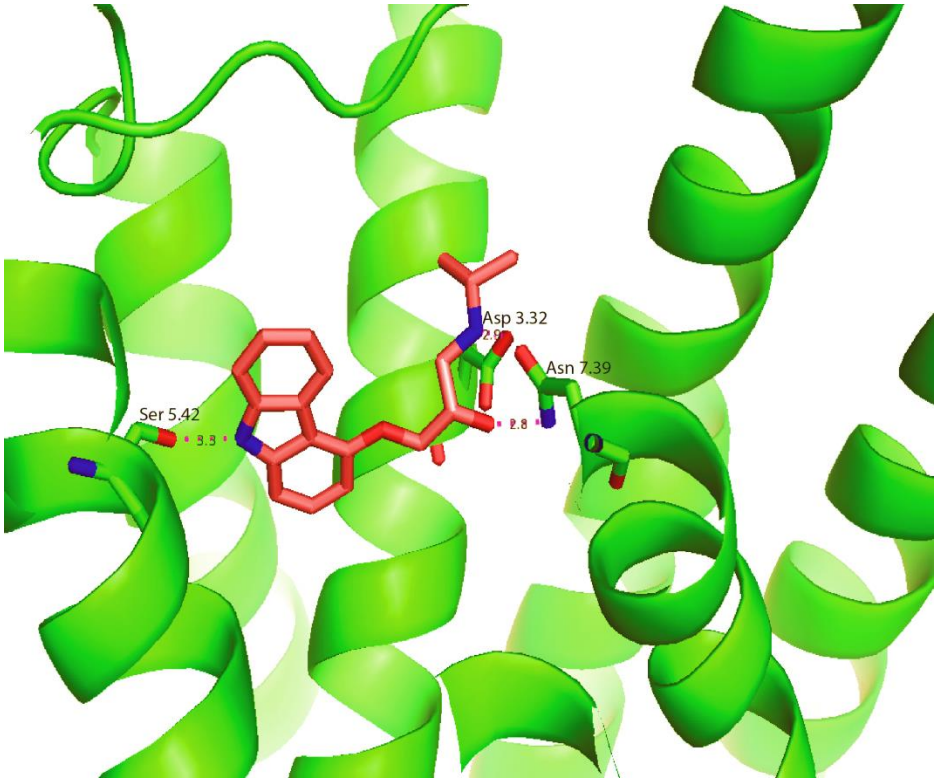

Figure 1.7 Crystal structures for β_2-adrenergic receptor. The crystal structure shows the inverse agonist carazolol (shown in red) bound to the receptor. Some of the key interactions that stabilize the ligand are formed with $Asp^{3.32}$, $Ser^{5.42}$ and $Asn^{7.39}$ as shown in the figure. Modified from Shonberg et al., 2015.

1.8 The endocannabinoid system

The endocannabinoid system primarily consists of two receptor subtypes i.e. CB_1 and CB_2 (Pertwee et al., 1997), the ligands acting at these receptors naturally synthesized in the body called endocannabinoids and the enzymes involved in their biosynthesis, transport and metabolism (Petrocellis et al., 2004). Screening of orphan GPCRs for binding to THC resulted in the identification of the CB_1 receptor (Devane et al., 1988; Bram et al., 2012). Later, the CB_2 receptor was identified by homology cloning (Munro et al., 1993). The two major endocannabinoids include anandamide (*N*-arachidonyl-ethanolamine) (AEA) (Devane et al., 1992) and 2-arachidonylglycerol (2-AG) (Sugiura et al., 1995). Other proposed endocannabinoids include N-arachidonoyl-dopamine (NADA), noladin ether and virodhamine (Petrocellis et al., 2004). Recently, a nonapeptide known as hemopressin has been identified as the first endogenously synthesized CB_1 inverse agonist, although further investigation of its pharmacology is needed (Heimann et al., 2007).

Biosynthesis of AEA occurs in a two-step process as shown in Figure 1.8. First, transfer of arachidonic acid from the sn-1 position of phosphatidyl choline to the nitrogen atom of phosphoethanolamine (PE) is mediated by a calcium-dependent transacylase to form N-arachidonoyl PE (NAPE). This acts as the precursor for AEA synthesis. A NAPE-specific phospholipase D (NAPE-PLD) enzyme then hydrolyzes NAPE to yield AEA (Marzo et al., 2009). However, no reduction in AEA levels were exhibited in NAPE-PLD knockout mice which led to the identification of alternate enzymes and pathways involved in AEA synthesis (Leung et al., 2005). These include alpha-beta hydrolase 4 which sequentially cleaves sn-1 and 2-acyl groups of NAPE to generate glycerophospho-AEA which is hydrolyzed by phosphodiesterase to yield AEA. Another biosynthetic route involves the enzyme phospholipase

A_2 which converts NAPE into 2-lyso-NAPE which is then followed by action of lysophospholipase D (Liu et al., 2008).

For the hydrolysis of AEA, the main enzyme involved is fatty acid amide hydrolase (FAAH) which hydrolyzes AEA to its corresponding fatty acids (shown in Figure 1.8). FAAH has emerged as an attractive target in recent studies since FAAH inhibitors can increase the endogenous levels of AEA which can maintain the temporal and spatial control of the CB_1 receptor as against a CB_1 agonist which can potentially activate all the receptors in the body and not maintain the timing of signaling. This can be used for the treatment of pain, inflammation and sleep disorders (Otrubova at el., 2011).

The biosynthesis of 2-AG has also been largely investigated and the chief enzymes for 2-AG biosynthesis are diacylglycerol lipase (DAGL) α and β (Bisogno et al., 2003). Phospholipase C hydrolyzes phosphatidylinositol or phosphatidic acid to generate DAG precursors which are hydrolyzed to 2-AG by DAGL. Monoacylglycerol lipase is the main enzyme involved in degradation of 2-AG (Blankman et al., 2007). Other alternate enzymes involved in 2-AG degradation are ABHD-6 (α,β-Hydrolase domain containing 6) and ABHD-12.

Recent evidence has suggested some non-CB_1 and non-CB_2 receptors bind the endocannabinoids. This includes the orphan receptor GPR55, a receptor with <20% sequence homology with CB_1 and CB_2. This receptor is activated by CP55,940 and demonstrates GTPγS binding with anandamide and virodhamine (Ryberg et al., 2007). Further investigations are needed to understand the pharmacology of this receptor.

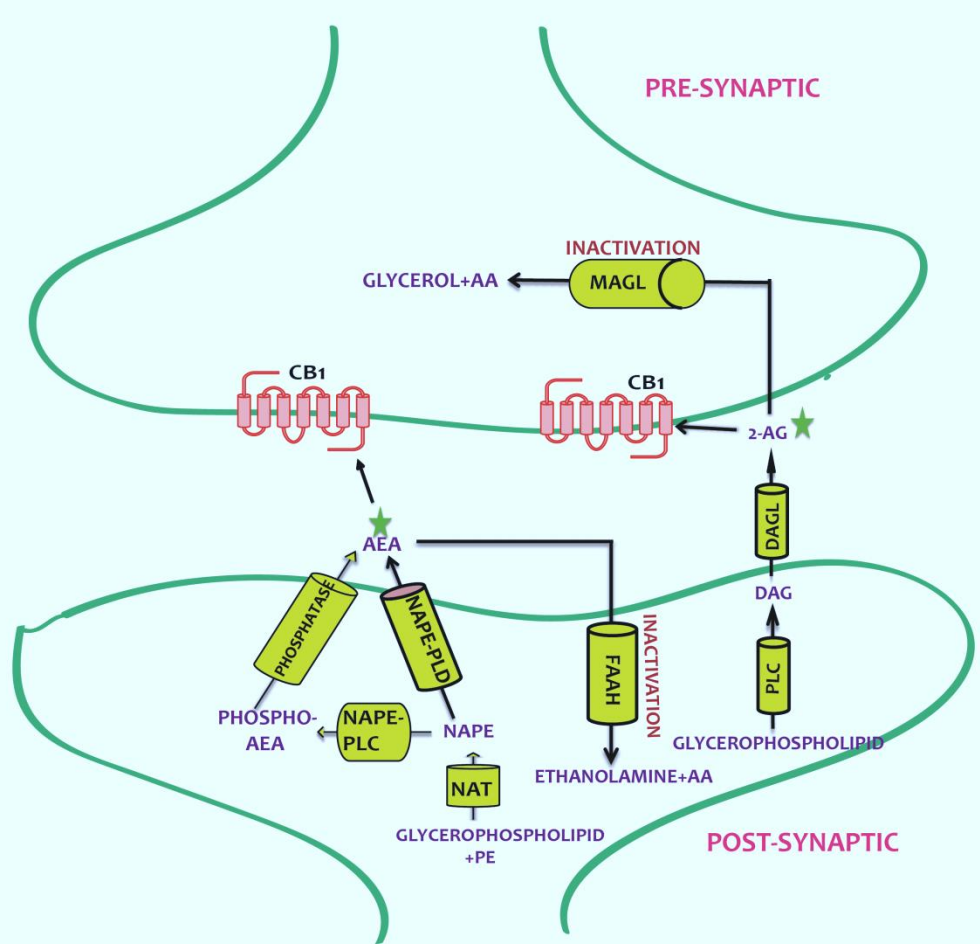

Figure 1.8 The endocannabinoid system represented in pre- and post-synaptic neurons. The two important endocannabinoids, AEA and 2-AG are shown with the enzymes involved in their synthesis and degradation. The enzymes involved in biosynthesis of anandamide are NAT (*N*-acyltransferase), NAPE (*N*-arachidonyl phosphatidylethanolamine), NAPE-PLD (*N*-arachidonyl phosphatidylethanolamine phospholipase D), NAPE-PLC (*N*-arachidonyl phosphatidylethanolamine phospholipase C) and phosphatase. Anandamide is inactivated by FAAH (fatty acid amide hydrolases). 2-AG is biosynthesized by PLC (phospholipase C) and DAGL (diacylglycerol lipase) and inactivation by MAGL (mono-acyl glycerol lipase)

1.9 Localization and tissue distribution of cannabinoid receptors

The CB_1 receptor is primarily expressed in the central nervous system (CNS) and is present on the presynaptic terminals (Katona et al., 1999; Marsicano et al., 1999, Tsou et al., 1999). However, recent studies have revealed that the CB_1 receptor is also expressed in peripheral tissues such as reproductive (Pertwee et al., 2001), digestive (Croci et al., 1998) and cardiovascular systems (Szabo et al., 2001). In the CNS, the CB_1 receptor is predominantly expressed in the hippocampus, caudate, putamen, globus pallidus, accumbens nucleus and horizontal limb of the diagonal band as shown in Figure 1.9 (Svizenska et al., 2008). These are important regions of the brain that influence mood, motor coordination, sensation, memory, cognition and autonomic function. The expression patterns of the receptor in the CNS can be correlated with many effects associated with cannabinoids. For example, the hippocampus region is involved in learning and memory processes and a high density of CB_1 receptors in this region relates to why chronic exposure to marijuana and other cannabinoids can impair memory and cognition (Herkenham et al., 1990; Herkenham et al., 1991b). Alterations in the expression of the CB_1 receptor in different parts of the brain have been attributed to the progression of diseases such as Parkinson's (Glass et al., 1993) and Huntington's disease (Sanudo-Pena et al., 1998). Differences in CB_1 expression levels between rat and human cerebellum explains why defects in gross motor functioning following marijuana use are subtle in humans compared to rats where acute administration of cannabinoids results in deleterious effects on motor function in the form of immobility, ataxia and catalepsy (Ameri et al., 1999; Herkenham et al., 1990). CB_1 receptors have been suggested as a therapeutic target for pain management, which is explained by the high expression of the CB_1 receptor in the periaqueductal gray and dorsal horn of the spinal cord. CB_1

is expressed in the majority of the nociceptive neurons in the dorsal root ganglia with variable degrees of CB_1 mRNA detected in the dorsal root ganglia.

The CB_1 receptor also plays a key role in regulation of food intake, metabolism of lipids and glucose and fat accumulation both centrally and peripherally. Rimonabant (also called SR141716A), an inverse agonist of CB_1, was commercially available in the European market as an anti-obesity drug. Upon stimulation of CB_1 in the hypothalamus, CB_1 may interact and regulate the neuropeptides involved in food intake and lipogenesis such as corticotropin-releasing hormone (MCH), prepro-orexin, cocaine-amphetamine-regulated transcript (CART). The dopaminergic reward pathway is invigorated upon CB_1 stimulation in the accumbens nucleus which leads to motivation to eat and intake drugs of abuse (Maldonado et al., 2006).

Regions with moderate density of CB_1 expression include neocortex, medial hypothalamus, solitary nucleus and basal amygdala. Very low levels of CB_1 are seen in the thalamus and brain stem (Svizenska et al., 2008).

CB_2 receptors are considered to be peripheral cannabinoid receptors due to their primary expression in the immune system. In immune cells, CD4+ T cells, CD8+ Tcells, B cells, batual killer cells, monocytes and polymorphonuclear neutrophils show highest CB_2 density (Derocq et al., 1995; Schatz et al., 1997; Dittel et al., 2008; Atwood et al.; 2010). Apart from the immune system, expression of CB_2 receptors is also reported in bone cells such as osteocytes, osteoblasts and osteoclasts where they modulate bone growth (Ofek et al., 2006). Other regions of CB_2 expression include adipocytes (Roche et al., 2006), hepatic myofibroblasts (Julien et al., 2005), the trabecular meshwork cells in the eye (He et al., 2007), cardiomyocytes (Shmist et al., 2006) and sperm cells (Grimaldi et al., 2009).

Although considered to be a peripheral cannabinoid receptor, recent murine and rat studies have detected expression of CB_2 in the brain although the density of expression is much lower than CB_1. Microglia, the resident immune cells of the brain which monitor pathological damage in the brain show CB_2 mRNA and protein (Meresz et al., 2007; Beltramo et al., 2006). Migration of microglia to neurodegenerated areas in the brain is modulated by CB_2 (Atwood et al., 2010). RT-PCR studies to quantify mRNA, protein and functional expression have shown the expression of CB_2 mRNA in the brainstem in rats. The presence of CB_2 mRNA has also been reported in the granule cells and Purkinje cell layers in the mouse cerebellum (Atwood et al, 2010).

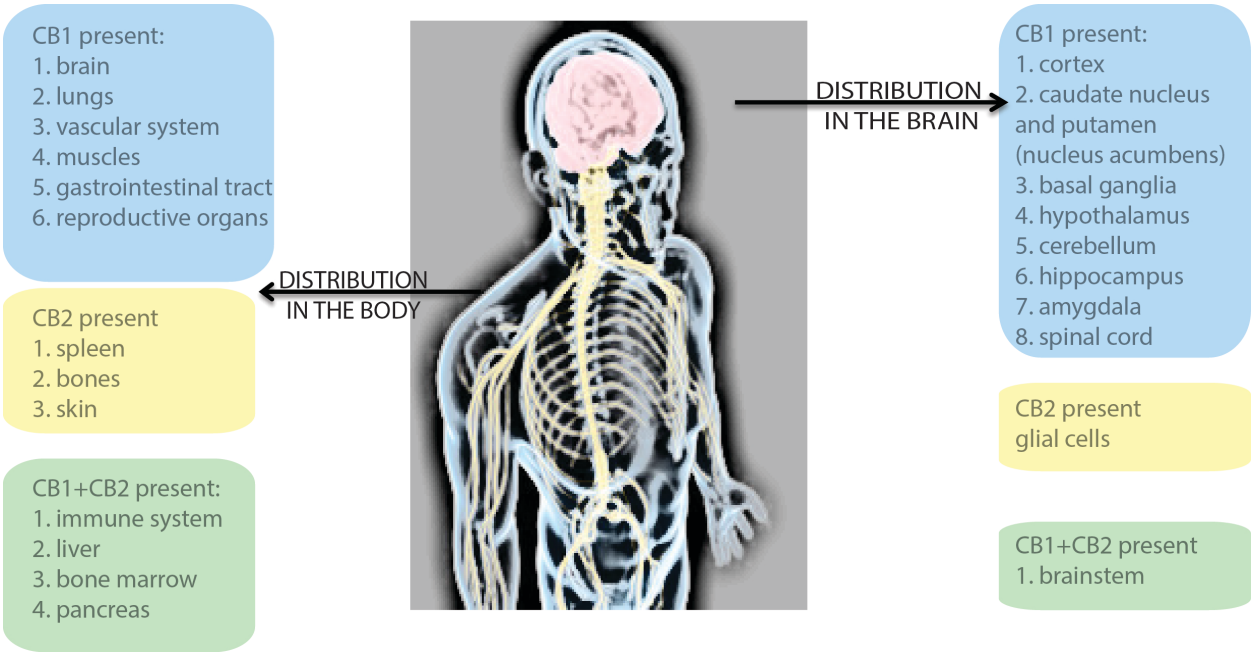

Figure 1.9 Tissue distributions of cannabinoid receptors in the body. The different systems of the body where CB_1 (in blue), CB_2 (in yellow) or both CB_1 and CB_2 (in green) are shown. The CB_1 receptor is primarily expressed in the CNS. Some of the key regions where CB_1 is expressed include hippocampus, basal ganglia, cortex and cerebellum. Lower expression levels are seen in amygdala, nucleus accumbens, thalamus, hypothalamus and spinal cord. CB_2 is primarily expressed in the immune system cells such as macrophages, B and T-lymphocytes, neutrophils and monocytes. CB_2 expression is also seen in bone cells, spleen and skin nerve fibres. Although low, expression of CB_1 is also been demonstrated in some areas of the CNS such as astrocytes, microglial cells and brainstem neurons.

1.10 Cannabinoid ligands and inactive-active state models

Research involving cannabinoid ligands developed from investigations on the plant material from marijuana (*Cannabis Sativa*). Since then, a number of CB_1 ligands, both natural and synthetic have been identified. CB_1 agonists can be divided into four major groups: classical cannabinoids, non-classical cannabinoids, aminoalkylindoles and eicosanoids. Recently, another class of agonists for CB_1 have been synthesized which are called hybrid cannabinoids.

Classical cannabinoids: The classical cannabinoids include the main psychoactive component of marijuana, Δ^9-THC; the equally active isomer of THC, Δ^8-THC and other active constituents from the plant material such as cannabidiol (CBD), cannabinol (CBN) and cannabichromene (CBC) (Pertwee et al., 2008). The classical cannabinoids also include synthetic analogs synthesized using Δ^9-THC which includes potent analogs such as 1′,2′-dimethylheptyl-pyran (DMHP) and (-)-11-Δ^8-THC-dimethylheptyl (HU-210). These ligands have a tricyclic ring system with a benzopyran moiety. The members of this group usually lack selectivity between CB_1 and CB_2 for binding. For example, Δ^9-THC is a partial agonist for both CB_1 (K_i= 39.5 nM) and CB_2 (K_i= 40 nM). HU-210 is a potent cannabinoid ligand but lacks subtype-specificity (K_i for CB_1=0.7 nM and K_i for CB_2= 0.2 nM) (Pertwee et al., 2005).

Non-classical cannabinoids: The non-classical cannabinoids include bicyclic (e.g. CP55,940) and tricyclic (e.g. CP55,244) analogs of Δ^9-THC developed by Pfizer. These ligands lacked the dibenzopyran ring present in classical cannabinoids since structure-activity relationship (SAR) studies on classical cannabinoids revealed that the benzopyran ring is not essential for activity and elimination of the pyran oxygen to make open phenol analogs showed higher affinity. CP55,940 shows higher affinity (K_i= 0.6 nM) and efficacy compared to Δ^9-THC (K_i= 39.5 nM). However, like Δ^9-THC, CP55,940 non-selectively binds to both CB_1 and CB_2. In the structure of

non-classical cannabinoids, it is the side chain and phenol that are key for maintaining activity at the cannabinoid receptors. The stereochemistry of the hydroxpropyl chain prefers a β-conformation although the chain is not necessary for activity (Reggio et al., 2008).

Hybrid Cannabinoids: This class of ligands was reported by the Makriyannis group and combined all the structural features of classical and non-classical cannabinoid ligands. These ligands used a southern aliphatic hydroxyl pharmacophore (SAH) not present in plant cannabinoids. The structure allowed three-dimensional access to the active sites which was not possible with the non-classical ligands. Using the SAH pharmacophore and optimizing it by introducing double bonds or triple bonds at the C2′′ position in the hydroxypropyl chain led to hybrid probes such as AM938 (Thakur et al., 2005).

Aminoalkylindoles: The prototypical ligand for this group is WIN-55,212-2, the structure of which bears no resemblance to classical or non-classical cannabinoids. First synthesized by the Sterling Research Group, WIN-55,212-2 has a high affinity for both CB_1 (K_i= 1.89 nM) and CB_2 (K_i= 0.28 nM). SAR on this structure by revealed that the aminoalkyl moiety in the molecule can be substituted for straight chain alkyl groups (Huffman et al., 1994). This lead to indole derivatives such as JWH-007 (1-pentyl-2-methyl-3-(1-naphthoyl)indole) with a high affinity for CB_1 (K_i=9.5 nM) and CB_2 (K_i= 2.9 nM) and JWH-015, the 1-propyl analog with a high affinity for CB_2 (K_i= 13.8 nM) (Reggio et al, 2008).

Eicosanoids: This class includes fatty acid derivatives that are endogenously synthesized cannabinoid ligands i.e. endocannabinoids. These are synthesized locally on demand and utilize cell membrane components for their biosynthesis. AEA and 2-AG are the primary endocannabinoids. AEA is easily hydrolyzed by FAAH (Deutsch et al., 1993). 2-AG is considered a primary endocannabinoid because it is present in higher amounts in the brain

although it has a lower binding affinity for CB_1(K_i=472 nM) compared to anandamide (K_i= 61 nM). Other ligands belonging to this category are 2-arachidonyl glyceryl ether (Noladin ether), virodhamine, N-docosatetraenoylethanolamine and N-arachidonoylglycine. Noladin ether shows a high binding affinity towards CB_1 (K_i= 21 nM) than CB_2 (K_i= >3000 nM) (Svizenska et al., 2008).

Inverse agonists

Hyperactivity of the endocannabinoid system is associated with the progression of many diseases. CB_1 hyperactivity has been associated with diseases such as obesity, overweight and the associated cardiovascular risks and substance abuse disorders for which inverse agonists of CB_1 have gained mounting interest. The first CB_1 inverse agonist, SR141716A, was first developed at Sanofi-Aventis and displayed a high affinity for CB_1 (K_i= 1.8 nM) and a reduced affinity for CB_2 (K_i= 514 nM). SR141716A affects the constitutive signaling of CB_1 promoting signaling responses opposite to those of agonists. It abrogates the constitutive G-protein signaling of CB_1. It antagonizes the inhibitory effects of CB_1 agonists on cAMP levels in rat brain membranes (Rinaldi-Carmona et al., 1994). Clinical effectiveness of rimonabant in obesity was based on its metabolic effects such as enhanced lipid oxidation and decreased lipogenesis in liver. However, reduction in food consumption with the drug is transient, which questions its ability to be an effective weight-control medicine (Henness et al., 2006; Patel et al., 2007). In 2008, this drug was withdrawn due to psychoactive side effects such as anxiety and depression associated with the drug (Kirilly et al., 2012). Other than SR141716A, AM251 and AM281 are inverse agonists of CB_1 with a diarylpyrazole pharmacophore. Capable of competing with SR141716A in CB_1 receptor membrane preparations, these ligands exhibit antagonizing properties to CB_1 agonists similar to SR141716A (Thakur et al., 2005).

Antagonists

Due to the side effects seen with inverse agonists of the CB_1 receptor, another pharmacological strategy to manipulate the CB_1 receptor that has emerged is the development of antagonists. Unlike CB_1 inverse agonists, these ligands do not affect the constitutive activity of CB_1 and thus only affect ligand-dependent CB_1 activation. Theoretically, the side effects seen with inverse agonists may be due to the abrogation of basal signaling tone of CB_1 receptor. Several antagonists of the CB_1 receptor have been developed. VCHSR, an analogue of SR141716A attenuates WIN55,212-2 induced inhibition of Ca^{2+} signaling by CB_1. However, as a neutral antagonist, it does not exhibit this effect in the absence of WIN55,212-2 unlike SR141716A. VCHSR lacks the hydrogen bonding in its C3 substituted region as exhibited by SR141716A (Hurst et al., 2002).

Another series of CB_1 antagonists were developed as sulphonamide analogs of Δ^8-THC with acetylenic side chains to yield O-2050 which showed neutral antagonism in mouse isolated vas deferens (Martin et al., 2002; Pertwee et al., 2005). Another analogue of SR141716A, NESS 0327 has been reported. NESS 0327 shows high specificity for CB_1 (Ki= 0.00035 nM) as opposed to CB_2 (21 nM) with 60000 times more readily binding to CB_1 than CB_2 and is more potent as an antagonist than CB_1 (Ruiu et al., 2003; Pertwee et al., 2005).

Structures of some of the important ligands discussed above along with their binding affinities at CB_1 receptor are shown in Figure 1.10.

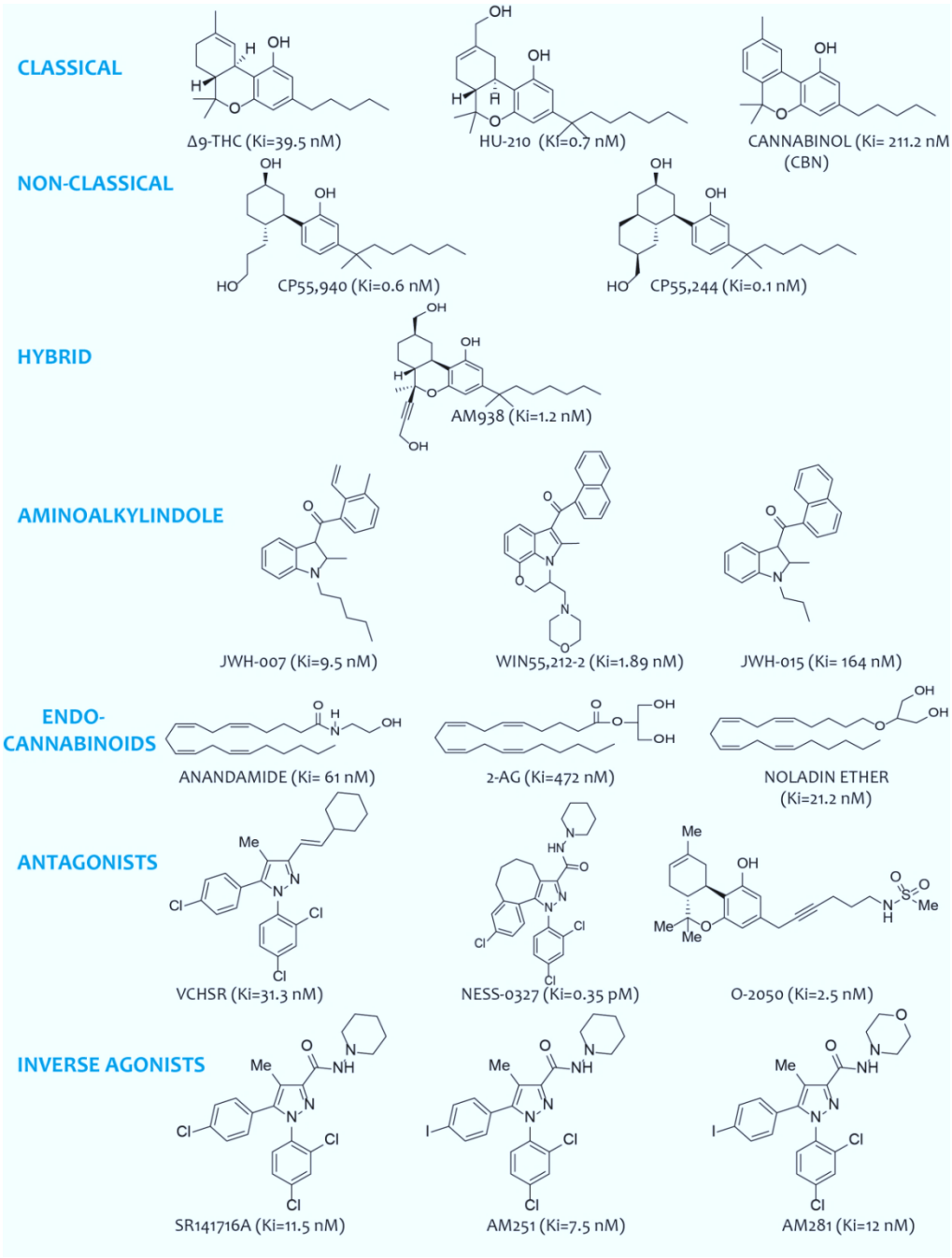

Figure 1.10 CB_1 ligand structures and K_i values for binding at CB_1 receptor. Representative agonists (classical, non-classical, aminoalkylindoles and endocannabinoids), antagonists and inverse agonists of CB_1 are shown with K_i values in brackets (K_i values reported from Pertwee et al., 2010).

1.11 Signaling via CB_1 receptors: G-protein dependent and independent-pathways

The CB_1 receptor is involved in multiple downstream signaling pathways which can be dependent on G-protein or could involve G-protein independent pathways. On activation by ligand, CB_1 receptors undergo conformational changes and on the intracellular side of the receptor, a heterotrimeric G-protein binds. There is a guanosine-nucleotide exchange of GDP for GTP and the G-protein dissociates into α and βγ subunits which are coupled to downstream effector molecules which drive different signaling pathways as shown in Figure 1.11.

CB_1 primarily couples to $G_{i/o}$ protein which on activation causes inhibition of adenylate cyclase. Coupling to $G_{i/o}$ protein may also lead to manipulation of different ion channels (Howlett et al., 1986). CB_1 activation causes stimulation of G-protein coupled inwardly rectifying potassium channels through $G_{i/o}$ protein (Mackie et al., 1995). In cerebral vessels, it has been reported that CB_1 activation causes inhibition of L-type calcium channels (Gebremedhin et al., 1999). Inhibition of N-type calcium channels has also been previously reported, which may be important for retrograde signaling by CB_1 (Brown et al., 2004).

Under certain circumstances such as treatment with pertussis toxin (PTX), CB_1 may couple to G_s protein, which causes activation of cAMP formation via activation of adenylate cyclase (Glass & Felder 1997, Abadji *et al.* 1999, Calandra *et al.* 1999, Kearn *et al.* 2005). Certain cannabinoid ligands have been reported to generate signaling via activation of $G_{q/11}$ protein. For example, HEK293 cells expressing the CB_1 receptor, when treated with the CB_1 agonist WIN55,212-2 causes a G_q-mediated calcium signaling (Lauckner et al., 2005). However, in NG108-15 cells, calcium signaling induced upon CB_1 stimulation was pertussis-toxin sensitive suggesting the involvement of $G_{i/o}$ protein (Sugiura et al., 1996), indicating that these cell-type specific results could be a result of different G-protein pools in different cell types. The CB_1 receptor also

activates pathways associated with mitogen-activated protein kinases (MAPKs). Activation of MAPKs can lead to pathways that ultimately activate phosphorylation of ERK1/2 (Howlett et al., 2005), c-Jun N-terminal kinase (JNK), p38 MAPK or ERK5 proteins (Turu et al., 2010). Activation of the CB_1 receptor leads to phosphorylation of ERK1/2 in a variety of cell types. Mechanisms leading to ERK1/2 activation include activation of $G_{i/o}$ proteins (Howlett et al., 2005), phosphatidylinositol 3-kinase (Galve-Roperh et al., 2002), Src tyrosine kinase (Derkindersen et al., 2003) and G-protein independent mechanisms mediated by β-arrestins (Turu et al., 2010).

Stimulation of the CB_1 receptor has been reported to activate JNK1/2 and p38 in a variety of cells. In Chinese hamster ovary (CHO) cells, stimulation of CB_1 via THC leads to activation of JNK-1/2 and p38 MAPK. Activation of JNK was mediated by $G_{i/o}$ proteins (Reuda et al., 2000). In rat hippocampal cells, p38 MAPK was activated by cannabinoids but no JNK1/2 activation was seen (Derkindersen et al., 2011). In Neuro 2a cells, ERK1/2 stimulation but not JNK1/2 or p38 activation was seen following treatment with HU-210 (Graham et al., 2006; Turu et al., 2010).

Other partners that CB_1 interacts with include adaptor protein AP-3 (Rosenfeld et al., 2008), adaptor protein FAN (Sanchez et al., 2001) and GPCR-associated sorting protein (GASP-1) (Martini et al., 2007) to control signaling and trafficking. Overall, the CB_1 receptor demonstrates the principle of stimulus trafficking where different ligands can evoke different signaling pathways depending upon the G-protein coupling and effector molecules stimulated.

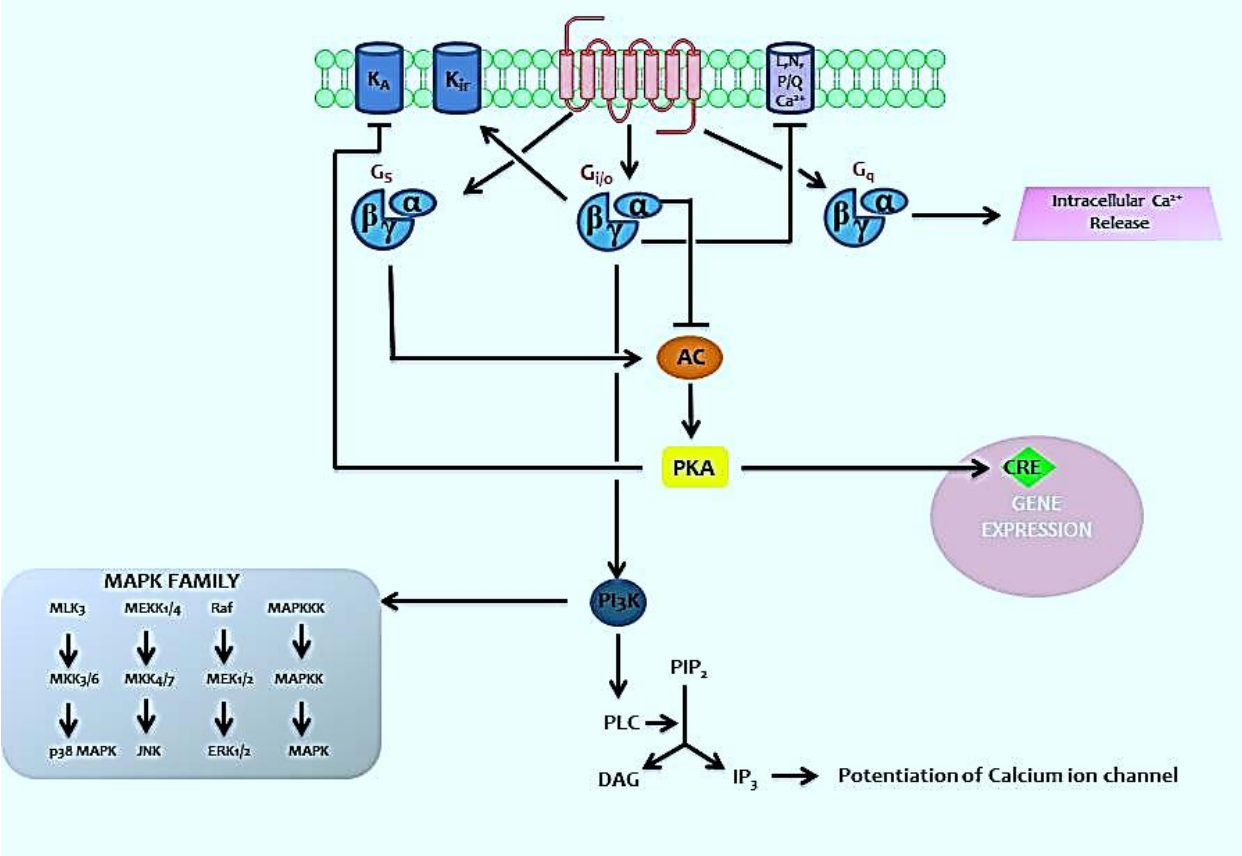

Figure 1.11 Complex signaling pathways followed by cannabinoid receptor activation. Both CB_1 and CB_2 primarily couple to $G_{i/o}$ and cause inhibition of adenylyl cyclase activity decreasing cAMP levels. CB_1 regulates many ion channels such as Ca^{2+} and K^+ channels. It causes negative regulation of voltage-gated Ca^{2+} channels and positive stimulation of inwardly-rectifying (K_{ir}) and voltage-dependent (K_A) potassium channels. CB_1 receptor is also involved in activation of MAPK family causing phosphorylation of ERK1/2, JNK and p38. Coupling of CB_1 to G_s protein has been reported in some cell lines and cause activation of adenylyl cyclase. CB_1, under certain conditions may couple to G_q protein which causes release of intracellular Ca^{2+}. Adopted and modified from Bosier et al., 2010.

1.12 Functional motifs on the CB_1 receptor: orthosteric binding site

It is now well understood that different ligands may induce different conformational states which in turn governs the G-protein it couples to. Different functional residues may be involved in binding of different class of ligands in the orthosteric binding pocket. The complexity in understanding binding efficacy of ligands in GPCRs is further heightened because most of the known X-ray crystal structures available for GPCRs are for the inactive state of the receptor (Edwards et al., 2004; Cherezov et al., 2007; Warne et al., 2008; Zazula et al.,2008) because the receptor is very dynamic in the active state and difficult to crystallize. No X-ray crystals are available for the CB_1 receptor. However, multiple functional residues have been identified for CB_1 through a combined approach of mutational analyses and computational modeling. Homology models are often built for CB_1 for docking ligands using X-ray crystal structures from the rhodopsin family. Sequence alignment with rhodopsin and others such as β_2-adrenergic receptor, alpha-adrenergic receptor 2A (AA_{2A} R) show that CB_1 shares some motifs that are conserved in GPCRs, which have been previously discussed in this chapter. Functional residues important for ligand binding that have been identified through mutagenesis require careful examination because introduction of a point mutation in a receptor can greatly alter the ligand-binding properties.

The key initial contacts of CP55,940 binding to the CB_1 receptor involved TM3-E2-TM5 region. At a later stage of receptor activation, TM6 and TM7 are also involved. The residues identified through many different mutagenesis studies have identified F268, P269, H270 and I271 in the extracellular loop 2 (EC2) (Ahn et al., 2009) and $Y275^{5.29}$ (McAllister et al., 2002) and $C355^{6.47}$ (Picone et al., 2005) as the residues which form direct contact with CP55,940 for binding to the CB_1 receptor. Computational modeling studies have suggested that $S383^{7.39}$ is

important to maintain a kink in the TM7, which is necessary for CP55,940 binding. Loss of CP55,940 binding occurs when this residue is mutated to alanine which causes reduction in the TM7 kink (Kapur et al., 2007). Thus, this residue results in an indirect loss of binding through the conformation formed that results in a loss of activation. For the aminoalkylindoles particularly WIN55,212-2, the aromatic microdomain in the TM3-4-5 and TM6 is the proposed region of binding. The residues which form a direct contact for WIN55,212-2 binding include G195$^{3.31}$ (Chin et al., 1999), F200$^{3.36}$ (McAllister et al., 2003), Y275$^{5.39}$ (McAllister et al., 2007), W279$^{5.43}$ (McAllister et al., 2003) and V282$^{5.46}$ (Song et al., 1999). Another residue important for WIN55,212-2 binding is D163$^{2.50}$, a highly conserved residue in GPCRs. The mutant D163N exhibits a 400-fold loss of binding of WIN55,212-2 and loss of cAMP signaling. Although the residue does not form direct contacts with WIN55,212-2, this mutation results in an altered ligand binding pocket and thus play a critical role in the binding of WIN55,212-2 to the CB_1 receptor (Abood et al., 1998).

AEA, an endocannabinoid for the CB_1 receptor, primarily binds in the TM2-3-5 region. Not many contacting residues for anandamide binding are known. Y275$^{5.39}$ is involved in H-bonding with AEA, since 13-fold loss of binding in a Y275F mutant and a complete loss of ligand binding in a Y275I mutant was observed. Another important residue involved in direct contacts with anandamide is F189$^{3.25}$ which forms aromatic/π interactions with the C5-C6 double bond of anandamide.

SR141716A, the highly subtype-specific inverse agonist for CB_1 binds in the TM3-5-6-7 region. The binding site is located deep in the receptor core and residues in direct contact with SR141716A include F200$^{3.36}$, W279$^{5.43}$, W356$^{6.48}$ (McAllister et al., 2003) and C386$^{7.42}$ (Fay et al., 2005). The two residues, W279$^{5.43}$ and W356$^{6.48}$ are part of the aromatic microdomain of

CB_1. The residues which indirectly affect SR141716A include C257 and C264 from the EC2 loop (Fay et al., 2005), which when mutated to alanine results in loss of SR141716A binding. The authors suggested that mutation of these cysteines to alanine may result in loss of intra-loop disulfide bonds, causing a conformation change that affects the ligand binding pocket architecture.

A residue $K192^{3.28}$ has been reported to be a crucial amino acid which is involved in binding of CP55,940, anandamide, SR141716A and HU-210. Mutations to this residue have been reported to modify the geometry of the binding pocket such that the mutated receptors show complete loss of binding for CP55,940, HU-210 and anandamide and 17-fold loss of SR141716A in K192A receptors (Song et al., 1996; Chin et al., 1998; Hurst et al., 2002).

Overall, the key residues for diverse classes of ligands discussed above suggest that although there is an overlap in the motifs for binding ligands to CB_1, each class of ligands shows some unique interactions with CB_1 which may dictate the functional selectivity seen with these ligands.

1.13 Mechanism of Activation of CB_1 Receptor: inactive to active state transition

Modeling and mutagenesis studies have helped to determine the multi-step activation of the CB_1 receptor with agonists such as CP55,940 as shown in Figure 1.12. The ligand CP55,940 interacts with the residues $F268^{E2}$, $P269^{E2}$, $H270^{E2}$, $I271^{E2}$, $Y275^{5.29}$ and $C355^{6.47}$. Aromatic interactions are formed between F268 and Y275 with the aromatic ring of the ligand. The C3 side chain of CP55,940 embeds deep in the core.

The residue $W356^{6.48}$, which is a part of the rotamer toggle switch, has been shown by

homology models to be molecularly constrained by aromatic stacking interactions with F200$^{3.36}$ and F170$^{2.57}$ and an extensive H-bond network formed by residues C355$^{6.47}$, L359$^{6.51}$, C383$^{7.38}$ and C386$^{7.42}$. This extensive network of H-bonds is broken by the interaction of the hydrophobic C3 chain of CP55,940 with L359$^{6.51}$. This causes interference with the CWxP motif and the W356$^{6.48}$ is freed from the molecular constraints to rotate. Coupling movements of TM5 and TM7 by ligand binding allows rotation of TM6. Due to this, the C355$^{6.47}$ residue whose side chains are embedded in the core in inactive CB_1 is now exposed and accessible to CP55,940. The activation switch for breaking ionic locks in GPCRs involves N389$^{7.45}$ and D163$^{2.50}$. The hydrogen bond between N389 and D163 breaks when the TM6 moves outwards. This causes N389 to come in contact with TM6. Also upon receptor activation, Y294$^{5.58}$ and Y397$^{7.52}$ come closer and contribute to breaking the ionic lock (Shim et al., 2009; Shim et al., 2010).

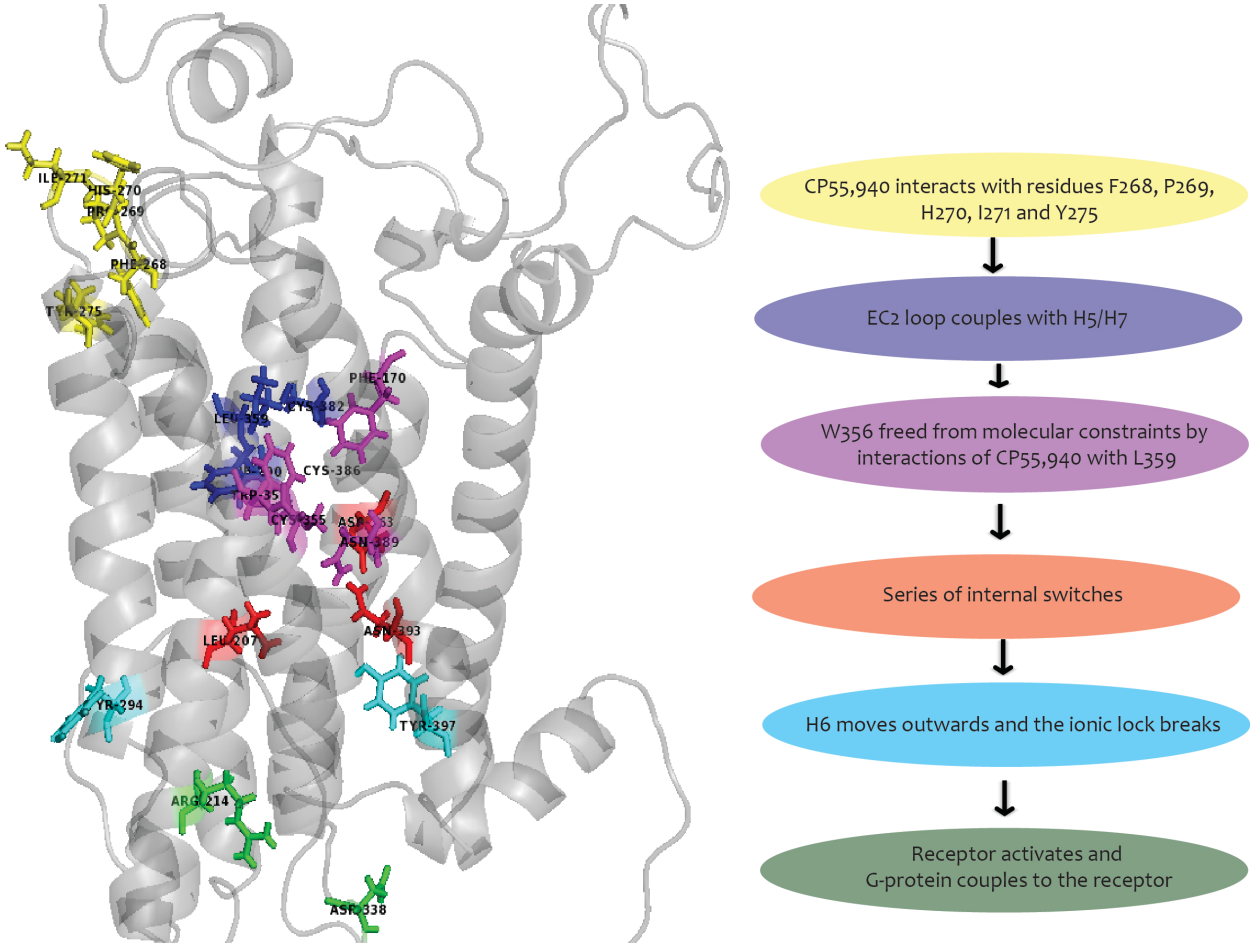

Figure 1.12 Schematic representation of the series of steps of activation of CB_1 receptor upon binding of CP55,940. Based on an inactive model of CB_1 (Shim et al., 2010), activation of CB_1 receptor to generate G-protein signaling involves a sequence of changes at molecular level to transfer signal from extracellular to intracellular side. These include binding of ligand (as shown in yellow) which causes coupling of EC2 loop to TM5/TM7 (as shown in purple). The residue $W356^{6.48}$ of the proposed rotamer toggle switch moves to break the H-bond between $W356^{6.48}$ and $N389^{7.45}$ (as shown in pink). Interactions between $L207^{3.43}$ and $N393^{7.49}$ (as shown in orange) and interaction between $Y294^{5.58}$ and $Y397^{7.52}$ (as shown in cyan) occurs which act as the internal switches to allow breakage of the ionic lock between $R214^{3.50}$ and $D338^{6.30}$ (as

shown in green). As a result, rigid body movements occur in TM6 and TM7 which expands a crevice on the intracellular side and allows receptor activation. Modified from Shim et al., 2010. To generate the inactive state model, the software MODELLER was used.

1.14 Allosteric modulation of CB_1 receptor

Identification of several allosteric modulators of CB_1 have opened opportunities to develop subtype-specific modulators since most of the orthosteric ligands for CB_1 known so far bind non-specifically to both CB_1 and CB_2. Some of the known allosteric modulators for the CB_1 receptor include 5-chloro-3-ethyl-N-(4-(piperidin-1-yl)phenethyl)-1H-indole-2-carboxamide (ORG27569) (Price et al., 2005), 1-(4-chlorophenyl)-3-(3-(6-(pyrrolidin-1-yl)pyridin-2-yl)phenyl)urea (PSNCBAM-1) (Horsewill et al., 2010) , 3-(4-chlorophenyl)-5-(8-methyl-3-p-tolyl-8-azabicyclo[3.2.1]octan-2-yl)isoxazole (RTI-371) (Navarro et al., 2009) and the endogenous ligand (5S,6R,9E,11Z,13E,15S)-5,6,15-trihydroxyicosa-9,11,13-trienoic acid (lipoxin A4) (Pamplona et al.,2012), which are positive allosteric modulators of CB_1. Negative allosteric modulation of the CB_1 receptor has been reported by a new family of peptide endocannabinoids (Pepcans) (Bauer et al., 2012).

ORG27569 is a prototypical allosteric modulator for CB_1 receptor. First developed and synthesized at Organon, UK, the pharmacological profile of this compound is interesting. It increases the binding affinity of CP55,940, an orthosteric agonist of CB_1. However, it decreases CP55,940-induced G-protein coupling at CB_1 receptor (Price et al., 2005; Ahn et al. 2012). A similar trend is seen with PSNCBAM-1. Thus, although these compounds are positive allosteric modulators of CP55,940 binding, they are antagonists for G-protein coupling. Previously, the Kendall lab showed that ORG27569 binding to the CB_1 receptor induces ERK1/2

phosphorylation in a G_i protein-independent manner. Yet, they showed that it acts as a positive allosteric modulator for signaling mediated by β-arrestin-1. It was further demonstrated that ORG27569 activates the receptor and enhances its affinity for CP55,940 (Ahn et al., 2012).

Not only do the allosteric modulators of CB_1 show pathway specificity, they also exhibit probe dependence. A group of researchers evaluated the impact of ORG27569 and PSNCBAM-1 on different pathways with three classes of orthosteric agonists i.e. CP55,940 (classical cannabinoids), WIN55,212-2 (aminoalkylindoles) and anandamide (endocannabinoids) (Baillie et al., 2013). In GTPγS assays in mouse brain membranes, both ORG27569 and PSNCBAM-1 displayed a concentration-dependent decrease in E_{max} of induced G-protein coupling by CP55,940, WIN55,212-2 and anandamide. However, a lesser reduction in GTPγS levels was seen with WIN55,212-2-induced G-protein coupling than those with CP55,940 and anandamide. The effect of ORG27569 on CB_1 agonist-mediated inhibition of forskolin-stimulated cAMP production was measured in cell membranes epressing hCB_1R. ORG27569 reduced the inhibition of CP55,940-mediated inhibition of foreskolin-stimulated cAMP production with the signaling completely abolished at 10 nM ORG27569. However, it was less effective in reducing WIN55,212-2-mediated inhibition of foreskolin-stimulated cAMP production. In contrast to the inhibitory effects, ORG27569 increases the ERK1/2 phosphorylation levels induced by CP55,940. No significant effect was seen on WIN55,212-2 mediated ERK1/2 phosphorylation levels. This clearly demonstrates the probe dependence exhibited by ORG27569. (Baillie et al., 2013).

1.15 Therapeutic potential of CB_1 receptor

Three cannabinoid ligands are commercially available which are Sativex, Cisamet and Marinol. All three are cannabis-based therapeutics with Δ^9-THC as the active ingredient. Marinol and Cesamet are approved for nausea and vomiting in cancer and AIDS patients and Sativex is approved for treatment of neuropathic pain and plasticity in patients with Multiple Sclerosis. However, other than the conditions stated above, cannabinoid receptors have been implicated to have therapeutic potential for treatment of many disorders.

The cannabinoid-based therapeutics that have received most attention are the antagonists and inverse agonists of CB_1, primarily as anti-obesity drugs. CB_1 receptors, when activated promote expression of fatty-acid synthase in hepatocytes and hypothalamus (Osei-Hyiaman et al., 2005) and activity of lipoprotein lipase in adipocytes (Cota et al., 2003). Thus, CB_1 receptors regulate energy balance both centrally and peripherally. CB_1 antagonists and inverse agonists, in preclinical studies have demonstrated a decrease in food consumption and long-term efficacy in weight loss (Black et al., 2004). Apart from weight loss, CB_1 antagonists and inverse agonists demonstrate improved lipid metabolism through peripheral mechanisms. Thus, these compounds show promise for developing anti-obesity drugs. Rimonabant (Acomplia) or SR141716A, an inverse agonist for CB_1 was commercially available as anti-obesity drug but was withdrawn from the market due to psychiatric issues. As a result, CB_1 antagonists primarily acting through peripheral mechanisms have been a focus of intense research in the past (Mackie et al., 2005).

Another area of application of CB_1 antagonists is in treatment of 'craving disorders". CB_1 receptor activation has also been associated with the reward behavior that is seen with opioids. In

rats treated with heroin, treatment with CB_1 antagonists decrease reinstatement (Solinas et al., 2003). In CB_1 knockout-mice, the rewarding properties of opioids are attenuated. Apart from the therapeutic role in opioid abuse, another potential therapeutic application of CB_1 antagonism is for alcohol abuse. Blocking CB_1 receptors via antagonists have shown to reduce alcohol consumption. CB_1 receptors are also being investigated as a promising target for other drugs of abuse such as nicotine and in smoking cessation (Mackie et al., 2005).

Another therapeutic area of intense interest for CB_1 agonists has been antinociception especially in treatment of inflammatory and neuropathic pain. The CB_1 receptor is densely expressed in brain regions involved in perception and modulation of nociceptive information such as thalamus, amygdala, and midbrain periaqueductal grey matter and in the substantia nigrosa of spinal cord. Arachidonyl-2-chloroethylamide (ACEA), a selective agonist of the CB_1 receptor, has been shown to induce antinociceptive effects in rat models with inflammatory pain. The CB_1 receptor agonists such as HU-210, Δ^9-THC, *R*-(+)-WIN55,212-2 and anandamide show antinociceptive effects in animal models of acute thermal, anti-inflammatory and neuropathic pain. (Manzanares et al., 2006)

Other potential areas where ligands of CB_1 may be of therapeutic value include neurodegenerative disorders such as Parkinson's disease and Alzheimer's disease. In Alzheimer's disease, agonists such as WIN55,212-2, ACEA and CBD inhibit tau protein hyper-phosphorylation which is one of the main biomarkers for Alzheimer's disease pathology. This effect was mediated by CB_1 which causes down-regulation of inducible nitric oxide synthase (Aso et al., 2014).

CHAPTER 2

Indole-2-Carboxamides as Allosteric Modulators of the CB_1 Receptor

This is an adaptation of an article that appeared in an ACS publication. ACS has not endorsed the content of this adaptation or the context of its use. Part of this chapter has been incorporated from published material (Khurana, L., Ali, H.I., Olszewska, T., Ahn, K. H., Damaraju, A., Kendall, D.A., Lu, D. "Optimization of Chemical Functionalities of Indole-2-Carboxamides to Improve Allosteric Parameters of the Cannabinoid Receptor 1 (CB_1)." Journal of Medicinal Chemistry 57(7) (2014): 3040-3052 (http://pubs.acs.org/doi/full/10.1021/jm5000112). Compound syntheses was done by collaborators from Dr. Dai Lu's lab at Texas, A&M.

2.1 Background

This chapter describes the optimization of indole-2-carboxamides to generate analogs with improved allosteric parameters at the CB_1 receptor. The compounds were synthesized to evaluate the impact of modifying chemical functionalities of the indole-2-carboxamide scaffold on parameters that define the affinity for binding to the receptor and efficacy of allosteric modulation at the receptor. Cannabinoid agonists have been a subject of intense research to develop therapeutics in many diseases that the CB_1 receptor is involved. For example, Δ^9-THC has been demonstrated to be an effective antinociceptive agent in animal models of neurodegenerative and inflammatory disease states (Guindon et al., 2009; Pryce et al., 2012; Fagan et al., 2014). However, due to the global activation of CB_1 receptors in the brain and periphery by these ligands, these agonists pose side effects such as substance abuse, dependence

and impaired memory (Justinova et al, 2003; Cooper et al., 2009). However, endogenous ligands are synthesized on demand and metabolize easily and thus may have lesser side effects (Dimarzo et al., 1999; Ignatowska-Jankowska et al., 2015). PAMs of the CB_1 receptor, thus offer the potential to alter the endogenous signaling without generating the side effects posed by other cannabinoid-based therapeutics. Here, we have identified some PAMs of CB_1 receptor. These allosteric modulators demonstrated biased agonism for β-arrestin 1 mediated pathways. Thus, these allosteric modulators hold promise to develop therapeutics which are not only subtype-specific but also pathway specific.

2.2 Introduction

The CB_1 receptor is the most abundant GPCR expressed in the CNS (CNS), where it attenuates the release of excitatory and inhibitory neurotransmitters (Howlett et al., 2004; Mackie et al., 2008; Mackie et al., 2008). The CB_1 receptor is also present in lower concentrations in a variety of peripheral tissues, including, spleen, tonsil, gastrointestinal tract, liver, kidney, and heart (Gerard et al., 1991; Straiker et al., 1999; Galiegue et al., 1995). It regulates a variety of physiological functions including neuronal development, neuromodulatory processes, metabolism, nociception, and cardiovascular as well as reproductive functions (Howlett et al., 2004; Pertwee et al., 2006; Mackie et al., 2006). While CB_1 preferentially couples to $G_{i/o}$ type G proteins, it can interact with G_s (Glass et al., 1997) or G_q (Lauckner et al., 2005) under some conditions. The CB_1 receptor also modulates the activation of mitogen-activated protein kinases (MAPKs) (Turu et al., 2010), inhibits N- and P/Q-type voltage-gated Ca2+ channels, activates A-type and inwardly rectifying K+ channels (Howlett et al., 2005). Moreover, the CB_1 receptor can interact with non-G protein partners such as β-arrestins, adaptor protein AP-3, GPCR-associated

sorting protein 1 (GASP1) and the adaptor protein FAN to control receptor signaling or trafficking (Howlett et al., 2010; Smith et al., 2010). The complex signaling network of the CB_1 receptor suggests the existence of finely-controlled modulatory mechanisms of receptor functions.

Traditionally, the functions of the CB_1 receptor is regulated through various agonists, partial agonists, antagonists and inverse agonists (Pertwee et al., 2006), which bind to the orthosteric site where the endogenous cannabinoids bind. Recently, several allosteric modulators of the CB_1 receptor have been identified, which bind to sites that are topologically distinct from the orthosteric binding site. These include 5-chloro-3-ethyl-N-(4-(piperidin-1-yl)phenethyl)-1H-indole-2-carboxamide (1, ORG27569) (Price et al., 2005), 1-(4-chlorophenyl)-3-(3-(6-(pyrrolidin-1-yl)pyridin-2-yl)phenyl)urea (PSNCBAM-1) (Horsewill et al., 2007), 3-(4-chlorophenyl)-5-(8-methyl-3-p-tolyl-8-azabicyclo[3.2.1]octan-2-yl)isoxazole (RTI-371) (Navarro et al., 2009) and the endogenous ligand (5S,6R,9E,11Z,13E,15S)-5,6,15-trihydroxyicosa-9,11,13-trienoic acid (lipoxin A4) (Pamplona et al., 2012). Allosteric modulators typically work cooperatively with orthosteric ligands and stabilize the receptor in various biological conformations that may be difficult to achieve by the orthosteric ligands (Wang et al., 2013). This increases the possibility of regulating receptor activities in more sophisticated ways than with orthosteric ligands. Thus, allosteric modulation can significantly expand the pharmacological repertoire for a given receptor (Wootten et al., 2013; Gao et al., 2013). Additionally, allosteric sites are less structurally conserved than the corresponding orthosteric site and thus provide new opportunities for the development of more selective therapeutics (Mackie et al., 2006; Christopoulos et al., 2002). The discovery of CB_1 allosteric modulators lays the foundation for receptor-selective and signaling-pathway-selective therapies.

Compound **1** was the first allosteric modulator identified for the CB_1 receptor (Price et al., 2005). It augments specific binding of the CB_1 agonist 2-[(1R,2R,5R)-5-hydroxy-2-(3-hydroxypropyl) cyclohexyl]-5-(2-methyloctan-2-yl)phenol ([^{3}H]CP55,940) but decreases the binding of the inverse agonist 5-(4-Chlorophenyl)-1-(2,4-dichloro-phenyl)-4-methyl-N-(piperidin-1-yl)-1H-pyrazole-3-carboxamide ([^{3}H]SR141716A) in membranes from cells expressing the CB_1 receptor (Price et al., 2005; Ahn et al., 2012). Despite acting as an enhancer of agonist binding, it antagonizes agonist-induced G- protein coupling to the receptor (Price et al., 2005; Ahn et al., 2012). It was further demonstrated that **1** in the absence of any orthosteric agonist can induce cellular internalization of the CB_1 receptor and downstream activation of ERK signaling mediated by β-arrestins (Ahn et al., 2012; Ahn et al., 2013; Baillie et al., 2013), as a consequence of CB_1 receptor activation. This indicates that allosteric modulators of the CB_1 receptor offer the potential to develop drugs capable of generating therapeutic effects via ligand-biased signaling pathways.

Following the discovery of **1** (Price et al., 2005), structure activity relationship (SAR) studies have revealed that the indole-2-carboxamide scaffold is a viable template for developing CB_1 allosteric modulators (Ahn et al., 2013; Piscitelli et al., 2012; Mahmoud et al., 2013). The general structure of this class of compounds can be divided into two moieties comprising the bicyclic aryl fragment and the amide fragment (Figure 2.1).

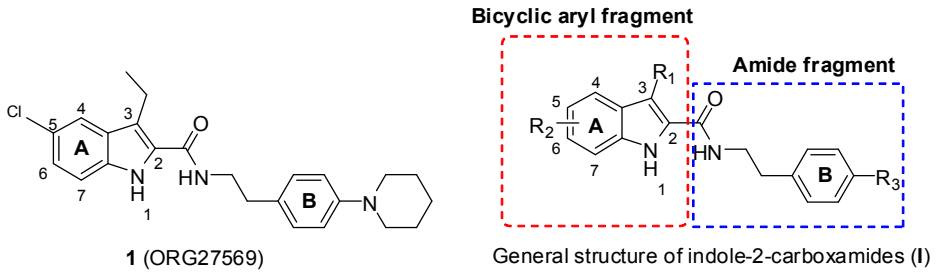

Figure 2.1 Compound 1 and general structure of indole-2-carboxamides.

Earlier results from us (Ahn et al., 2013; Mahmoud et al., 2013) and others (Piscitelli et al., 2012) have identified several key SARs within this class of compounds (**I**). These include 1) the indole ring of **I** (Figure 2.1) impacts the ligand's capability to bind to the allosteric site more than the ligand's capability to modulate the orthosteric site (Mahmoud et al., 2013); 2) the presence of a linear alkyl group at the C3 position of the indole ring is instrumental and its length has a profound influence on the allosteric modulation of the orthosteric binding site (Ahn et al., 2013; Mahmoud et al., 2013); 3) the amide functionality at the C2 position of the indole ring is critical for the allosteric effects on the orthosteric site (Piscitelli et al., 2012); 4) shortening the linker between the amide bond and the phenyl ring B abolished the allosteric modulation of the orthosteric binding site (Mahmoud et al., 2013); 5) replacing the piperizinyl group of **1** with various functional groups (Piscitelli et al., 2012; Mahmoud et al., 2013) generally led to reduced allosteric modulation except for the methylamino (Piscitelli et al., 2012) and dimethylamino groups (Piscitelli et al., 2012; Mahmoud et al., 2013). Along with **1**, a few other indole-2-carboxamides (Price et al., 2005; Ahn et al., 2013; Piscitelli et al., 2012) have also shown allosteric modulation of the CB_1 receptor. These molecules 5-chloro-3-pentyl-*N*-(4-(piperidin-1-yl)phenethyl)-1*H*-indole-2-carboxamide (**2**, ICAM-b) (Ahn et al., 2013), *N*-(4-(dimethylamino)phenethyl)-3-ethyl-5-fluoro-1*H*-indole-2-carboxamide (**3**, ORG27759) (Price et al., 2005), 5-chloro-*N*-(4-(dimethylamino)phenethyl)-3-ethyl-1*H*-indole-2-carboxamide (**4**)

(Piscitelli et al., 2012) and 5-chloro-*N*-(4-(dimethylamino)phenethyl)-3-pentyl-1*H*-indole-2-carboxamide (**5**) (Mahmoud et al., 2013) are shown in Figure 2.2. K_B and α values for some of these compounds is shown in Table 2.1.

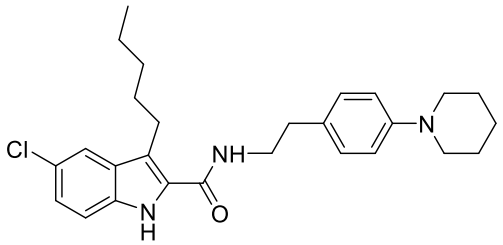

2

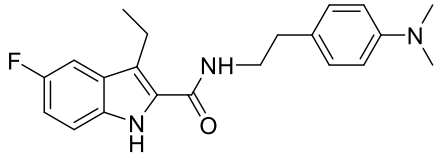

3

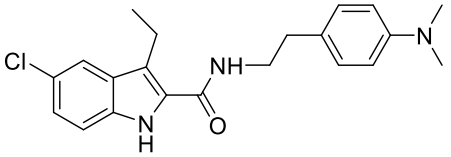

4

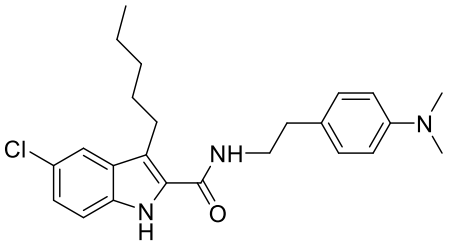

5

Figure 2.2 Representative indole-2-carboxamides showing CB_1 allostery.

In this context, we expanded our SAR studies of indole-2-carboxamides. Our efforts include elongation of the linker between the amide bond and the phenyl ring B, further investigation of the requirement of the C3 alkyl group (i.e. R_1) and modification of the

substitutions (i.e. R_2) on the phenyl ring A of the bicyclic aryl fragment. To date, most of the reported indole-2-caboxamides showing CB_1 allostery was developed from a 5-chloro-indole-2-carboxamide template (Price et al., 2005; Ahn et al., 2013; Piscitelli et al., 2012; Mahmoud et al., 2013) except **3** (Price et al., 2005). Hence, we investigated the impact of different substitutions of the phenyl ring A (Figure 2.1) on the allosteric effects. This effort led to the compounds **21a-d** (Table 2). The allosteric effects of these compounds are evaluated by two essential parameters (Christopoulos et al., 2002; May et al., 2007): the equilibrium dissociation constant (K_B), which reflects the binding affinity of the ligands to the allosteric site, and the binding cooperativity factor (α) that denotes the allosteric interaction between the orthosteric and allosteric ligands when they both occupy the receptor, i.e. it quantifies the direction of and magnitude by which the affinity of one ligand is changed by the other ligand when both are bound to the receptor to form the ternary complex (Christopoulos et al., 2004). When α is 1.0, the test modulator does not alter orthosteric ligand binding. If α is less than 1.0, the test modulator reduces orthosteric ligand binding (negative allosteric modulation of orthosteric ligand binding). If α is greater than 1.0, the modulator increases orthosteric ligand binding (positive allosteric modulation of orthosteric ligand binding) (Christopoulos et al., 2002). The α and K_B values were analyzed according to the allosteric ternary complex model (Price et al., 2005). Selected allosteric modulators were assessed for their effects on agonist-induced G-protein coupling activity and β-arrestin mediated ERK1/2 phosphorylation.

Chemistry

Dr Dai Lu's lab used the following procedures to carry out the chemical synthesis of compounds **12a-f**, **21a-d** and **26**:

The syntheses of C3-alkylated indole-2-carboxamides (**12a-f**) were achieved through the methods illustrated in Figure 2.3. The C3 substituents were introduced through Friedel-Crafts acylation of the ethyl 5-chloroindole-2-carboxylate (**6**), which is commercially available. Acylation of **6** with various selected acyl chlorides (**7a-c**) provided the desired 3-acyl-5-chloroindole-2-carboxylates (**8a-c**). Reduction of their ketone groups by triethylsilane generated the C3 alkylated 5-chloroindole-2-carboxylates (**9a-c**), which were then hydrolyzed in basic conditions to yield the key intermediate indole-2-carboxylic acids (**10a-c**). The final compounds (**12a-f**) were prepared by coupling commercially available amines (**11a-b**) with the acids (**10a-c**) individually in the presence of BOP and diisopropylethyl amine (DIPEA) in anhydrous DMF at room temperature.

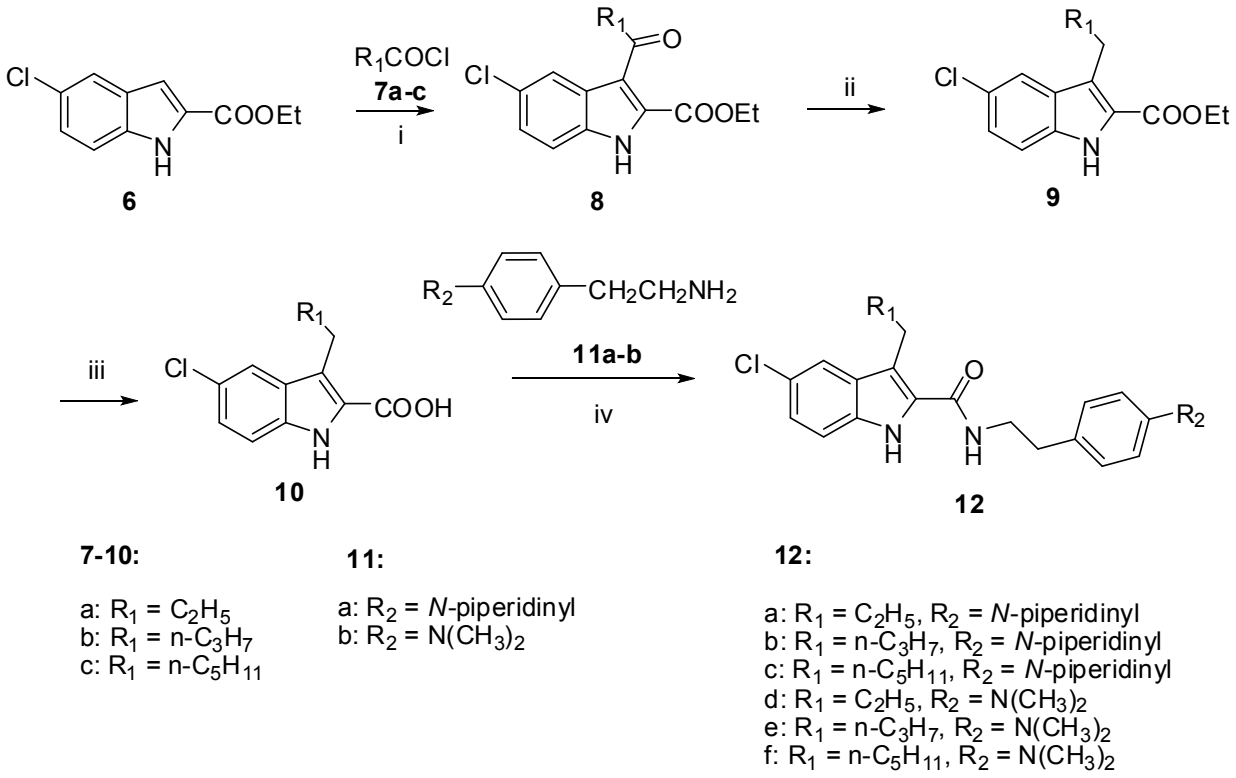

Figure 2.3 Synthesis of 3-alkyl-5-chloroindole-2-carboxamides **12a-f**. *Reagents and Conditions*: (i) $AlCl_3$, 1,2-dichloromethane, reflux, 2-3 h; (ii) $(Et)_3SiH$, CF_3COOH, 0°C-rt, 4-12 h; (iii) 3N NaOH, EtOH, reflux, 2 h; (iv) BOP, DIPEA, DMF, rt, 4-12 h.

To access the indole-2-carboxamides with different substituents on the phenyl ring A (**21a-d**), we employed Hemetsberger-Knittel indole synthesis (Hemetsberger et al., 1972), by which the required indole-2-carboxylate **17** can be obtained through Knoevenagel condensation of methyl 2-azidoacetate **14** with the substituted benzaldehyde **15** followed by a thermolysis of the azide of the resultant methyl-2-azidocinnamate **16** and an electrophilic cyclization. The synthesis of indole-2-carboxylate **17** through Hemetsberger-Knittel reaction depends on the reaction conditions, which include the reaction temperature and stoichiometry of reactants in the Knoevenagel condensation (step ii, Figure 2.4) and the concentration of reactant in the

subsequent thermolytic cyclization (step iii, Figure 2.4). We optimized the reaction conditions to obtain **16** and **17** in good yield to proceed with the synthesis . The cyclization of **16d** provided two regioisomers the 5- and 7-substituted indole-2-carboxylates (**17d** and **17e**) with the 5-regioisomer (**17d**) being slightly favored over the 7-regioisomer (**17e**). The structures of the two regioisomers were assigned by comparison of their ^{1}H NMR with the reported data (Yamazaki et al., 2003; Vieira et al., 2008). Acylation of **17a-17d** by Friedel-crafts reaction led to the major product as the desired 3-acyl-indol-2-carboxylates **18a-18d**. However, acylation of **17e** generated the 4-acyl-indole-2-carboxamide as the major product, which is not suitable for SAR study in this series; hence, the 4-acylated product was not further pursued in the synthesis of corresponding indole-2-carboxamide **21.** Following the preparation of 3-acylated indole-2-carboxylates **18a-18d,** we synthesized the corresponding final products **21a-21d** by following Figure 2.3 (steps i-iv).

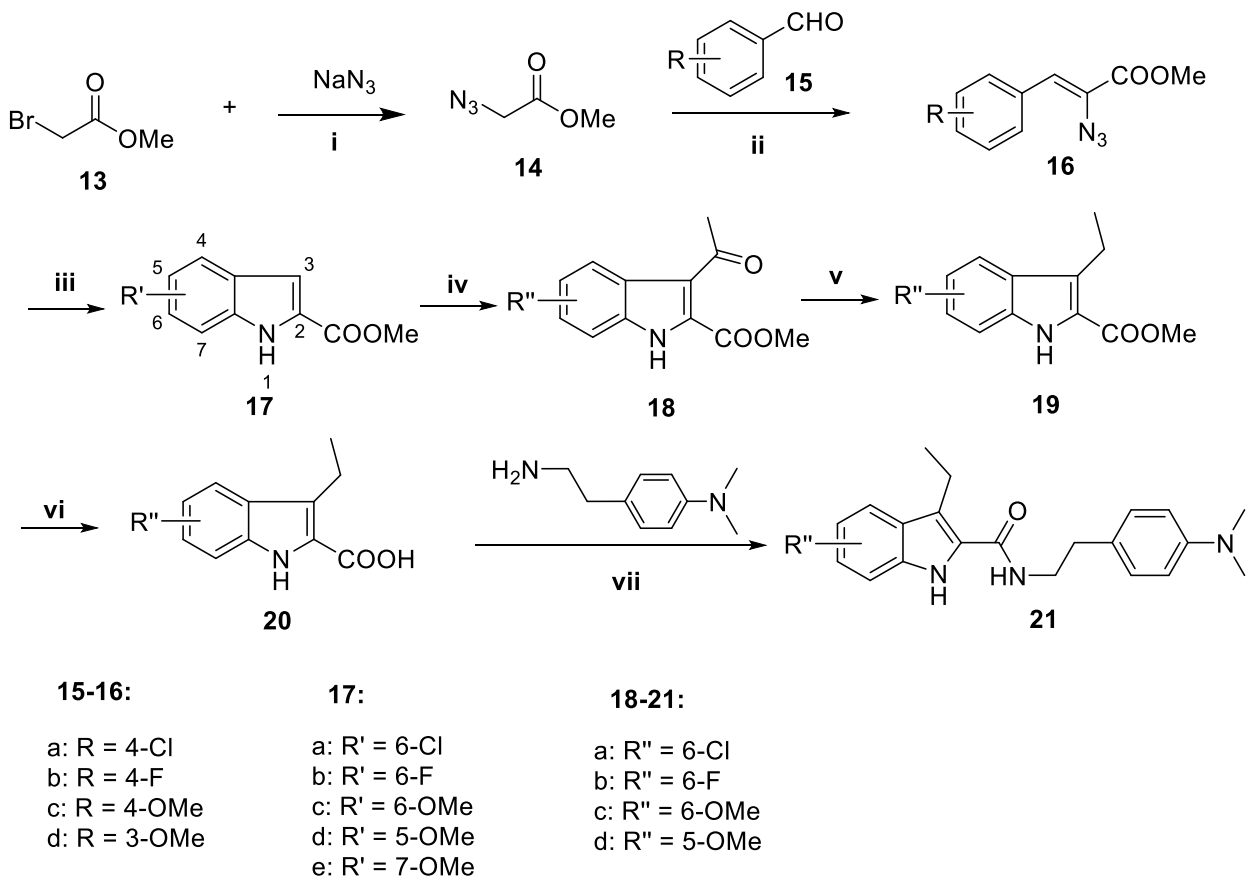

Figure 2.4 Synthesis of 3-ethyl indole-2-carboxamides **21a-d**. *Reagents and Conditions*: (i) NaN_3, DMF, rt, 1.5 h; (ii) $NaOCH_3/CH_3OH$, –20 °C, 5 h; (iii) xylene, reflux, 3 h; (iv) $AlCl_3$, 1,2-dichloromethane, reflux, 2.5 h; (v) $(Et)_3SiH$, CF_3COOH, 0 °C-rt, 4 h; (vi) 3 N NaOH, EtOH, reflux, 2 h; (vii) BOP, DIPEA, DMF, rt, 4-12 h.

The indole-2-carboxamide **26** was synthesized according to the route illustrated in Figure 2.5. It was prepared through coupling of 4-(3-aminopropyl)-*N*,*N*-dimethyl aniline **24** with 5-chloro-3-ethyl-1*H*-indole-2-carboxylic acid **25**, which was synthesized according to the reported method (Mahmoud et al., 2013). For the synthesis of **24,** 4-dimethylaminobenzaldehyde **22** was condensed with acetonitrile through aldol condensation in strong basic conditions to yield a

mixture of (*E*)- and (*Z*)-3-(4-(dimethylamino)phenyl)acrylonitrile **23** which was reduced to yield amine **24**.

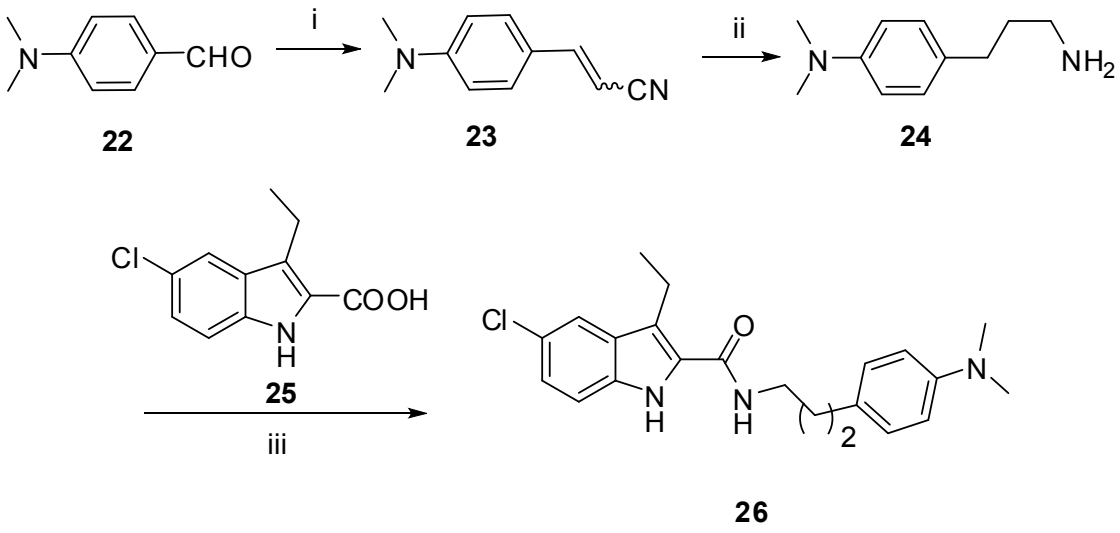

Figure 2.5 Synthesis of indole-2-carboxamide **26**. *Reagents and Conditions*: (i) CH_3CN, KOH, reflux, 10 min; (ii) THF, $LiAlH_4$, $AlCl_3$, reflux, 1 h; (iii) BOP, DIPEA, DMF, rt, 4-12 h.

2.3 Materials and Methods

Compounds. Tested compounds (**12a-12f** and **21a-21d)** were synthesized for this study except **1**, which was purchased from Tocris Bioscience (Minneapolis, MN). Compounds **2** (Ahn et al., 2013) and **12g**, **12h** and **5** have previously been reported by us (Mahmoud et al., 2013) and were cited in this report for comparison. Compound **4** was earlier reported (Piscitelli et al., 2012), and was resynthesized and tested in our laboratories for comparative purposes.

CB_1 Expression and membrane preparation. HEK 293 cells were maintained in Dulbecco's modified Eagle's medium supplemented with 10% fetal bovine serum and 3.5% mg/ml glucose at 37ºC in 5% CO2. One day prior to transfection, cells were seeded at approximately 900,000

cells/100 mm dishes. The cells were transiently transfected by the calcium phosphate precipitation method (Chen et al., 1987). At 24h post transfection, the cells were harvested and washed twice with phosphate buffered saline (PBS). The cells were resuspended in PBS solution containing mammalian protease inhibitor cocktail ((4-2-aminoethyl) benzene-sulfonyl fluoride, pepstatin A, E-64, bestatin, leupeptin, and aprotinin) (Sigma-Aldrich, St. Louis, MO) and lysed by nitrogen cavitation at 750 psi for 5 min using a Parr cell disruption bomb. The lysate was spun at 500 g for 10 min at 4ºC and the supernatant was subsequently spun at 100,000 g for 45 min at 4ºC. The membrane-containing pellet was resuspended in TME buffer (25 mM Tris-HCl, 5 mM $MgCl_2$, and 1 mM EDTA, pH 7.4) containing 7% w/v sucrose. For immunoblotting studies, HEK 293 cells were transfected using lipofectamine (Invitrogen, Carlsbad, CA) according to the manufacturer's instructions. 24 hr post-transfection, cells were washed and incubated for an additional 18 h in serum-free growth media. siRNA transfection was carried out as previously described (Ahn et al., 2013). Briefly, HEK293 cells in a 6-well plate were transfected with the plasmid encoding CB_1 and 2.6 micrograms of siRNA (Qiagen, Valencia, CA) targeting β-arrestin 1 or non-silencing RNA duplex for control.

Radioligand binding assay. Ligand binding assays were performed as previously described to determine the cooperativity between the orthosteric and allosteric ligands (Ahn et al., 2012). Briefly, 6μg of membrane preparation was incubated for 60 min with a fixed concentration of tracer [^{3}H]CP55940 (141 Ci/mmol, PerkinElmer Life Sciences (Boston, MA)) typically at its K_d which was determined from a saturation binding isotherm in a total volume of 200 μL of TME buffer containing 0.1% fatty acid-free BSA. Ligand depletion was avoided by adjusting the amount of membrane sample and total assay volume to keep the bound ligand less than 10% of the total. At least nine concentrations of unlabeled test compound (ranging between 100 pM and

100 μM) were used for the binding assays as described previously (Ahn et al., 2012). Nonspecific binding was determined in the presence of unlabeled CP55,940 (1 μM). The reaction was terminated by addition of 250 μL TME buffer containing 5% BSA followed by filtration with a Brandel cell harvester through Whatman GF/C filter paper followed by washing with ice cold TME buffer. Radioactivity was measured using liquid scintillation counting.

GTPγS Binding Assay. GTPγS binding assays were performed as described previously (Ahn et al., 2012). Briefly, 7.5 μg of membranes were incubated for 60 min at 30°C in a total volume of 200 μL GTPγS binding assay buffer (50 mM Tris-HCl, pH 7.4, 3 mM $MgCl_2$, 0.2 mM EGTA, and 100 mM NaCl) with unlabeled CP55,940 (at least nine different concentrations were used ranging between 100 pM and 100 μM), 0.1 nM [^{35}S]GTPγS (1250 Ci/mmol; PerkinElmer Life Sciences, Boston, MA), 10 μM GDP (Sigma, St. Louis, MO), and 0.1% (w/v) BSA in the absence and presence of varying concentrations of the allosteric compounds as indicated. Nonspecific binding was determined with 10 μM unlabeled GTPγS (Sigma, St. Louis, MO). The reaction was terminated by rapid filtration through Whatman GF/C filters. The radioactivity trapped in the filters was determined by liquid scintillation counting.

Ligand and GTPγS Binding Data Analysis. All ligand binding assays were carried out in duplicate. Data are presented as the mean ± S.E. or the mean with the corresponding 95% confidence limits from at least three independent experiments. The interactions between the orthosteric radiolabeled agonist [^{3}H]CP55,940 and the test modulators were analyzed by nonlinear regression using Prism 6.0 (Graphpad Software Inc., San Diego, CA) as previously described (Ahn et al., 2012).

Immunoblotting Studies. Cells expressing the CB_1 receptor and siRNA targeting β-arrestin 1 or non-silencing RNA duplex were washed twice with PBS and exposed to varying concentrations of allosteric modulators (**2**, **12d** or **12f**) in the presence of 0.2 μM CP55,940 for 5 min. To observe the effect of the modulators on pertussis toxin (PTX)-insensitive ERK1/2 phosphorylation, cells were treated with 5 ng/ml PTX for 16 h at 37 °C prior to compound treatment. The media were aspirated and the cells were washed with ice-cold PBS and lysed in ice-cold lysis buffer (150 mM NaCl, 1.0% IGEPAL® CA-630, 0.5% sodium deoxycholate, 0.1% SDS, 50 mM Tris, pH 7.5) and a protease inhibitor cocktail (4-(2-aminoethyl)benzenesulfonyl fluoride (AEBSF), pepstatin A, E-64, bestatin, leupeptin, and aprotinin; Sigma, St Louis, MO). Solubilized cell extracts were centrifuged at 18,500 g for 15 min at 4 °C and the supernatant was transferred to a new tube and heated at 95°C for 3 minutes. 12 μg of total protein was resolved by 10% SDS-PAGE, and transferred to polyvinylidene fluoride (PVDF) membrane. After washing with blocking reagent (Fisher Scientific, Pittsburgh, PA), the membrane was incubated for 1h at rt with the primary antibody (1:3000 phospho-p44/42 and p44/42 antibodies; Cell Signaling Technology, Danvers, MA). After washing with PBS, the membrane was incubated with anti-rabbit peroxidase-conjugated secondary antibody (1:5000; Cell Signaling Technology, Danvers, MA) for 60 min at rt. Immunoreactivity was visualized and quantified as reported earlier (Ahn et al., 2013).

Synthesis. All chemical reagents and solvents were purchased from Sigma-Aldrich Chemical Company unless specified otherwise and used without further purification. All anhydrous reactions were performed under a static argon atmosphere in dried glassware using anhydrous solvents. Organic phases in the work up were dried over anhydrous Na_2SO_4, and removed by evaporation under reduced pressure. The crude compounds were purified by a Combiflash *Rf*

chromatography system (Teledyne Technologies, Inc, Thousand Oaks, CA) unless specified otherwise. Purities of the intermediates were established by Thin-layer Chromatography (TLC), melting point, ^{1}H NMR, and mass spectrometry. Analytical Thin-layer Chromatography (TLC) was run on pre-coated silica gel TLC aluminum plates (Whatman®, UV_{254}, layer thickness 250 μm), and the chromatograms were visualized under ultraviolet (UV) light. Melting points were determined on a capillary Electrothermal® melting point apparatus and are uncorrected. ^{1}H NMR spectra of intermediates were recorded on a Bruker Avance DPX-300 spectrometer operating at 300 MHz. ^{1}H NMR spectra of the final compounds were recorded on a Bruker AV-500 spectrometer operating at 500 MHz. All NMR spectra were recorded using $CDCl_3$ or DMSO-d_6 as solvent unless otherwise stated and chemical shifts are reported in ppm (parts per million) relative to tetramethylsilane (TMS) as an internal standard. Multiplicities are indicated as br (broadened), s (singlet), d (doublet), t (triplet), q (quartet), m (multiplet), bs (broadened singlet) and coupling constants (J) are reported in hertz (Hz). Low resolution mass spectra were performed at the School of Chemical Sciences, University of Illinois at Urbana-Champaign. The purity of each tested compound was analyzed by combustion elemental analysis and was confirmed to be greater than 99%. (Roberson Microlit laboratories, Madison, NJ).

The hemesberger-knittel reaction. The hemesberger-knittel reaction (step ii and iii, Figure 2.4) is postulated to proceed via a highly electrophilic singlet nitrene species, which then inserts into the phenyl ring to form the indole derivatives (Hemetsberger et al., 1972; Hemetsberger et al., 1969; O'Brien et al., 2011). In some circumstances, the Knoevenagel condensation (step ii, Figure 2.4) requires highly excessive quantities of the reactant azidoacetate and the catalytic base (e.g. benzaldehyde:azidoacetate:methoxide = 1:10:10 molar ratio) to achieve high yields (Condie et al., 2005). We tried different stoichiometries of the reactants in the condensation of **14** with **15**

and found when the molar ratio of reactants (benzaldehyde:azidoacetate:methoxide) is 1:3:3, it provided an acceptable yield ranging from 58% to 74% for the products **16a-d**. When the molar ratio of reactants used was benzaldehyde:azidoacetate:methoxide = 1:10:10, the yields for **16a** and **16b** were increased from 59% and 58% to 93% (**16a**) and 69.6% (**16b**), respectively. Additionally, the yield of the 2-azidocinnamate from the Knoevenagel condensation also depends on the reaction temperature (Murakami et al., 1997). We found that optimal yields can be obtained when the reaction was firstly carried out at -20°C for 30 minutes and then at -5-0°C for 6-19 h (depending on the benzaldehyde employed). To obtain the indole-2-carboxylates **17** via thermolytic cyclization of **16** (step iii, Figure 2.4), there are many thermolysis conditions reported, which include carrying the reaction with microwave and flow chemistry facilitated thermolytic cyclization (Lehmanna et al., 2009; O'Brien et al., 2011; Ranasinghe et al., 2013), and employment of various catalysts to facilitate the indole ring formation (Stokes et al., 2007; Bonnamour et al., 2011). We tried various conditions including carrying the thermolytic reaction in different solvents such as regular xylene, anhydrous xylene, anhydrous toluene, and anhydrous THF heated in a pressure tube, as well as using iron (II) triflate to catalyze the reaction in THF (Bonnamour et al., 2011). We found that carrying the reaction in dilute and freshly prepared anhydrous xylene solution (i.e. 1 g of azidocinnamate 16 in ~100 mL xylene, approximately 40 mM) for 30 minutes generally led to good yield of the products (88.6-94.6%) except **17b** (53%). Specific details of synthesis of each compound can be found in the original publication.

2.4 Results and Discussion

Our previous investigations revealed that structural variation at the C3 position of indole-2-carboxamide has a profound influence on CB_1 allostery. We found that the C3 position prefers a linear alkyl group (Mahmoud et al., 2013). When the C3 ethyl group of **1** was replaced with a

n-pentyl group (**2**), it led to the enhancement of the allosteric effect, which is reflected by an improvement in the cooperativity factor α from 6.9 (**1**) to 17.6 (**2**) (Ahn et al., 2013). However, further increasing the length of the C3 alkyl to *n*-heptyl (**12g (LDK1218)**) and *n*-nonyl (**12h (LDK1219)**) groups did not improve the allosteric effects on CB_1 (Mahmoud et al., 2013). Here, we elaborated our investigation of the C3 position with variations of the linear alkyl groups such as *n*-propyl, *n*-butyl and *n*-hexyl groups. The allosteric parameters of the analogs are presented in Table 2.1. The results reflect that a specific length of the linear alkyl group is required at the C3 position. Increasing the length of the C3 alkyl group of **1** to *n*-propyl (**12a** (**LDK1259**)), *n*-butyl (**12b** (**LDK1260**)) and *n*-pentyl (**2**) led to the significant enhancement of binding cooperativity (α). When the length was further elongated to *n*-hexyl (**12c** (**LDK1261**)), *n*-heptyl (**12g** (**LDK1218)**) and *n*-nonyl (**12h** (**LDK1219**)), the binding cooperativity (α) decreased to a level comparable to **1**. Notably, the significant increase of the binding cooperativity factor (α) of **12a** (**LDK1259**) and **12b** (**LDK1260**) was accompanied by reduced binding affinities to the allosteric site. This reflects that an allosteric modulator can induce a receptor conformation that enhances orthosteric ligand binding despite having a relatively low affinity for the allosteric site. As has been shown previously, the affinity of an allosteric modulator (K_B) and the allostery (α) it exhibits for the orthosteric compound are not necessarily correlated (Christopoulos et al., 1999; May et al., 2005). In this series of modifications (entry 1-7, Table 2.1), the C3 *n*-propyl provided markedly enhanced allosteric modulation of the orthosteric site (binding cooperativity factor α = 26.7). We further assessed the effects of the length of C3 alkyl chain on allosteric properties using **4** as a scaffold because replacing the *N*-piperidinyl group of **1** with a dimethylamino group resulted in improvement of the allosteric effects of indole-2-carboxamides (Piscitelli et al., 2012; Mahmoud et al., 2013). This effort led to the analogs **12d-f** with improved allosteric parameters.

The results suggest that the dimethylamino group on the phenyl ring B is superior to the *N*-piperidinyl group of the indole-2-carboxamides yielding modulators with higher binding affinity for the allosteric site and greater cooperativity to the orthosteric site (e.g. **12d** (**LDK1256**) *vs* **12a** (**LDK1259**), **12e** (**LDK1257**) *vs* **12b** (**LDK1260**), **5** *vs* **2**, and **4** *vs* **1,** Table 2.1). Strikingly, the *n*-hexyl substituent (**12f** (**LDK1258**)) improved the equilibrium dissociation constant (K_B) to 89.1 nM with an α comparable to **1**. Binding curves for compounds 12a-1f are shown in Figure 2.6.

Table 2.1 Allostery of indole-2-carboxamides **12a-f** and some referenced compounds.

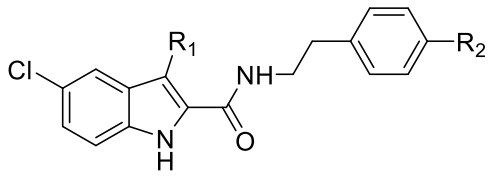

Entry	Compd	R^1	R_2	K_B (nM)[a]	α[b]
1	**1**[c]	C_2H_5	*N*-piperidinyl	217.3 (170.3-277.2)	6.9
2	**12a** (**LDK1259**)	n-C_3H_7	*N*-piperidinyl	1746 (377.8-8065)	26.7
3	**12b** (**LDK1260**)	n-C_4H_9	*N*-piperidinyl	1985 (775.1-5082)	17.7
4	**2**[d]	n-C_5H_{11}	*N*-piperidinyl	469.9 (126.2-1750)	17.6
5	**12c** (**LDK1261**)	n-C_6H_{13}	*N*-piperidinyl	310.6 (110.5-873.2)	4.6
6	**12g**[e] (**LDK1218**)	n-C_7H_{15}	*N*-piperidinyl	651.2 (81.51-5203)	7.4
7	**12h**[e] (**LDK1219**)	n-C_9H_{19}	*N*-piperidinyl	259.7 (87.56- 770)	6.8
8	**4**[e]	C_2H_5	$N(CH_3)_2$	207.4 (155.9-2759)	19.7
9	**12d** (**LDK1256**)	n-C_3H_7	$N(CH_3)_2$	259.3 (19.8-3365)	24.5
10	**12e** (**LDK1257**)	n-C_4H_9	$N(CH_3)_2$	209.0 (62.7--696.7)	12.8
11	**5**[e]	n-C_5H_{11}	$N(CH_3)_2$	167.3 (23.39-1197)	16.5
12	**12f** (**LDK1258**)	n-C_6H_{13}	$N(CH_3)_2$	89.1 (47.08-168.4)	5.1

[a]K_B: equilibrium dissociation constant of a potential allosteric ligand. [b]α: binding cooperativity factor for the tested allosteric modulator. Both parameters were tested using [^{3}H]CP55,940 as the orthosteric ligand. [c] Data cited for **1** are from our earlier report (Ahn et al., 2012) and are given for comparison. [d]Data cited for **2** are from our earlier report (Ahn et al., 2013) and are given for comparison. [e]Data cited for compounds **4**, **5**, **12g and 12h** (**LDK1219**) are from our earlier report (Mariam et al., 2013) and are given for comparison.

Table 2.2 Allostery of indole-2-carboxamides **21a-d** and **26**.

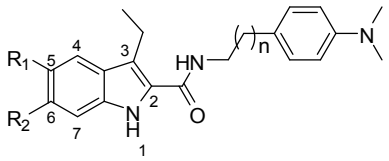

Entry	Compd	R_1	R_2	n	K_B (nM)[a]	α[b]
13	**4**[c]	Cl	H	1	207.4 (155.9-2759)	19.7
14	**21a** (**LDK1265**)	H	Cl	1	3673 (1048-12880)	16.0
15	**21b** (**LDK1266**)	H	F	1	1580 (328.7-7599)	22.9
16	**21c** (**LDK1269**)	OCH_3	H	1	2708 (973.4-7535)	6.2
17	**21d** (**LDK1264**)	H	OCH_3	1	4084 (1213-13750)	11.9
18	**26** (**LDK1257**)	Cl	H	2	ND[d]	ND[d]

[a]K_B: equilibrium dissociation constant of a potential allosteric ligand. [b]α: binding cooperativity factor for the tested allosteric modulator. Both parameters were tested using [^{3}H]CP55,940 as the orthosteric ligand. [c] Data cited for **4** are from our earlier report (Mariam et al., 2013) and are given for comparison. [d]ND: no detectable modulation of [^{3}H]CP55,940 binding using up to 32 μM of test compound.

The indole-2-caboxamide 4 (Piscitelli et al., 2012; Mahmoud et al., 2013) was used as a reference compound to vary the substitutions (Table 2.2) on the phenyl ring A (Figure 2.1). The

C5-chloro group of 4 is an electron withdrawing group (EWG) inductively and is electron donating by resonance. To evaluate the impact of the substitution position, we moved the C5-chloro group of 4 to the C6 position. This modification (**21a** (**LDK1265**)) drastically reduced the binding affinity to the allosteric site (K_B = 3673 nM), but not the allosteric modulation of the orthosteric ligand binding (α = 16.0). Because a fluoro group has a greater electron-withdrawing inductive effect than a chloro group, we replaced the C6-chloro group with a C6-fluoro group (**21b** (**LDK1266**)), this modification did not improve the binding affinity to the allosteric site (K_B = 1580 nM) while the allosteric modulation on orthosteric ligand binding is well preserved (α = 22.9) in comparison with 4 (α = 19.7). The result from **21b** (**LDK1266**) along with an earlier result of **3**, which is a 5-fluro-indole-2-carboxamide (Price et al., 2005), suggested that fluoro as a substituent on ring A is suboptimal than a chloro group. Taken the fact that chloro group is an EWG inductively and is electron donating group (EDG) by resonance, we replaced it with a methoxy group, which is purely an EDG. This modification led to **21c** (**LDK1269**), which exhibited a significantly decreased cooperativity factor (α = 6.2) and the binding affinity (K_B = 2708 nM) in comparison with **4** (α = 19.7, K_B = 207.4 nM). Moving the methoxy group to the C6-position (**21d** (**LDK1264**)) also reduced the allosteric effect on the orthosteric site and the binding affinity to the allosteric site. This series of compounds (entry 13-17) suggested that the nature and the position of the substituent on the phenyl ring A are critical for both the binding affinity (K_B) to the allosteric site and the binding cooperativity with the orthosteric site. Binding curves for the compounds 21a-21d and 26 are shown in Figure 2.7.

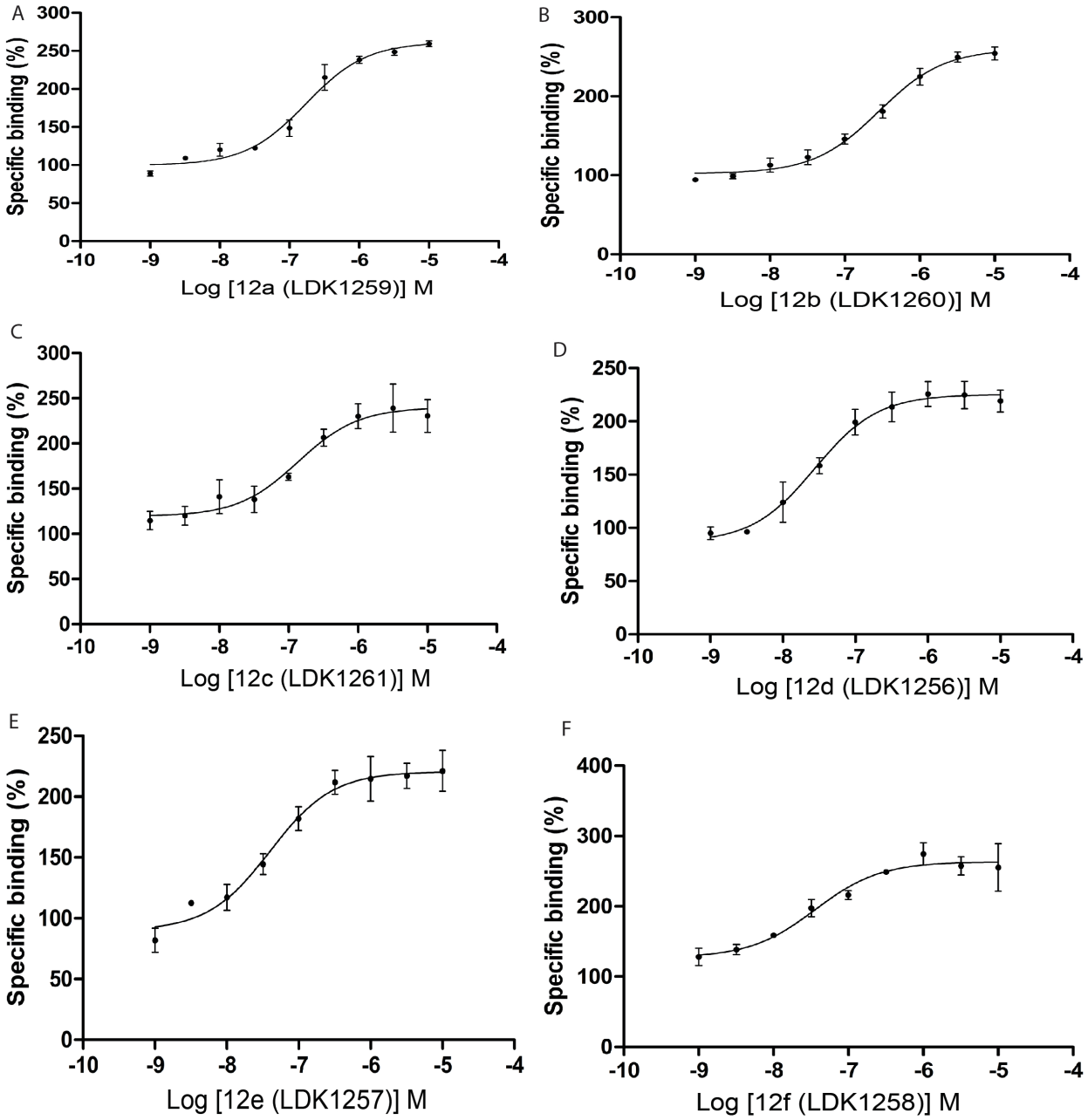

Figure 2.6 Binding curves for analogs 12a-12f. The binding curves show the impact of varying concentrations of test compounds 12a (A), 12b (B), 12c (C), 12d (D), 12e (E) and 12f (F) on the binding of [^{3}H]CP55,940.

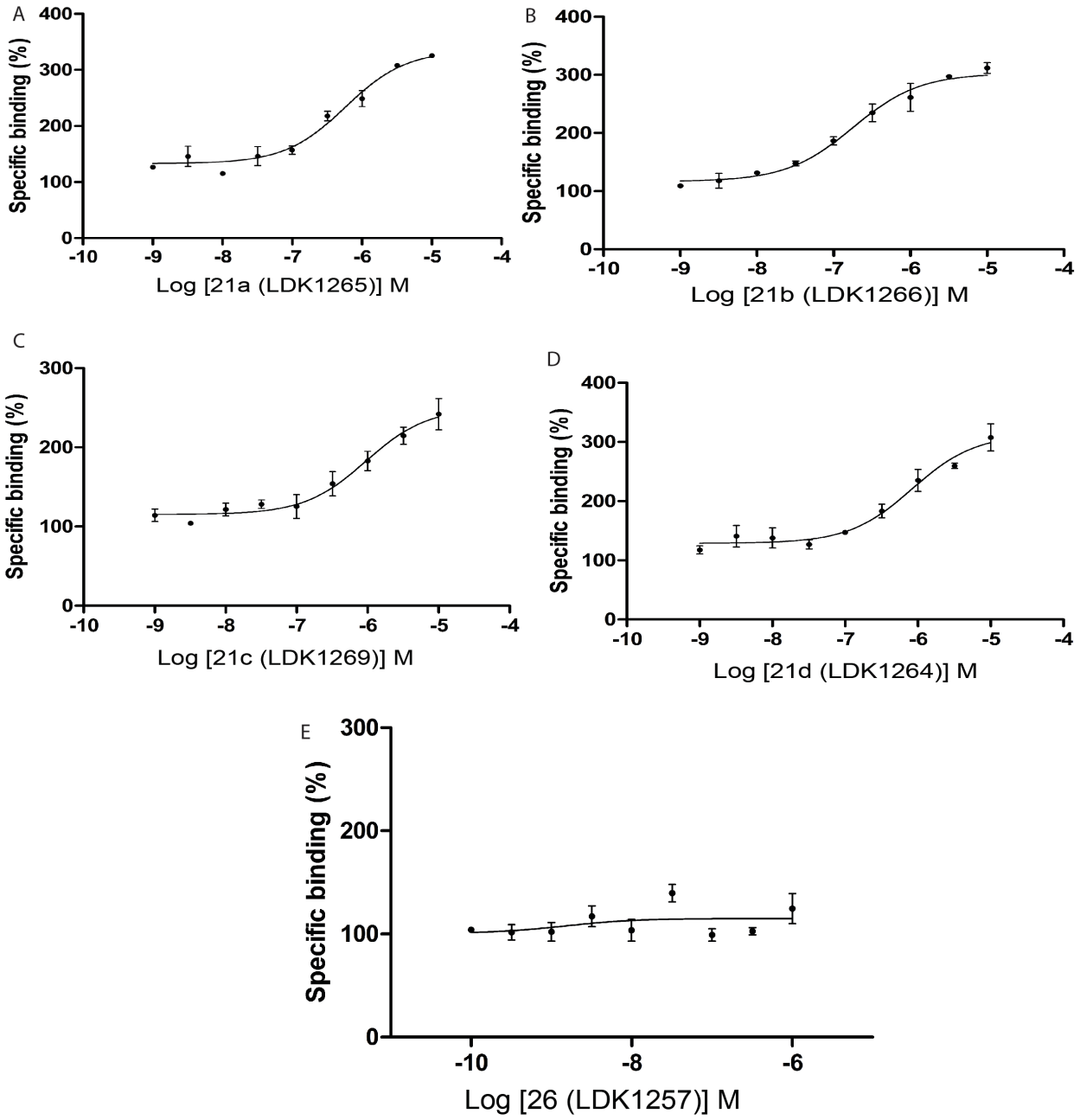

Figure 2.7 Binding curves for analogs 21a-21d and 26. The binding curves show the impact of varying concentrations of test compounds 21a (A), 21b (B), 21c (C), 21d (D) and 26 (E) on the binding of [^{3}H]CP55,940.

In line with our earlier finding that the one carbon linker between the amide bond and the phenyl ring B (Figure 2.1) abolished the allostery of this class of compounds on CB_1 receptor (Mahmoud et al., 2013), the loss of allosteric modulation of orthosteric agonist CP55,940 binding with **26** (**LDK1257**) indicated the critical role of the 2-carbon linker between the amide bond and the phenyl ring B of the amide fragment within the structure of indole-2-carboxamides (**I**, Figure 2.1).

The two robust allosteric modulators **12d** (**LDK1256**) and **12f** (**LDK1258**) were further tested for their effect on CP55,940-induced G-protein coupling activity. It was found that both the compounds showed a concentration-dependent inhibition of agonist-induced GTPγS binding as shown in Figure 2.8

.

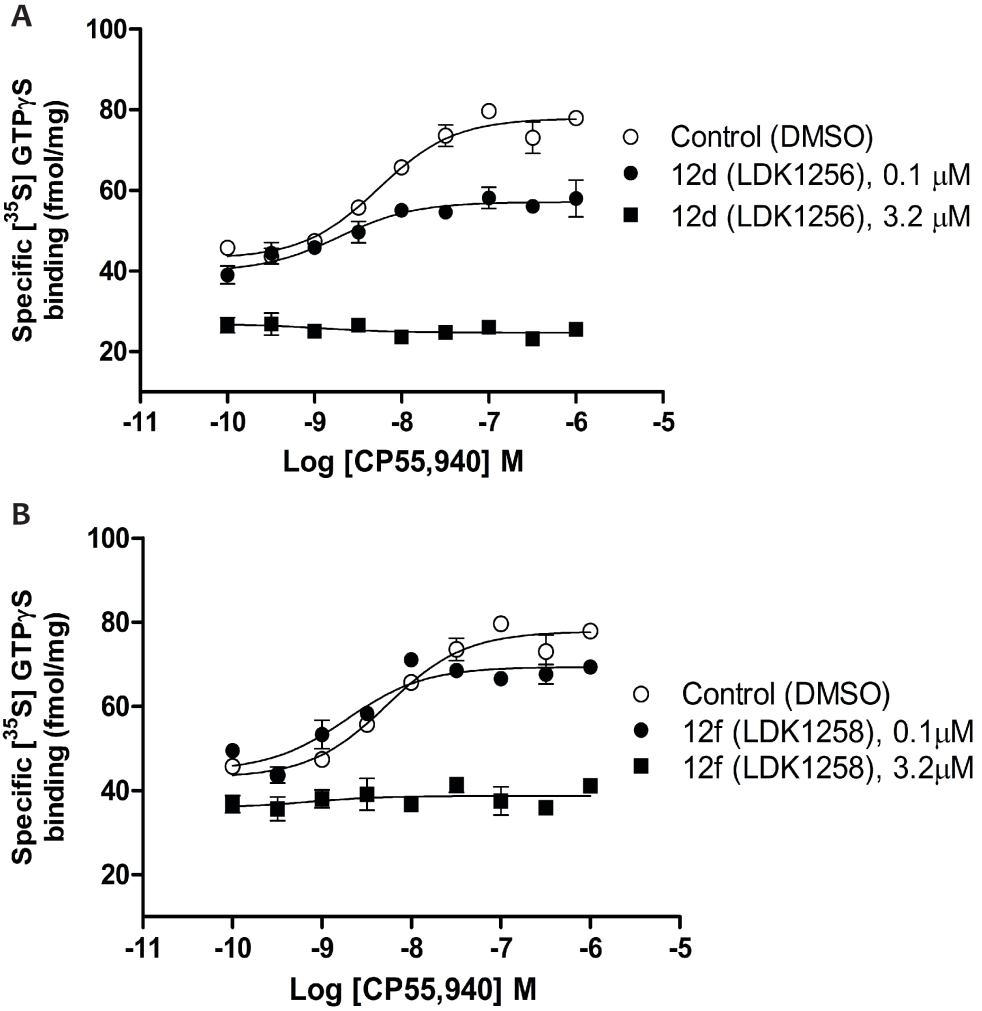

Figure 2.8 Dose−response curves for CP55,940-induced [^{35}S]GTPγS binding to HEK293 cell membranes expressing the CB_1 receptor in the absence and presence of compounds **12d** (**LDK1256**) (A) and **12f** (**LDK1258**) (B) at the indicated concentrations. Nonspecific binding was determined in the presence of 10 μM unlabeled GTPγS. Data is presented as specific binding of GTPγS (fmol/mg) to the membranes. Each data point represents the mean ± S.E. (error bars) of at least three independent experiments performed in duplicate.

We previously demonstrated that ERK1/2 can be activated via CB_1 in a G-protein-dependent manner by CP55,940 alone and a G-protein-independent manner in the presence of **1**

or **2** and CP55,940 (Ahn et al., 2012; Ahn et al., 2013; Ahn et al. 2013). In agreement, CP55,940-induced ERK1/2 phosphorylation was substantially attenuated by pertussis toxin (PTX) but not by β-arrestin knockdown indicating alone it is G_i-protein mediated (Figure 2.9A). In contrast, yet in-line with the observed inhibition of G protein coupling activity (Figure 2.8), ERK1/2 phosphorylation due to **12f** (**LDK1258**) treatment was PTX insensitive (Figure 2.9A) suggesting utilization of a β-arrestin mediated pathway. Furthermore, Figure 2.9B-D show that co-treatment of **2**, **12d** (**LDK1256**) or **12f** (**LDK1258**) and CP55,940 induce concentration-dependent ERK1/2 phosphorylation that is β-arrestin-1 sensitive; the β-arrestin 1 knockdown resulted in substantial inhibition of ERK1/2 phosphorylation induced by **2**, **12d** (**LDK1256**) and **12f** (**LDK1258**). These results indicate that **2**, **12d** (**LDK1256**) and **12f** (**LDK1258**) are functionally positive allosteric modulators, at least for ERK1/2 phosphorylation. Interestingly, **12d** (**LDK1256**) and **12f** (**LDK1258**) reached a plateau at 5 μM of the modulator whereas 2 required 10 μM to achieve comparable levels of ERK1/2 phosphorylation (Figure 2.9E). This may reflect the higher binding affinity of **12d** (**LDK1256**) and **12f** (**LDK1258**) relative to that of **2** (Table 2.1).

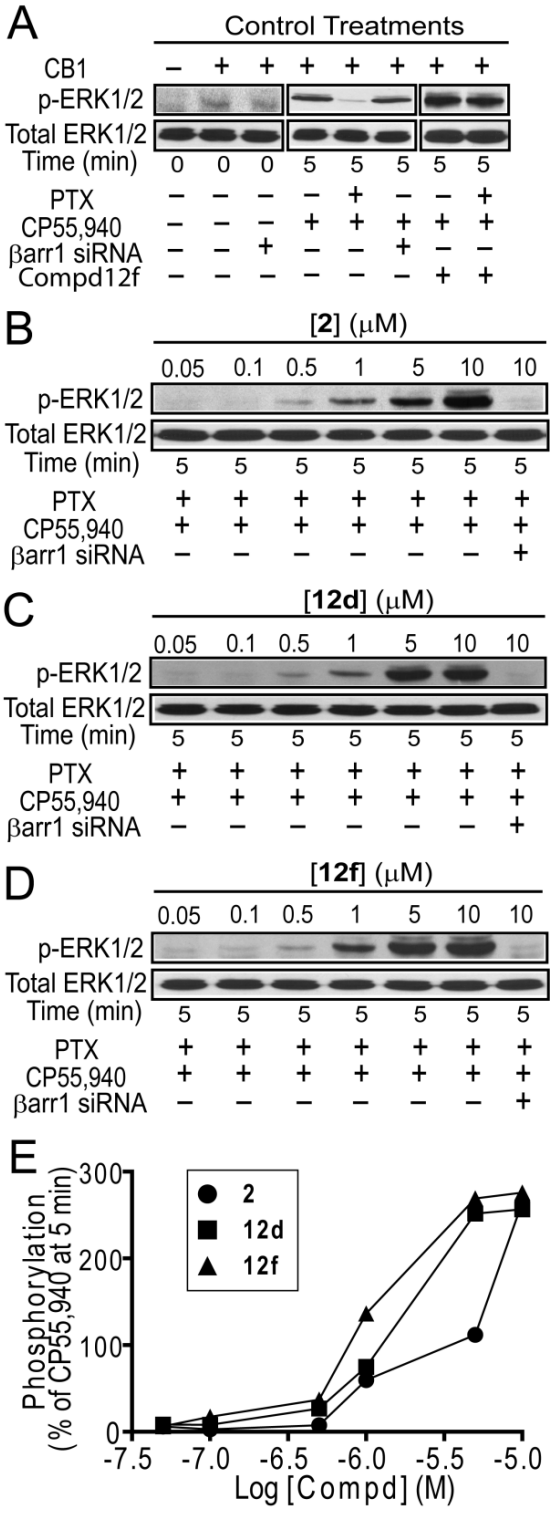
A
Control Treatments
CB1
p-ERK1/2
Total ERK1/2
Time (min)
PTX
CP55,940
βarr1 siRNA
Compd12f
B
[2] (μM)
C
[12d] (μM)
D
[12f] (μM)
E
2
12d
12f
Phosphorylation (% of CP55,940 at 5 min)
Log [Compd] (M)

Figure 2.9 Effect of 12d and 12f on ERK1/2 phosphorylation**.** (A) Mock-transfected and treatment conditions for CP55,940 (0.2 μM), PTX, and siRNA knockdown of HEK293 cells expressing CB_1 are indicated and shown for comparison. (B-D) HEK293 cells expressing CB_1 receptors were exposed to 0, 0.05, 0.1, 0.5, 1, 5, 10 μM of **2** (B), of **12d** (C) or of **12f** (D) in the presence of 0.2 μM CP55,940 for 5 min with PTX pre-treatment for 16 hrs. Cell lysates were separated on SDS-PAGE and analyzed by western blots probed with phospho-ERK1/2 (p-ERK1/2). The total level of ERK1/2 was detected for comparison. Note that the two bands correspond to the predominant isoforms, p42 (ERK2) and p44 (ERK1) for ERK1/2. (E) Graphs provide the quantified ERK1/2 phosphorylation levels induced by each compound for 5 min. Data represent the mean ± S.E. and are expressed as a percent of the level of CP55,940-induced ERK1/2 phosphorylation (Done by Kwang H. Ahn).

2.5 Conclusions and Future Directions

The results from the newly synthesized indole-2-carboxamides along with our earlier findings (Mahmoud et al., 2013) elucidated key structural requirements of indole-2-carboxamides for allosteric modulation of the CB_1 receptor. The critical structural factors include: 1) the chain length of the C3-alkyl group is critical with *n*-propyl being preferred for allosteric modulation of orthosteric ligand binding and *n*-hexyl being preferred for enhancing affinity of the allosteric modulator to the CB_1 receptor; 2) an electron withdrawing group needs to reside at the C5 position of the indole ring; 3) the linker between the amide bond and the phenyl ring B must be an ethylene group whereas shortening or elongating the linker abolishes allosteric effects; and 4) the substituent on the phenyl ring B explicitly influences both the binding to the allosteric site and the binding cooperativity with the orthosteric ligand, with the *N*,*N*-dimethyl amino group being preferred over the piperidinyl functionality of the prototypical CB_1 allosteric modulator **1**. These SARs will guide the future design and synthesis of more potent CB_1 allosteric modulators based on the indole-2-carboxamide scaffold. The therapeutic usefulness of CB_1 allosteric modulators is becoming evident. For instance, the CB_1 allosteric modulator PSNCBAM-1 exhibits acute hypophagic effects (Horsewill et al., 2007) and antagonism of neuronal excitability (Wang et al., 2011), which have the potential for the treatment of obesity and some CNS disorders. The endogenous CB_1 allosteric modulator Lipoxin A4 is capable of protecting neuronal cells from β-amyloid-induced neurotoxicity (Pamplona et al., 2012) that has been implied in the etiology of Alzheimer's disease. Given the nature of biased signaling of some CB_1 allosteric modulators from the indole-2-carboxamide class, selective regulation of signaling-pathway-specific functions of the CB_1 receptor is possible and this may be therapeutically beneficial. The angiotensin II receptor, for example, may exhibit G-protein dependent or β-

arrestin-dependent signaling. Biased agonism of this receptor to promote β-arrestin mediated effects only, may provide a beneficial cytoprotective response and obviate a deleterious increase in blood pressure that is observed in a G-protein manner (Kenakin et al., 2010). This offers tremendous opportunities for developing drugs for many disorders that have been linked to the CB_1 receptor in the CNS and periphery.

Further optimization of the allosteric modulators presented in this chapter to improve the binding affinity and cooperativity of these compounds will be useful for therapeutic purposes. It would be of great interest to utilize these compounds and evaluate their allosteric effects on endocannabinoids such as AEA and 2-AG. Such information will aid in providing more information about the pharmacological profile of these compounds.

Also of interest will be to evaluate the impact of these compounds on other kinases such as JNK1/2/3. CREB, Akt and heat shock proteins. This will allow us to identify other signaling pathways that may be modulated by these allosteric modulators. Evaluation of these compounds in animal models to establish their therapeutic utility is also needed. Recent studies on ORG27569 in animal models demonstrated attenuation of cue- and drug-induced reinstatement of cocaine and methamphetamine. However, the involvement of CB_1 receptor in these effects was not determined (Jing et al., 2014). This necessitates further studies of other allosteric modulators of CB_1 receptor such as those shown in this chapter.

CHAPTER 3

Pyrimidinyl Biphenylureas as Allosteric Modulators of CB_1 receptor: Establishing Structure-Activity Relationships

3.1 Background

This chapter focuses on utilizing another scaffold, pyrimidinyl biphenylureas and modifying this scaffold to identify chemical groups important for allostery at the CB_1 receptor. PSNCBAM-1, which has been previously reported as an allosteric modulator of CB_1 with a diarylurea scaffold was modified by replacing the pyridine ring for a pyrimidine ring and two regioisomers were generated. Modifications were made with these regioisomers to introduce changes in the substituents on ring A of the scaffold (Figure 3.1) or modifications were made in the substituents on the pyrimidine ring to generate 30 different compounds, which were further evaluated for allostery at the CB_1 receptor.

Considerable interest has been generated in development of allosteric modulators of CB_1 due to the many advantages posed by these over their orthosteric counterparts. PSNCBAM-1 has been of particular interest due to its effects in acute food intake studies on rat models. PSNCBAM-1 showed a decrease in cumulative food intake and overall change in the body weight, suggesting that this allosteric modulator can be used to develop anti-obesity drugs. CB_1 receptor has been a target of intense research to develop anti-obesity drugs in the past. Rimonabant (also called SR141716A), an inverse agonist of CB_1 has been previously marketed as an anti-obesity drug. However, it was withdrawn from the market to its psychiatric side effects. With PSNCBAM-1 showing promise as an anti-obesity drug, these compounds synthesized by modifications in

PSNCBAM-1 may help generate therapeutics with anorexic effects. Recently, PSNCBAM-1 has also been investigated for its role in decreasing neuronal excitability. It was demonstrated that PSNCBAM-1 reduces CP55,940 induced neuronal excitability in cerebellum. This decrease in the excitability was not seen in the absence of CP55,940, thus exhibiting that no intrinsic changes to neuroexcitability occur with PSNCBAM-1 (Wang et al., 2011). This is an advantage of utilizing PSNCBAM-1 over CB_1 orthosteric agonists which demonstrate intrinsic changes in neuronal excitation, which is undesirable as was seen with Rimonabant. Thus, these allosteric modulators can be alternative pharmacological agents for therapeutic modulation of CB_1 receptors in diseases of the CNS exhibiting cerebellar dysfunction.

3.2 INTRODUCTION

The endocannabinoid system (ECS) consists of two-well characterized receptor subtypes, the cannabinoid receptor 1 (CB_1) and the cannabinoid receptor 2 (CB_2), the eicosanoid ligands synthesized in the body called endocannabinoids and several metabolic proteins (e.g. fatty acid amide hydrolase, monoacylglycerol lipase) (Petrocellis et al., 2004). Both the receptors are activated by Δ^9-tetrahydrocannabinol (THC), the psychoactive component of marijuana (*Cannabis sativa*) and belong to class 1A rhodopsin-like G-protein coupled receptors (GPCRs). Moreover, CB_1 is one of the most abundant GPCRs expressed in the central nervous system (CNS) (Howlett et al., 2004; Mackie et al., 2008). Upon activation, the CB_1 receptor primarily couples to $G_{i/o}$ protein, which causes downstream inhibition of adenylyl cyclase. The CB_1 receptor can also activates inwardly rectifying and A-type outward potassium channels (Mackie et al., 1995; Mu et al., 1999) and inhibit N-type and P/Q type of calcium channels (Mackie et al., 1992; Gebremedhin et al., 1999). The CB_1 receptor can also activate different members of mitogen-activated protein kinases including p44/42 MAP kinase, p38 kinase and JUN-terminal

kinase through G-protein mediated pathways or pathways independent of G-proteins via arrestins (Pacher et al., 2006; Turu et al., 2010). Due to its complex signaling network, CB_1 has been implicated in the pathology of many disorders and thus is a promising therapeutic target for ameliorating diseases including nausea, obesity, neurodegenerative disorders, pain and substance abuse disorders (Pacher et al., 2006; Mackie et al., 2006). However, despite extensive efforts to generate cannabinoid-based therapeutics, only three medications from cannabinergic compounds (i.e. Cesamet, Marinol and Sativex) are commercially available due to the extensive side effects associated with CB_1 orthosteric ligands. Another CB_1 ligand, SR141716A (rimonabant), which was initially developed as an anti-obesity drug, was withdrawn from the market due to its psychiatric side effects (Cridge et al., 2013).

To overcome challenges posed by orthosteric ligands (ligands which compete with the endogenous ligands for the same site), recent research in GPCRs including CB_1 has shifted focus to allosteric modulators that bind to a topographically distinct site called the allosteric site. Allosteric modulators offer many therapeutic advantages over their orthosteric counterparts. First, due to less evolutionary pressure, allosteric binding pockets have amino-acid sequences which are not highly conserved like the orthosteric sites and thus are more specific for each receptor subtype. Second, the allosteric modulators have a ceiling effect due to their limited allosteric cooperativity and thus can be used to generate titrated pharmacological responses (Christopoulos et al., 2002; Bridges et al., 2008). Third, the allosteric modulators can be used to fine-tune endogenous signaling without affecting the spatial and temporal aspects of endogenous ligand-receptor signaling (Burford et al., 2013).

Allosteric modulators, upon binding to a receptor, can induce an array of distinct conformations that can be very different from those stabilized by orthosteric ligands and thus

have expanded the spectrum of biological conformations between the inactive and active states. Several classes of allosteric modulators of CB_1 have been identified (Figure 3.1), which include 5-chloro-3-ethyl-N-(4-(piperidin-1-yl)phenethyl)-1H-indole-2-carboxamide (**1**, ORG27569) (Price et al., 2005), 1-(4-chlorophenyl)-3-(3-(6-(pyrrolidin-1-yl)pyridin-2-yl)phenyl)urea (**2**, PSNCBAM-1) (Horsewill et al., 2007), 3-(4-chlorophenyl)-5-(8-methyl-3-p-tolyl-8-azabicyclo[3.2.1]octan-2-yl)isoxazole (**3**, RTI-371) (Navarro et al., 2009), the endogenous ligand (5S,6R,9E,11Z,13E,15S)-5,6,15-trihydroxyicosa-9,11,13-trienoic acid (**4**, lipoxin A4) (Pamplona et al., 2012) and 6-methyl-3-(2-nitro-1-(thiophen-2-yl)ethyl)-2-phenyl-1H-indole (**5**, ZCZ011) (Ignatowska-Jankowska et al., 2015). All of these ligands are positive allosteric modulators (PAMs) of the CB_1 receptor in terms of enhancing orthosteric agonist binding. A family of peptide endocannabinoids (Pepcans) represented by pepcan-12 (**6**) has recently been reported to exhibit negative allosteric modulation (NAM) on the CB_1 receptor at the levels of regulating the orthosteric agonist binding as well as on the signaling functions of CB_1 receptor (Bauer et al., 2012). Since allosteric modulators can induce distinct conformations than those induced by orthosteric ligands, they offer potential to generate pharmacological responses that may be difficult to achieve with orthosteric ligands alone. The different receptor states induced by allosteric modulators can be biased for a certain intracellular signaling pathways as is seen with many allosteric modulators including ORG27569 for the CB_1 receptor and thus, they offer promising avenues to develop subtype-specific and pathway-specific therapeutics (Kenakin et al., 2012; Kenakin et al., 2010).

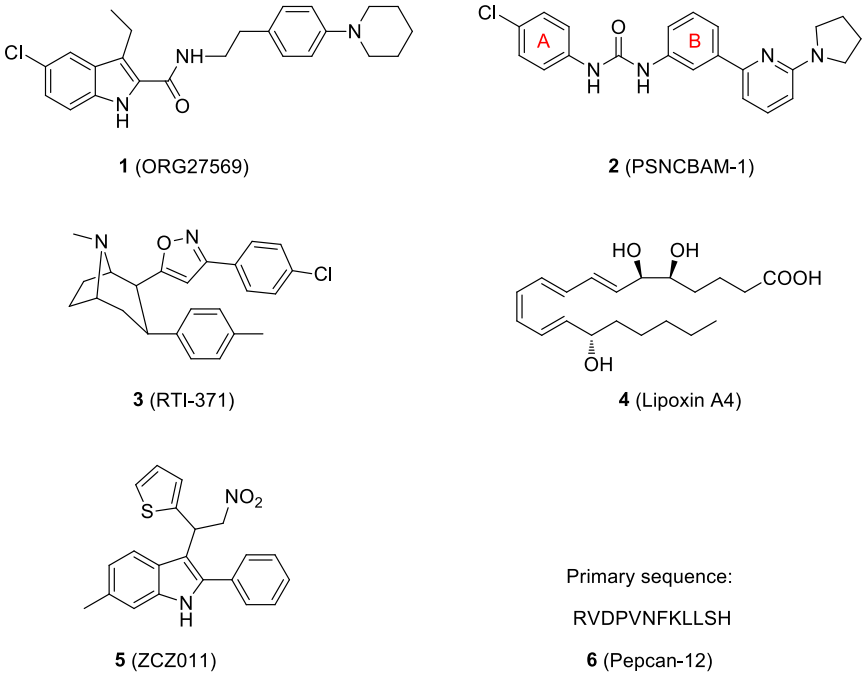

Figure 3.1. Structures of representative allosteric modulators of the CB_1 receptor.

Some *in vivo* pharmacological assessment indicated that these allosteric modulators can generate therapeutic effects relevant to various clinical therapies. For instance: **1** was demonstrated effective to inhibit reinstatement of drug-seeking behavior (Jing et al., 2014); **4** was found to reduce β-amyloid-provoked neurotoxicity (Pamplona et al., 2012). The positive CB_1 allosteric modulator **5** was shown to generate antinociceptive effects without psychoactive effects typically found in orthosteric ligands of CB_1 receptor (Ignatowska-Jankowska et al., 2015). Interestingly, **2** was found capable of reducing food intake and body weight in an acute feeding study (Horsewill et al., 2007). Thus, this scaffold holds promise for the development of anti-obesity drugs by targeting the allosteric sites. A recent SAR study of **2** has revealed that two structural variations can preserve the activity of **2**. These include the replacement of the chloro group with either a fluoro (F) or a cyano (CN) group and the replacement of pyrrolidine ring

with *N,N*-dimethyl amino group. Using a calcium mobilization assay, these analogs exhibited a dose-dependent reduction of E_{max} values with the CB_1 agonist CP55940, as expected for CB_1 G-protein NAMs (German et al., 2014). In order to increase the structural diversity from this scaffold, we designed novel analogs with the hypothesis that a pyrimidinyl ring can be employed to replace the pyridinyl ring of **2**. This effort led to our syntheses and assessment of novel analogs **7a-7h** and **8a-8u** whose structures are shown in Figure 3.2.

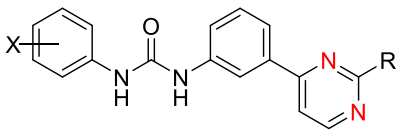

7

7a (LDK1283). X = *p*-Cl, R = pyrrolidine
7b (LDK1284). X = *p*-Br, R = pyrrolidine
7c (LDK1297). X = *p*-F, R = pyrrolidine
7d (LDK1285). X = *p*-CN, R = pyrrolidine
7e (LDK1293). X = *p*-F, R = *N,N*-dimethyl
7f (LDK1292). X = *p*-CN, R = *N,N*-dimethyl
7g (LDK1298). X = *p*-I, R = *N,N*-dimethyl
7h (LDK1295). X = *m*-F, R = *N,N*-dimethyl

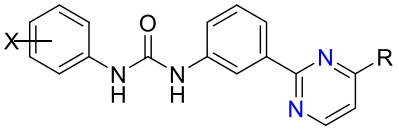

8

8a (LDK1286). X = *p*-Cl, R = pyrrolidinyl
8b (LDK1287). X = *p*-Br, R = pyrrolidinyl
8c (LDK1294). X = *p*-F, R = pyrrolidinyl
8d (LDK1288). X = *p*-CN, R = pyrrolidinyl
8e (LDK1290). X = *p*-F, R = *N,N*-dimethyl
8f (LDK1289). X = *p*-CN, R = *N,N*-dimethyl
8g (LDK1296). X = *p*-**I**, R = *N,N*-dimethyl
8h (LDK1291). X = *m*-F, R = *N,N*-dimethyl
8i (LDK1304). X = *p*-CF_3, R = pyrrolidinyl
8j (LDK1303). X = *p*-$CH_3C(O)$, R = pyrrolidinyl
8k (LDK1302). X = p-EtOC(O), R = pyrrolidinyl

8l (LDK1310). X = *p*-COOH, R = *N*-pyrrolidinyl
8m (LDK1301). X = *p*-OCH3, R = *N*-pyrrolidinyl
8n (LDK1311). X = *p*-OH, R = *N*-pyrrolidinyl
8o (LDK1300). X = *m*-CN, R = *N*-pyrrolidinyl
8p (LDK1312). X = *p*-CN, R = *N*-azetidinyl
8q (LDK1309). X = *p*-CN, R = *N*-piperidinyl
8r (LDK1307). X = *p*-CN, R = $N(Et)_2$
8s (LDK1306). X = *p*-CN, R = $CH_3CH_2NCH_3$
8t (LDk1308). X = *p*-CN, R = *N*-cyclopropyl amino

Figure 3.2. The designed and synthesized pyrimidinyl biphenyl ureas. (LDK numbers for the corresponding analogs are written in brackets.

CHEMISTRY

Dr. Dai Lu's lab used the following procedures to synthesize the compounds **7a-h** and **8a-u**.

The syntheses of the target compounds **7** and **8** were achieved through the routes illustrated by Figure 3.3 and Figure 3.4 respectively. To obtain compounds **7a**-**7h**, the synthesis of intermediate 3-(2-chloropyrimidin-4-yl)aniline (**12**) is critical. Coupling of the commercially available 2,4-dichloropyrimidine **9** with (3-nitrophenyl)boronic acid **10** under typical Suzuki reaction condition gave exclusively the 2-chloro-4-(3-nitrophenyl)pyrimidine **11**. We found that this Suzuki coupling reaction only took place at the 4-chloro position of starting material **9**, whilst its 2-chloro group was spared. The structure of the Suzuki coupling product **11** was confirmed by NOESY signals between the protons H-8 and H-12 with proton H-5 of **9** (see supporting information for 2D ^{1}H NMR of **9**). Upon reduction of **9** catalyzed with tin chloride dihydrate, the desired intermediate 3-(2-chloropyrimidin-4-yl)aniline (**12**) was obtained in an acceptable yield (45%). Reaction of the pyrimidinyl aniline **12** respectively with properly substituted isocyanate (**13a**-**13f**) yielded the key intermediates **14a**-**14f**. Thereafter, amination of the pyrimidinyl ring of individual **14** with either pyrrolidine or *N*,*N*-dimethyl amine in THF generated the final compounds **7a**-**7h**.

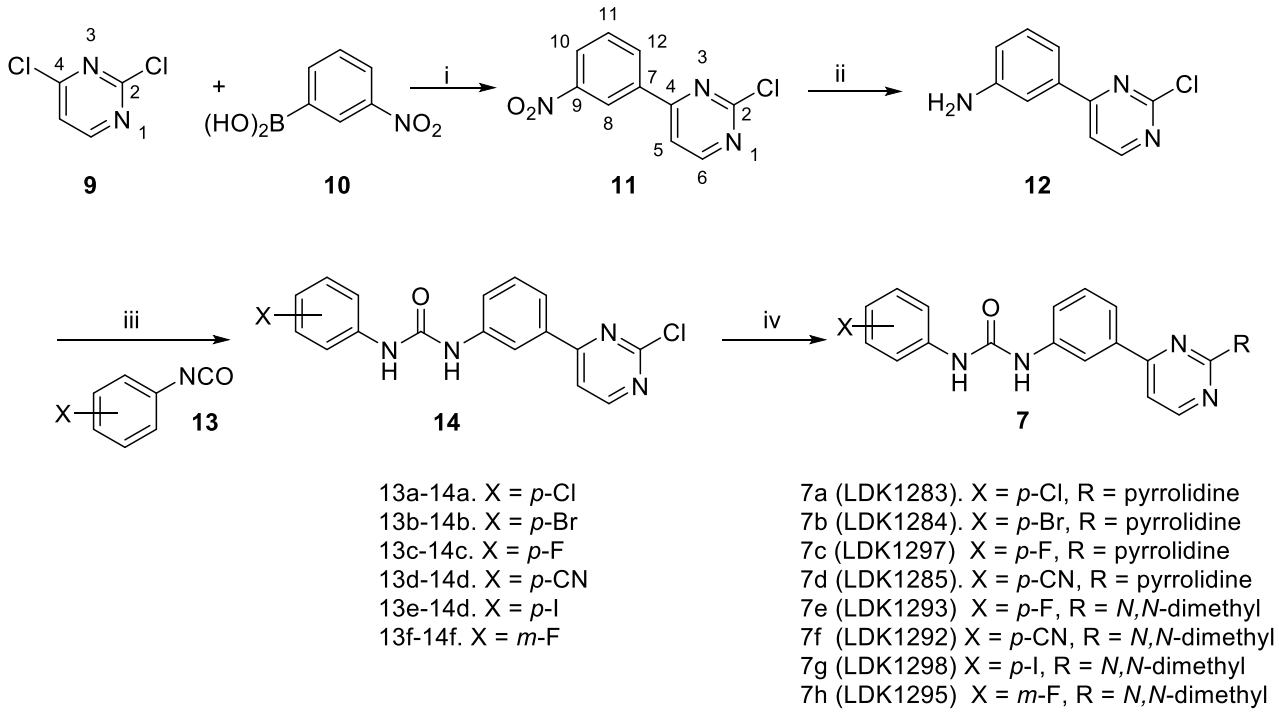

Figure 3.3 Synthesis of compounds 7a-7h. Reagents and conditions: (i) Na_2CO_3, $Pd(PPh_3)_4$, DME, H_2O; 90 ^oC, 7 h, 60%; (ii) $SnCl_2{\cdot}2H_2O$, DCM/MeOH (1:1), 0 ^oC then reflux at 60 ^oC, 4 h, 45%; (iii) DCM, 0 ^oC to rt, 2 h, 60-80%; (iv) pyrrolidine (for **7a-7d**) or *N*,*N*-dimethyl amine (for **7e-7h**), THF, reflux, 100 ^oC, 2-4 h, 60-80%. LDK numbers for the corresponding analogs is written in brackets.

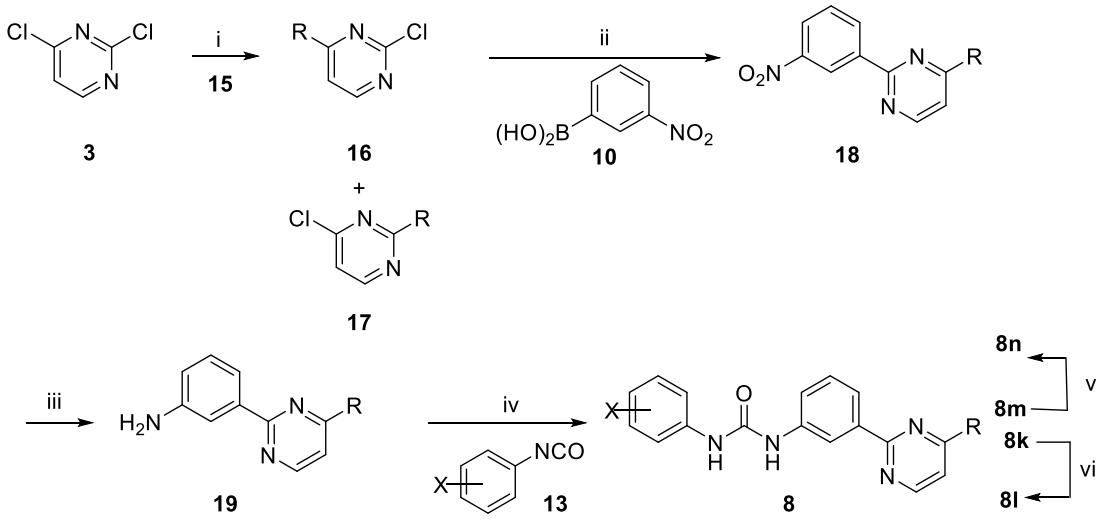

16a-19a. R = *N*-pyrrolidinyl
16b-19b. R = *N,N*-dimethyl
16c-19c. R = *N*-ethyl-*N*-methyl
16d-19d. R = diethyl amino
16e-19e. R = *N*-piperidinyl
16f-19f. R = *N*-cyclopropyl amino
16g-19g. R = *N*-azetidinyl

8a (LDK1286). X = *p*-Cl, R = pyrrolidinyl
8b (LDK1287). X = *p*-Br, R = pyrrolidinyl
8c (LDK1294). X = *p*-F, R = pyrrolidinyl
8d (LDK1288). X = *p*-CN, R = pyrrolidinyl
8e (LDK1290). X = *p*-F, R = *N,N*-dimethyl
8f (LDK1289). X = *p*-CN, R = *N,N*-dimethyl
8g (LDK1296). X = *p*-**I**, R = *N,N*-dimethyl
8h (LDK1291). X = *m*-F, R = *N,N*-dimethyl
8i (LDK1304). X = *p*-CF_3, R = pyrrolidinyl
8j (LDK1303). X = *p*-$CH_3C(O)$, R = pyrrolidinyl
8k (LDK1302). X = *p*-EtOC(O), R = pyrrolidinyl

8l (LDK1310). X = *p*-COOH, R = *N*-pyrrolidinyl
8m (LDK1301). X = *p*-OCH3, R = *N*-pyrrolidinyl
8n (LDK1311). X = *p*-OH, R = *N*-pyrrolidinyl
8o (LDK1300). X = *m*-CN, R = *N*-pyrrolidinyl
8p (LDK1312). X = *p*-CN, R = *N*-azetidinyl
8q (LDK1309). X = *p*-CN, R = *N*-piperidinyl
8r (LDK1307). X = *p*-CN, R = $N(Et)_2$
8s (LDK1306). X = *p*-CN, R = $CH_3CH_2NCH_3$
8t (LDK1308). X = *p*-CN, R = *N*-cyclopropyl amino

Figure 3.4 Synthesis of Compounds 8a-8t. Reagents and conditions: (i) amine **15** (**15a**: pyrolidine; **15b**: $NH(CH_3)_2$; **15c**: MeNHEt; **15d**: $NH(Et)_2$; **15e**: piperidine; **15f**: cyclopropylamine; **15g**: azitidine), THF, rt, 2 h, 77.3%-80%; c) ; (ii) Na_2CO_3, $Pd(PPh_3)_4$, 1,4-dioxane, H_2O (4:1), 110 ^oC, 10 h, 60-65%; (iii) 10% Pd/C, H_2, EtOAc or ethanol, rt, 4 h, 90-95%; (iv) corresponding phenyl isocyanate **13**, DCM, 0 ^oC-rt, 2 h, 65-85%; (v) LiOH, THF/H_2O, rt; (vi) BBr_3, DCM, 0 ^oC-rt. LDK numbers for the corresponding residues is written in brackets.

To synthesize the compounds of series **8**, we first tried to obtain compound **18** bearing a chloro functionality (R=Cl) so that the further variation at this position with different amino substitutions could be facilitated. However, the Suzuki coupling reaction between **9** and **10** only produced compound **11**, and no structure **18** (R= Cl) was formed. Therefore, we took the route illustrated in Figure 3.4 and aminated the 2,4-dichloropyrimidine **9** first. This yielded two regioisomers **16** and **17**. The 4-amino pyrimidine **16** was obtained as the major product while the 2-amino pyrimidine **17** is the minor product. The structures of individual compounds **16** and **17** were determined by proton NMR, mass and compared to data reported in the literature. Coupling the 4-amino pyrimidine **16a-16g,** respectively with (3-nitrophenyl)boronic acid **10** under Suzuki reaction conditions yielded the desired 2-(3-nitrophenyl)pyrimidin-4-amines **18a-18h** in acceptable yields (46%-75%). Hydrogenation of **18** produced the desired 2-(3-aminophenyl)-pyrimidin-4-amines **19** in good yield (87-97%). Coupling the selected isocyanate **13** with amines **19** yielded the final compounds **8a-8j**, **8m** and **8o-8t**. The compound **8l (LDK1310**) was further derived from **8k (LDK1302)** through hydrolysis, and **8n (LDK1311)** was further derived from **8m (LDK1301)** through removal of the methyl group by boron tribromide.

3.3 Materials and Methods

Cell line and culture conditions. Human embryonic kidney cells (HEK293T) was a kind gift from Dr. Randall Walikonis (Department of Physiology and Neurobiology, University of Connecticut). The cell line was cultured in DMEM medium with 10% FBS (v/v) and glucose (3.5 mg/ml). Cultures were maintained at 37 °C in humidified incubators with 5% CO_2/ 95% air.

CB_1 expression and membrane preparation. HEK293 cells were seeded at approximately 800,000 cells/100 mm dishes and transiently transfected using the calcium-phosphate

precipitation method. Membrane preparation was made as described previously (Chen et al., 1987). Briefly, 24 hours post-transfection, the cells were harvested and washed with phosphate buffered saline (PBS). The cells were resuspended in PBS solution containing mammalian protease inhibitor cocktail ((4-2-aminoethyl) benzene-sulfonyl fluoride, pepstatin A, E-64, bestatin, leupeptin, and aprotinin) (Sigma-Aldrich, St. Louis, MO) followed by lysis by nitrogen cavitation at 750 psi for 5 min using a Parr cell disruption bomb. The cell lysate was spun at 500 *g* for 10 min at 4ºC to remove nuclei, cell debris and intact cells. The supernatant was collected and spun at 100,000g for 45 min at 4ºC. The membrane containing pellet was resuspended in TME buffer (25 mM Tris-HCl, 5 mM $MgCl_2$, and 1 mM EDTA, pH 7.4) containing 7% w/v sucrose. The protein concentration was determined using Bradford assay (Bradford, M.M., 1976). The membrane preparation was then stored at -70ºC.

Radioligand binding assay. To determine the allosteric parameters K_B and α, ligand binding assays were performed as previously described (Ahn et al., 2012). Membrane preparation expressing the CB_1 receptor was incubated with at least nine different concentrations (ranging between 100 pM and 100 μM) of unlabeled allosteric compound, in the presence of 0.5 nM [^{3}H]CP55,940 (141.2 Ci/mmol, PerkinElmer Life Sciences (Boston, MA)) which is an orthosteric ligand of CB_1 and was used as a tracer. TME containing 0.2% fatty acid-free BSA was used as a buffer to make a final volume of 200 μl. Nonspecific binding was determined by incubating the membranes with a high concentration of unlabeled CP55,940 (1 μM). The reaction was terminated by adding 300 μl TME buffer containing 5% BSA and subsequent filtration through Whatman GF/C filter paper with a Brandel cell harvester. This was followed by washing with ice cold TME buffer and collecting the filter paper sections corresponding to each sample. Radioactivity was measured using liquid scintillation counting.

[^{35}S]GTPγS evaluation. To evaluate the impact of the test compounds on the G-protein coupling efficiency of the CB_1 receptor, GTPγS assays were performed as described previously (Ahn et al., 2012). Briefly, 7.5 μg membrane preparation expressing the CB_1 receptor was incubated with a saturating concentration of CP55,940 (1 μM), 0.1 nM [^{35}S]GTPγS (1250 Ci/mmol; PerkinElmer Life Sciences, Boston, MA), 5 μM GDP (Sigma, St. Louis, MO) and 0.1% (w/v) BSA in the absence and presence of varying concentrations of the test allosteric modulators. GTPγS binding assay buffer (50 mM Tris-HCl, pH 7.4, 3 mM $MgCl_2$, 0.2 mM EGTA, and 100 mM NaCl) was used to make a total volume of 200 μL and the membranes were incubated at 30°C for an hour. Nonspecific binding was determined with 10 μM unlabeled GTPγS (Sigma, St. Louis, MO). For the controls, membrane preparations expressing CB_1 receptor were treated with DMSO or a high concentration of the inverse agonist SR141716A (1 μM). Membrane preparations from the same cells not transfected with CB were also evaluated for the G-protein coupling levels to determine non-CB_1 mediated GTPγS binding. The reaction was terminated by filtration through Whatman GF/C filter papers followed by washing with cold TME buffer. The filter paper sections were collected and radioactivity was measured by liquid scintillation counting.

Data Analysis. All ligand binding and GTPγS assays were carried out in duplicate and at least three independent experiments were performed for each curve. For the ligand binding assays, data are presented as a mean with the corresponding 95% confidence limits. Data were analyzed by nonlinear regression using Prism 6.0 (Graphpad Software Inc., San Diego, CA) as previously described (Ahn et al., 2012).

3.4 RESULTS AND DISCUSSION

The synthesized analogs were firstly evaluated for allostery, using the orthosteric agonist, CP55,940 and two key parameters: K_B, the equilibrium dissociation constant of the allosteric modulator which reflects the affinity of the allosteric modulator for the receptor and α, the binding cooperativity factor which defines the magnitude and direction of the allosteric effect on the binding of the orthosteric ligand, when both occupy the receptor. Modulators with an $\alpha>1$ promote orthosteric ligand binding and are classified as positive allosteric modulators (PAMs) whereas modulators with $\alpha<1$ inhibit orthosteric ligand binding and are classified as negative allosteric modulators (NAMs). Compounds with no allosteric activity on orthosteric ligand binding have an α equaling to 1 and are classified as silent allosteric modulators.

To evaluate the scaffold **7** and **8**, we first compared **7a (LDK1283)** and **8a (LDK1286)** with the lead compound **2**. The results shown in Table 3.1 and 3.2 (entry 2 and 10) suggested that replacing the pyridine ring of **2** with a pyrimidine ring reduced the binding affinity while the modulation on orthosteric ligand binding were enhanced (i.e. the α values are increased). This promoted our further investigation of the two new scaffolds by optimizing the substituents. We synthesized and assessed compounds **7b-7h** and their counterpart compounds **8b-8h**. The results shown in Table 3.1 (entry 3-9) and Table 3.2 (entry 11-17) revealed that the scaffold **7** and **8** do not show significant difference in binding affinity (K_B) and binding cooperativity factor (α) except when the A ring was substituted with a *para*-cyano group and the pyrimidine ring was substituted with a pyrrolidinyl group (**8d (LDK1288)**). It also appears that a *N*,*N*-dimethyl amino substituent on the pyrimidinyl ring is suboptimal than a pyrrolidinyl group within each series of compound from scaffold **7** and **8**. By far, only compound **8d (LDK1288)** showed activity comparable to the lead compound **2**.

A cyano group is a strong electron-withdrawing group (EWG). To investigate if other substituent on the phenyl ring A can increase the binding affinity and allosteric effects, we synthesized and assessed the compounds **8i-8n** (Table 3.2), which bear either various EWG including CF_3 (**8i (LDK1304)**), acetyl (**8j (LDK1303)**), ethoxyacyl (**8k (LDK1302)**) and COOH (**8l (LDK1310)**) or an electron-donating group (EDG) such as OMe (**8m (LDK1301)**) and OH (**8n (LDK1311)**). However, none of them surpassed the cyano-substituted compound **8d (LDK1288)**. Introducing EDGs on the phenyl ring A (i.e. compound **8m (LDK1301)** and **8n (LDK1311)**) significantly reduced the binding affinity to the allosteric site. Some of the EWGs are able to retain some binding affinity to the allosteric site (i.e. **8i (LDK1304)** and **8k (LDK1302)**). These suggested that variation of the electron density of the phenyl ring A alone is unable to enhance the binding affinity. It seems that the cyano group is not only to polarize the adjacent electron density on the A ring but also is likely involved in the molecular recognition process. The multiple biological functions of a cyano group have been well recognized (Fleming et al., 2010). Its functions include serving as carbonyl and halogen bioisosteres, a hydroxyl and carboxyl surrogate, an inducer of non-specific dipole interactions with amino acids and metal ions, and functionality able to replace a conserved water molecule from the binding domain (Fleming et al., 2010). Expulsion of a conserved water molecule from the binding domain by a cyano group may provide additional entropic improvement of binding affinity (Comer et al., 2001; Levinson et al., 2014).

Table 3.1. Allosteric parameters of analogs derived from scaffold **7** (**7a-7h**).

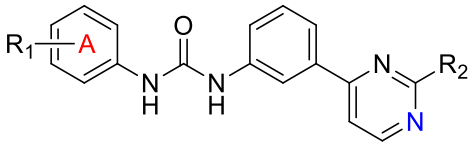

Entry	Compd	R_1	R_2	K_B (nM)[a]	α[b]
1	**2**	*p*-Cl	*N*-Pyrrolidinyl	54.3 (21.9-134.6)	7.3
2	**7a (LDK 1283)**	*p*-Cl	*N*-Pyrrolidinyl	226.9 (61.8-832.2)	11.6
3	**7b (LDK1284)**	*p*-Br	*N*-Pyrrolidinyl	394.9 (79.3-1964)	16.8
4	**7c (LDK 1297)**	*p*-F	*N*-Pyrolidinyl	195.6 (113.8-336.1)	3.5
5	**7d (LDK1285)**	*p*-CN	*N*-Pyrrolidinyl	167.8 (57.1-492.1)	10.5
6	**7e (LDK1293)**	*p*-F	$N(CH_3)_2$	1116 (506.6-2459)	7.3
7	**7f (LDK1292)**	*p*-CN	$N(CH_3)_2$	416.6 (308.1-563.2)	6.1
8	**7g (LDK1298)**	*p*-I	$N(CH_3)_2$	965.3 (629.0-1481)	2.7
9	**7h (LDK1295)**	*m*-F	$N(CH_3)_2$	967.4 (540.3-1722)	2.5

[a]K_B : equilibrium dissociation constant of a potential allosteric ligand. [b]α: binding cooperativity factor for the tested allosteric modulator. The two allosteric parameters were tested using [^{3}H]CP55,940 as the orthosteric ligand.

Table 3.2. Allosteric parameters of analogs derived from scaffold **8** (**8a-8q**).

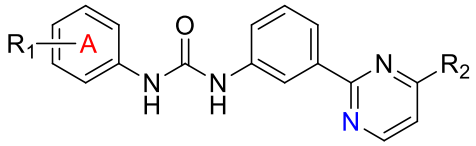

Entry	Compd	R_1	R_2	K_B (nM)[a]	α[b]
1	**2**	*p*-Cl	*N*-Pyrrolidinyl	54.3 (21.9-134.6)	7.3
10	**8a (LDK1286)**	*p*-Cl	*N*-Pyrrolidinyl	264.4 (61.9-1129)	18.1
11	**8b (LDK1287)**	*p*-Br	*N*-Pyrrolidinyl	101.9 (32.8-316.9)	6.1
12	**8c (LDK1294)**	*p*-F	*N*-Pyrrolidinyl	222.9 (154.2-322.1)	4.9
13	**8d (LDK1288)**	*p*-CN	*N*-Pyrrolidinyl	49.1 (27.9-86.3)	4.6
14	**8e (LDK1290)**	*p*-F	$N(CH_3)_2$	1221 (849.6-1755)	5.2
15	**8f LDK1289)**	*p*-CN	$N(CH_3)_2$	313.3 (216.2-454.2)	4.5
16	**8g LDK1296)**	*p*-I	$N(CH_3)_2$	997.1 (480.7-2068)	2.5
17	**8h (LDK1291)**	*m*-F	$N(CH_3)_2$	669.8 (173.6-2584)	2.0
18	**8i (LDK1304)**	*p*-CF_3	*N*-Pyrrolidinyl	144.2 (85.8-242.4)	3.8
19	**8j (LDK1303)**	*p*-$CH_3C(O)$	*N*-Pyrrolidinyl	2108 (1299-3422)	2.5
20	**8k (LDK1302)**	*p*-EtOC(O)	*N*-Pyrrolidinyl	463.0 (51.8-4132)	1.6
21	**8l (LDK1310)**	*p*-COOH	*N*-Pyrrolidinyl	NB[c]	NB[d]
22	**8m (LDK1301)**	*p*-OCH_3	*N*-Pyrrolidinyl	1826 (991.7-3364)	3.8
23	**8n (LDK1311)**	*p*-OH	*N*-Pyrrolidinyl	NB[c]	NB[d]
24	**8o (LDK1300)**	*m*-CN	*N*-Pyrrolidinyl	1980 (388.1-10100)	1.5

[a]K_B : equilibrium dissociation constant of a potential allosteric ligand. [b]α: binding cooperativity factor for the tested allosteric modulator. The two allosteric parameters were tested using [^{3}H]CP55,940 as the orthosteric ligand. [c]NB: no detectable binding to the receptor using up to 32 μM of test compound.

Table 3.3. Allosteric parameters of analogs derived from scaffold **8** (**8p-8t**).

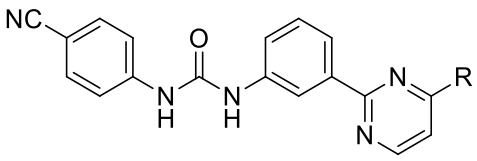

entry	Compd	R	K_B (nM)[a]	α[b]
13	**8d (LDK1288)**	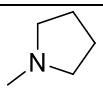	49.1 (27.9-86.3)	4.6
25	**8p (LDK1312)**		211.0 (100.7-442.0)	4.5
26	**8q (LDK1309)**	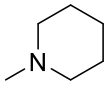	66.4 (24.9-176.4)	3.2
27	**8r (LDK1307)**	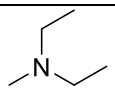	69.6 (20.1-240.3)	4.8
28	**8s (LDK1306)**		206.9 (110.3-388.1)	4.5
29	**8f (LDK1289)**		313.3 (216.2-454.2)	4.4
30	**8t (LDK1308)**	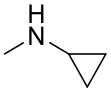	97.7 (13.4-711.0)	1.7

[a]K_B : equilibrium dissociation constant of a potential allosteric ligand. [b]α: binding cooperativity factor for the tested allosteric modulator. The two allosteric parameters were tested using [^{3}H]CP55,940 as the orthosteric ligand.

Following the identification of **8d (LDK1288)**, we investigated if other amino substituents on the pyrimidine ring can enhance activity (Table 3). We reduced the ring size to a 4-membered azetidinyl ring (**8p(LDK1312)**). This led to a decline of K_B. When the ring size was increased to a 6-membered piperidinyl ring (**8q (LDK1309)**), it showed a K_B comparable to **8d (LDK1288)** with slightly reduced binding cooperativity factor (α). This promoted our synthesis of analogs with acyclic amino substituents of the pyrimidinyl ring (i.e. **8r**-**8t**). The results (entry 27-29, Table 3.3) indicated that only the *N*,*N*-diethyl amino group (**8r (LDK1307)**) preserve the activity of **8d (LDK1288)**. The results from **8r to 8t** indicated that a dialkyl amino group is preferred as the substituent on the pyrimidinyl ring and each of the alkyl substitutions should be greater than methyl.

In summary, the efforts using pyrimidine in lieu of the pyridine ring led to two compounds (i.e. **8d** (**LDK1288**) and **8r** (**LDK1307**)) showing similar binding affinity (K_B) to the allosteric site as the lead compound **2**. Their allosteric effects on orthosteric agonist binding (i.e. the α values) are comparable to **2**. The graphs for the analogs evaluated are shown in Figures 3.5-3.10.

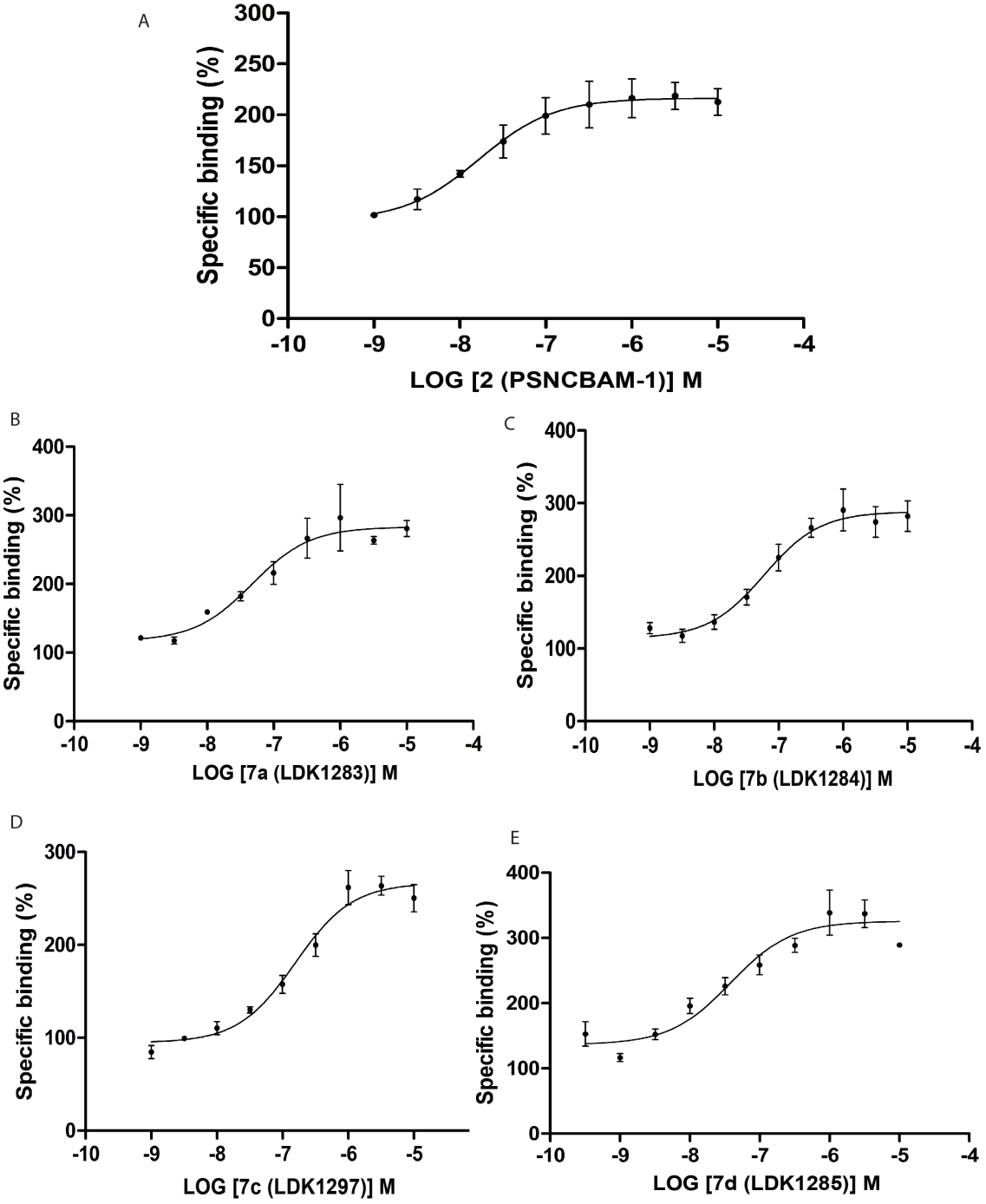

Figure 3.6 Binding curves for 2 (PSNCBAM-1) and analogs 7A-7D. The binding curves show the impact of varying concentrations of test compounds 2 (A), 7a (B), 7b (C), 7c (D) and 7d (E) on the binding of [^{3}H]CP55,940.

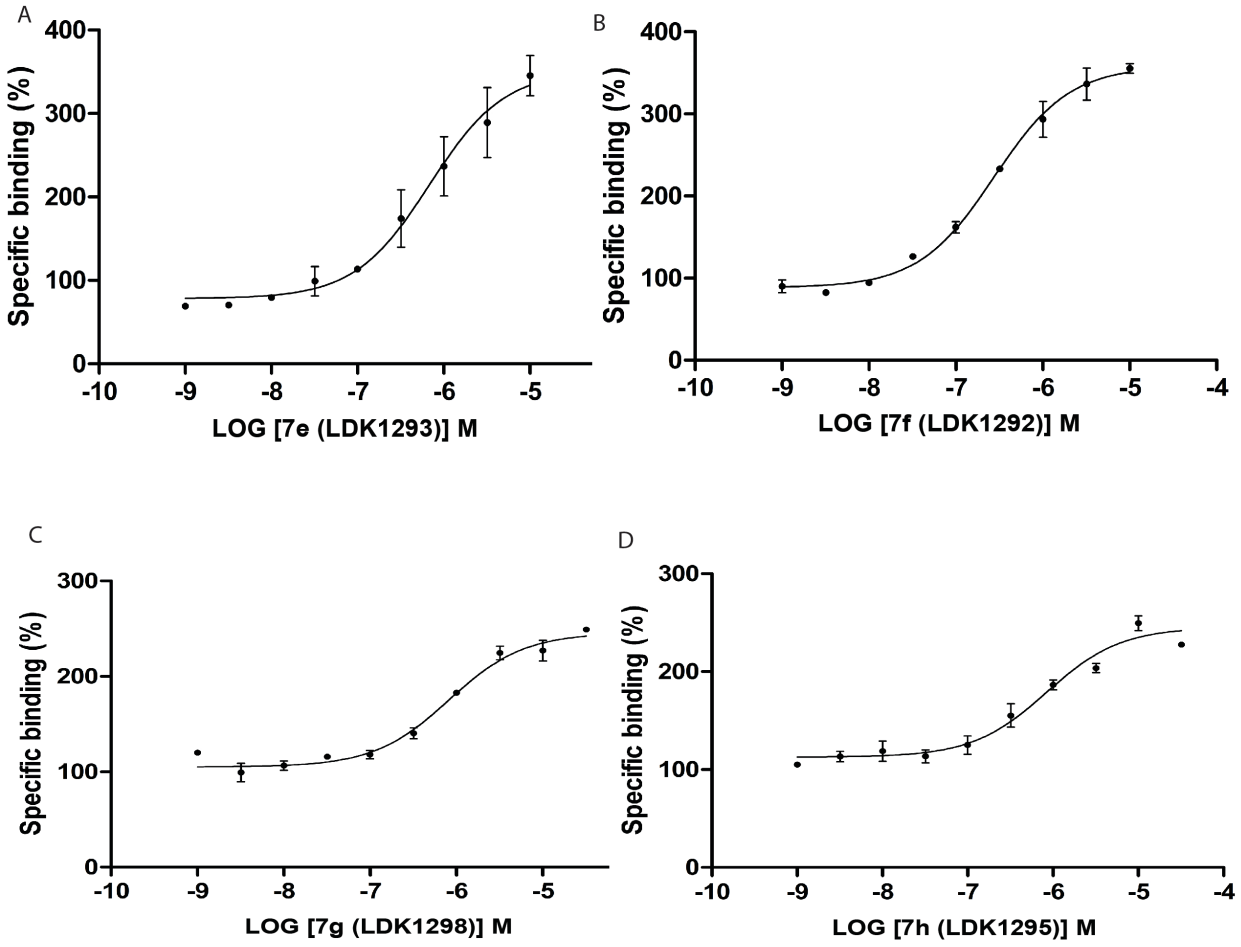

Figure 3.6 Binding curves for analogs 7e-7h. The binding curves show the impact of varying concentrations of test compounds 7e (A), 7f (B), 7g (C) and 7h (D) on the binding of [^{3}H]CP55,940.

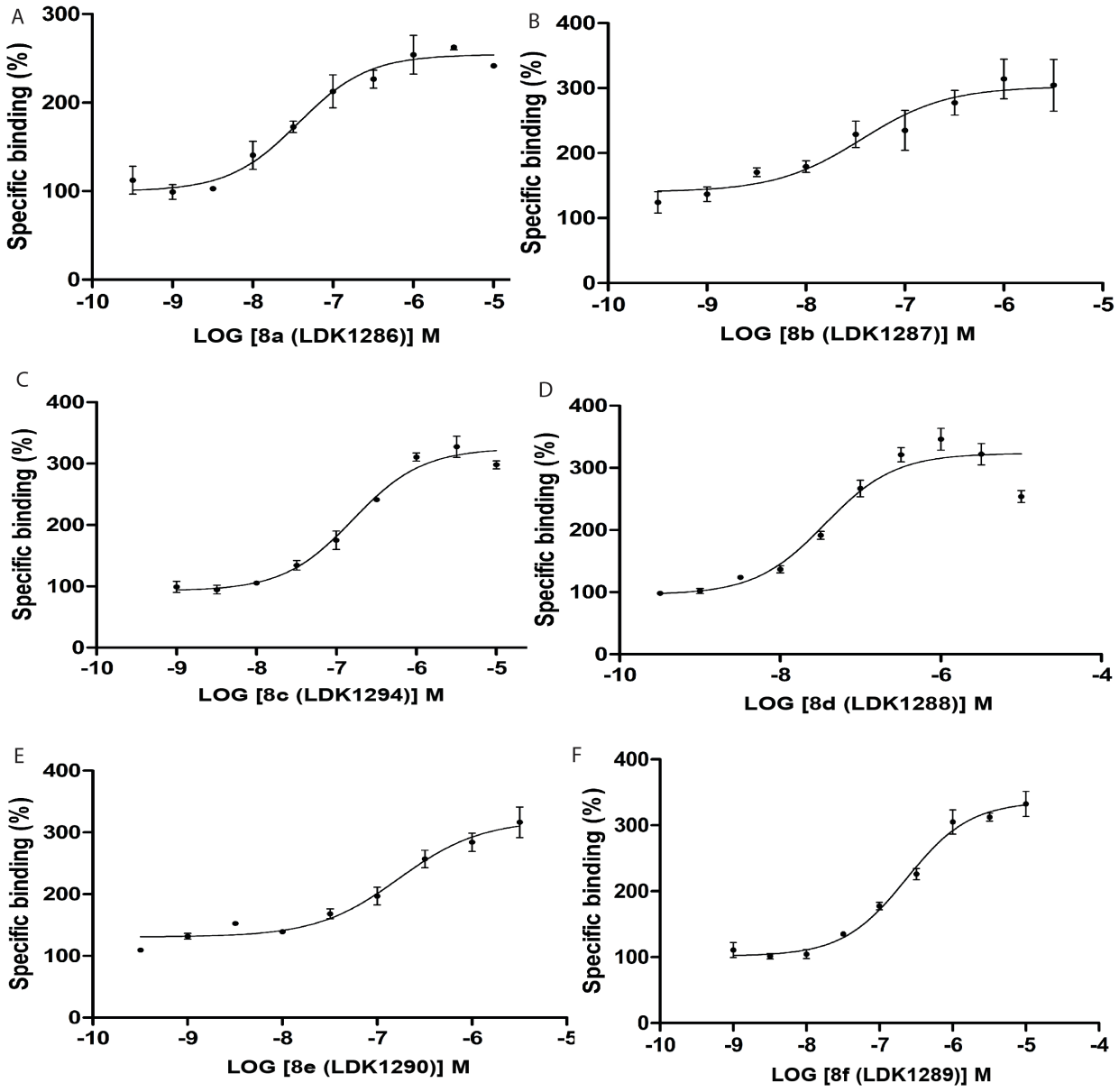

Figure 3.7 Binding curves for analogs 8a-8f. The binding curves show the impact of varying concentrations of test compounds 8a (A), 8b (B), 8c (C), 8d (D), 8e (E) and 8f (F) on the binding of [^{3}H]CP55,940.

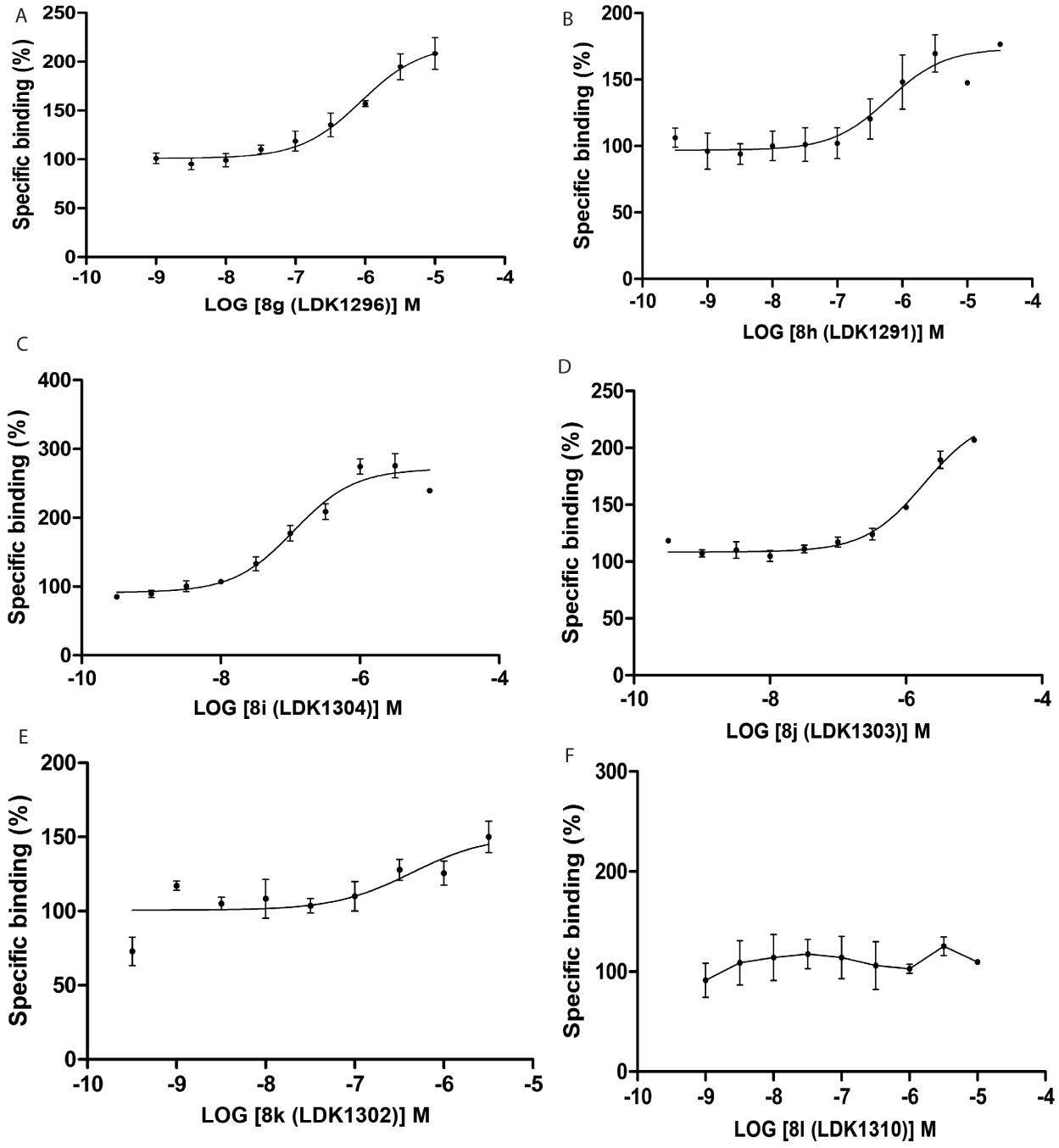

Figure 3.8 Binding curves for analogs 8g-8l. The binding curves show the impact of varying concentrations of test compounds 8g (A), 8h (B), 8i (C), 8j (D), 8k (E) and 8l (F) on the binding of [^{3}H]CP55,940 .

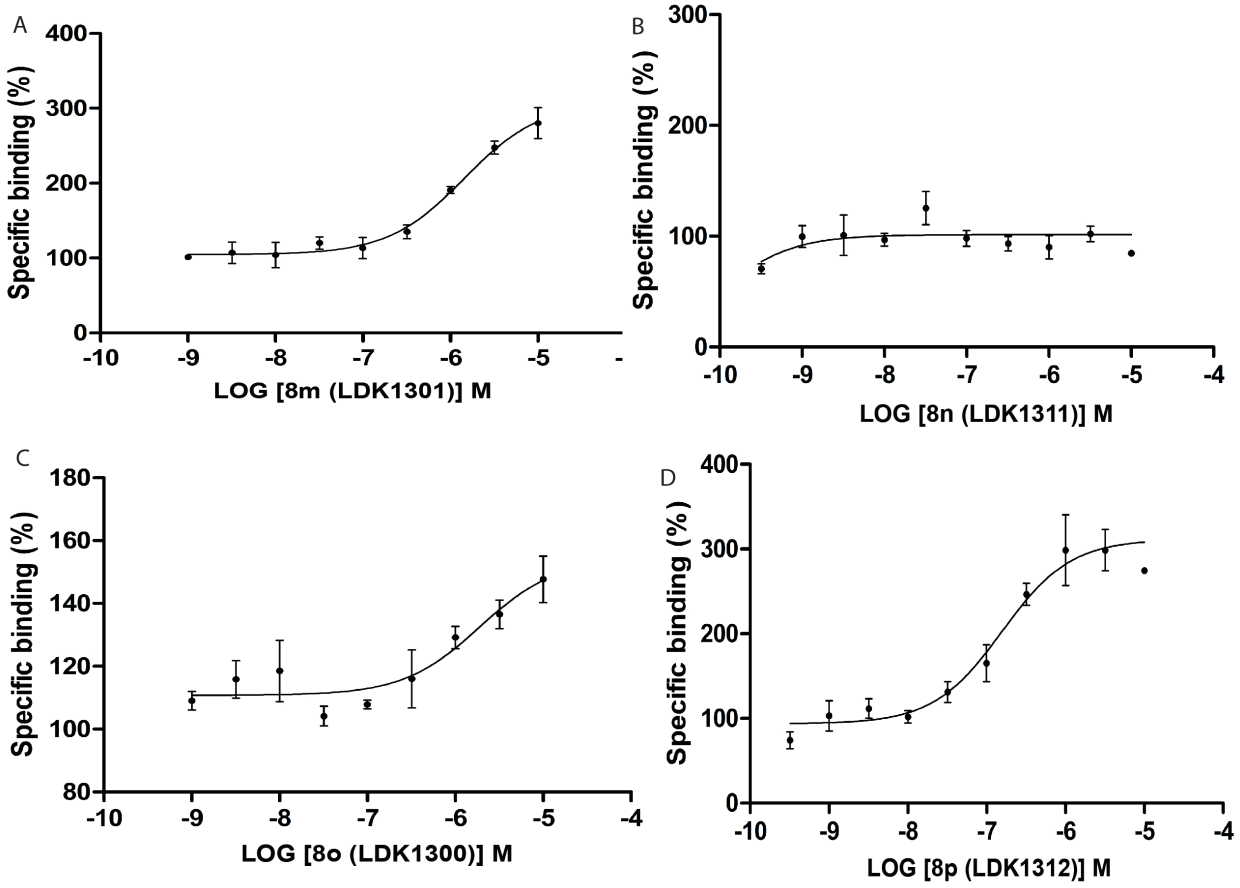

Figure 3.9 Binding curves for analogs 8m-8p. The binding curves show the impact of varying concentrations of test compounds 8m (A), 8n (B), 8o (C) and 8p (D) on the binding of [^{3}H]CP55,940.

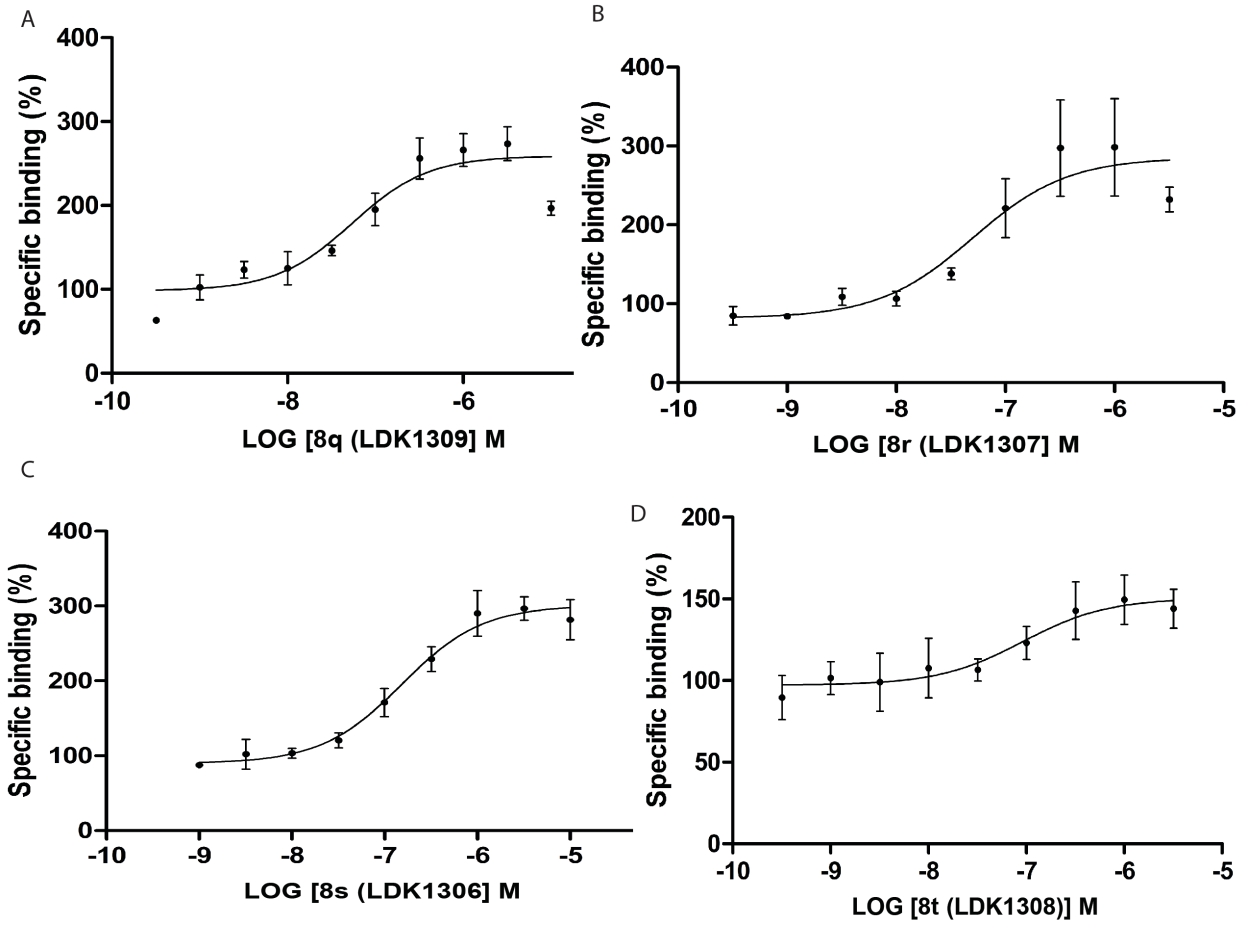

Figure 3.10 Binding curves for analogs 8q-8t. The binding curves show the impact of varying concentrations of test compounds 8q (A), 8r (B), 8s (C) and 8t (D) on the binding of [^{3}H]CP55,940.

To further confirm the value of the novel allosteric modulators, compounds **8d** (**LDK1288**), **8r** (**LDK1307**), **7a** (**LDK1283**), **8a** (**LDK1286**) and **7d** (**LDK1285**) were selected to compare with **2** in a [^{35}S]GTPγS binding assay indicative of G protein coupling. The results were shown in Figure 3.11. In the functional assay, compounds **7a** (**LDK1283**) and **8a (**LDK1286**)** are weaker antagonists than **2** in reducing the G-protein coupling to the CB_1 receptor. In contrast,

compounds **7d** (**LDK1285**) and **8d** (**LDK1288**) showed potency comparable to **2** in reducing the G-protein coupling. Notably, although **7d** (**LDK1285**) has a weaker binding affinity to the allosteric site than **8d** (**LDK1288**) and **8r** (**LDK1307**), it displayed potency similar to **8d** (**LDK1288**) and **2** in the functional assay. This was indicated by their relative potency at the 0.3 μM testing concentration in the [^{35}S]GTPγS binding assay. In combination with the allosteric binding parameters, we conclude that compounds **7d** (**LDK1285**) and **8d** (**LDK1288**) are viable CB_1 allosteric modulators showing a similar binding profile and functional activity to **2**.

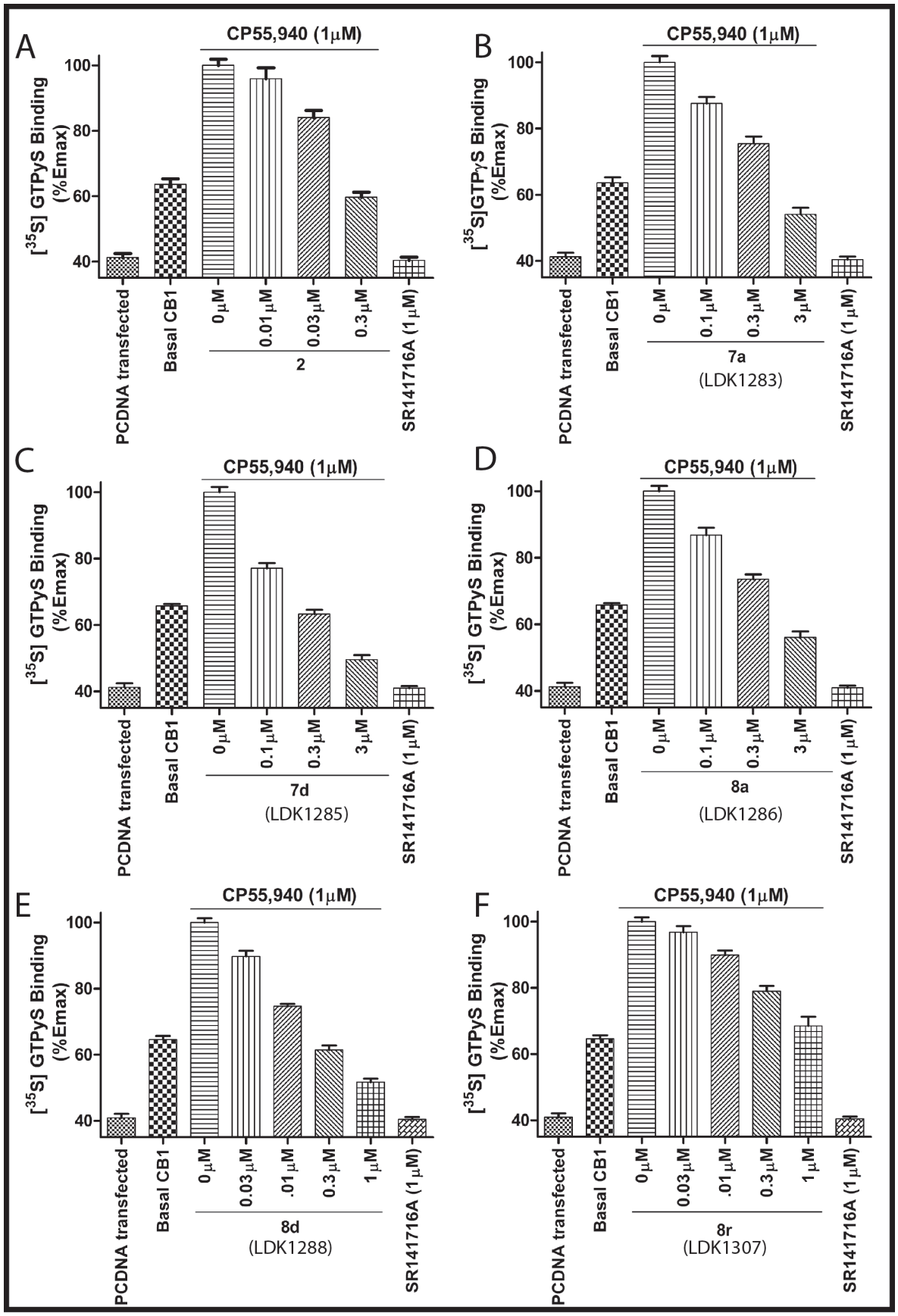
A
CP55,940 (1μM)
[35S] GTPyS Binding (%Emax)
100
80
60
40
PCDNA transfected
Basal CB1
0μM
0.01μM
0.03μM
0.3μM
2
SR141716A (1μM)
B
CP55,940 (1μM)
[35S]GTPγS Binding (%Emax)
PCDNA transfected
Basal CB1
0μM
0.1μM
0.3μM
3μM
7a
(LDK1283)
SR141716A (1μM)
C
CP55,940 (1μM)
[35S] GTPyS Binding (%Emax)
PCDNA transfected
Basal CB1
0μM
0.1μM
0.3μM
3μM
7d
(LDK1285)
SR141716A (1μM)
D
CP55,940 (1μM)
[35S] GTPyS Binding (%Emax)
PCDNA transfected
Basal CB1
0μM
0.1μM
0.3μM
3μM
8a
(LDK1286)
SR141716A (1μM)
E
CP55,940 (1μM)
[35S] GTPyS Binding (%Emax)
PCDNA transfected
Basal CB1
0μM
0.03μM
.01μM
0.3μM
1μM
8d
(LDK1288)
SR141716A (1μM)
F
CP55,940 (1μM)
[35S] GTPyS Binding (%Emax)
PCDNA transfected
Basal CB1
0μM
0.03μM
.01μM
0.3μM
1μM
8r
(LDK1307)
SR141716A (1μM)

Figure 3.11 CP55,940-induced GTPγS levels in the presence and absence of varying concentrations of test allosteric modulators. HEK293 cell membranes expressing the CB_1 receptor was tested for GTPγS levels in the absence and presence of compounds (A) PSNCBAM-1 (**2**), (B) **7a** (**LDK1283**), (C) **7d** (**LDK1285**), (D) **8a** (**LDK1286**), (E) **8d** (**LDK1288**) (F) **8r** (**LDK1307**) at the indicated concentrations in the presence of CP55,940 (1 μM). The basal levels of [^{35}S]GTPγS binding were also measured in the absence of any orthosteric and allosteric ligand (Basal CB_1), and the inhibition of it was tested by treatment with SR141716A (1 μM). Data are presented as a percentage of the GTPγS levels in the presence of CP55,940 (1μM). Each data point represents the mean ± SE (error bars) of at least three independent experiments performed in duplicate. Non-CB_1-mediated GTPγS levels were measured by obtaining [^{35}S]GTPγS binding to membrane preparations transfected with empty vector PCDNA3.1 (PCDNA transfected).

3.5 Conclusion and Future Directions

The recent identification of CB_1 allosteric modulators indicated a new approach for developing safer therapeutics based on regulating the pharmacologically important CB_1 receptor. Unlike CB_1 orthosteric ligands, which typically present undesired psychotropic and psychiatric side effects, allosteric modulators have a better chance to avoid untoward side effects. This is because modulation of the receptor can be more finely regulated. Furthermore, if biased signaling pathways are utilized, signal transduction is more pathway-specific. In contrast to the vast structural diversity of CB_1 orthosteric ligands, the structural diversity of CB_1 allosteric modulators are fairly limited. This work identified novel lead compounds from the biphenyl ureas that possess a pyrimidine ring in their structures. The new compounds showed biological activities comparable to the well-established CB_1 allosteric modulator PSNCBAM-1(**2**) that has a pyridine moiety. In comparison with pyridine, the pyrimidine structure offers more synthetic versatility. It has a π-electron density decreased to an even greater extent than pyridine (Brown et al., 2009). Therefore, nucleophilic aromatic substitution is facilitated. Synthetically, the electron-deficient nature of pyrimidine accounts for better opportunities than pyridine when nucleophilic aromatic substitution chemistry is employed in functionalization of the electron-deficient heteroaromatic ring (Brown et al., 2009). Collectively, the newly identified pyrimidinyl biphenyl urea analogs provide new opportunities for the development of novel and potent CB_1 allosteric modulators.

Since these allosteric modulators demonstrate a paradoxical behavior of improving binding affinity of orthosteric ligands, yet decreasing G-protein coupling efficacy of orthosteric ligands which is similar to what is seen with indole-2-carboxamides, it will of interest to investigate whether these ligands also demonstrate a positive modulation of β-arrestin mediated

pathways such as ERK1/2, JNK1/2/3 etc. Further investigation of different kinases impacted by these analogs may help to better evaluate how these analogs manipulate different signaling pathways mediated by CB_1. Also, investigation of these allosteric modulators in anti-obesity animal models will help translate the efficacy of these compounds from cellular models to animal models.

CHAPTER 4

Identifying the Allosteric Binding Site on the CB_1 Receptor

4.1 Background

Despite the advantages posed by allosteric modulation of CB_1 for developing therapeutics, structure-based drug design is difficult for CB_1 due to lack of information regarding the site(s) of binding of allosteric modulators. The difficulty in crystallizing these largely hydrophobic receptors further hinders the identification of key motifs that form the allosteric binding pocket on the CB_1 receptor. Different modeling and experimental data generated by different researchers have identified three different allosteric sites (Fay et al., 2012; Shore et al., 2013; Stornaiuolo et al., 2015)). However, no consensus exists so far as to which of these models truly identifies the allosteric binding site. In our efforts to identify the allosteric binding site on the CB_1 receptor, we chose a chimeric receptor construct approach to evaluate which regions of the receptor may be involved in the binding of allosteric modulators, ORG27569 and PSNCBAM-1. Chimeras of CB_1 and CB_2 were constructed where portions of low-affinity sequences of CB_2 replaced the corresponding pieces of high affinity sequences from the CB_1 receptor. Since these allosteric modulators bind to CB_1 and not CB_2 (Ahn et al., 2012; Horsewill et al., 2010), the chimeric constructs were evaluated for loss of binding affinity to identify motifs that may involve residues important for binding of allosteric modulators. In this chapter, we piloted this approach to negate some of the possible hypothesis of allosteric binding site and identify a region that may play a key role in allosteric ligand binding. This data will lay the basis for further investigating the regions that may be involved in binding of these allosteric modulators.

4.2 Introduction

Research in cannabinoid-based therapeutics has been severely impeded by the lack of subtype-specific drugs for CB_1 and CB_2 which may cause side-effects. The two subtypes of the cannabinoid receptor family, i.e. CB_1 and CB_2, have a transmembrane sequence identity of 51% (Shire et al., 1996) making subtype specific ligands that target this region in CB_1 difficult to generate. The discovery of ORG27569 as an allosteric modulator of the CB_1 receptor has demonstrated that at least one allosteric site exists on the CB_1 receptor. While most orthosteric ligands like CP55,940 bind non-selectively to both CB_1 and CB_2, ORG27569 doesn't bind CB_2 up to 10 μM (Ahn et al., 2012). Identifying the amino acid residues that confer specificity of binding to ORG27569 can help in defining the allosteric binding site. Identification of the allosteric binding site will allow an understanding of the mechanisms by which ORG27569 displays a contradictory profile i.e it increases CP55,940 binding while decreasing G-protein coupling associated with CP55,940 (Ahn et al., 2012). Identifying the allosteric binding pockets will also allow structure-based drug design for modulators with improved allostery at the CB_1 receptor.

Three different research groups have utilized different techniques to identify the putative allosteric binding pockets at the CB_1 receptor and investigate the mechanisms that could explain the contradictory profile of ORG27569 being a PAM for CP55,940 binding but an allosteric antagonist for G-protein coupling. However all three of the putative allosteric binding sites identified by these groups do not seem to overlap. Fay and colleagues (Fay et al., 2012) investigated how different conformations of the receptor are induced by ORG27569 which could explain the molecular pharmacology of ORG27569. Site-specific fluorescent labeling of the receptor was done to identify conformational changes in CB_1 upon binding of ORG27569. A

mutant of CB_1 lacking the cysteines was generated with only Cys-257 and Cys-264 not mutated as these two cysteines are involved in a disulfide bond formation and are necessary to retain a functional receptor. A cysteine was then introduced in the mutant at residue 342 which lies in the TM6 on the intracellular side. A bimane label was then used to label the cysteine at residue 342 and changes in fluorescence were monitored with the label introduced. The mutation was introduced at residue 342 as changes in TM6 have been reported for GPCR activation. The authors demonstrated that changes in fluorescence intensity occurs upon interaction of the mutant with agonist CP55,940. However, incubation of the receptor preparations with ORG27569 blocked the change in fluorescence intensity. It was thus concluded that ORG27569 arrests the receptor in an agonist-bound non-G-protein signaling state by blocking the movements in TM6 from the agonist). Further investigations by this group identified a disulfide bond in the N-terminus of the receptor to play an important role in the allosteric effects seen with ORG27569 and PSNCBAM-1. The disulfide bond was formed by Cys98 and Cys107. Interestingly, they found that reduction of this disulfide bond in the amino-terminus resulted in enhancement of the cooperativity effects seen with ORG27569 and PSNCBAM-1. The authors suggested that the allosteric modulators may bind to this region and alter the dissociation of the orthosteric ligand CP55,940, thus enhancing CP55,940 binding. However, the studies lacked a direct evidence to show the impact of the disulfide bridge on binding affinities of the allosteric ligands, thus suggesting that the disulfide bond may play an indirect effect of the allostery at CB_1 receptor but may not be be part of the allosteric binding pocket.

Shore and colleagues utilized molecular modeling, mutagenesis and G-protein coupling assays to define the allosteric binding pocket for ORG27569 (Shore et al., 2013). The approach for the identification of the allosteric site was based on the observation that ORG27569, in ligand

displacement assays, decreases the equilibrium binding of SR141716A, an inverse agonist of CB_1 receptor. Thus ORG27569 may have an overlapping binding site with SR141716A. Computational modeling of ORG27569 on the CB_1 receptor was done with docking the ligand manually in the TMH3-6-7 region. Modeling data suggested that the binding site for ORG27569 overlaps with the binding of SR141716A. Residues $K192^{3.28}$, $F200^{3.36}$, $W279^{5.43}$ and $W356^{6.48}$, which have previously been reported to be important for SR141716A binding were mutated to alanine and tested for their impact on G-protein coupling efficacy of CP55,940 with ORG27569. Incubation of CB1Wt membrane preparations with ORG27569 (1μM) showed a complete loss of CP55,940 induced G-protein coupling. Mutants that would cause a loss of ORG27569 binding would demonstrate decrease in the antagonism of G-protein coupling by ORG27569, which will be seen by higher G-protein coupling levels. Only K192A mutant showed an increase in G-protein coupling in presence of ORG27569 compared to CB1WT, suggesting this amino acid plays an important role in the binding of ORG27569. The computational modeling suggested that the piperidine nitrogen of ORG27569 is involved in forming hydrogen bonding with K192. However, K192 has also been reported to directly impact the binding of CP55,940 (Song et al, 1996, Shim et al., 2010). The authors showed that K192A mutant demonstrated a high EC_{50} (225 nM) for CP55,940-induced G-protein coupling because of its role in CP55,940 binding. However, ORG27569 could only antagonize 41% of the levels exhibited by CP55,940. Also, since this residue is conserved between CB_1 and CB_2, this mutation does not describe why ORG27569 binds to CB_1 and not CB_2. The computational modeling also predicts F268 from the EC2 loop to form aromatic stacking interactions with the indole-ring of ORG27569. No mutagenesis studies were reported for this residue.

Stornaiuolo and colleagues identified an entirely different site of binding for ORG27569 (Stornaiuolo et al., 2015). The group utilized computational modeling techniques using sphingosine 1-phosphate receptor to build a homology model of CB_1 receptor, to identify five different possible allosteric binding sites. Out of all the sites, the few residues that were different in CB_1 and CB_2 were mutated in CB_1 to the corresponding residues in CB_2 receptor. Fluorescence binding assays were done using a fluorescent tetra-methyl-rhodamine (TAMRA) labeled form of the CB_1 inverse agonist, AM251, namely T1117. The mutations were first evaluated for their impact on T1117 binding. The mutations that did not affect T1117 binding were then evaluated for change in T1117 binding in the presence of ORG27569. It has been previously demonstrated by the same group (Bruno et al., 2014) that binding of T1117 to CB_1WT is negatively impacted by ORG27569. Loss of T1117 binding would suggest that the mutations are not important for ORG27569 binding. If however, no change in T1117 binding is seen in the presence of ORG27569, the mutation is considered important for ORG27569 binding. Photoactivatable analogs of ORG27569 were also utilized to cross-link with CB_1 and residues important for binding were then evaluated from mass-spectrometry. The authors identified an intracellular binding site for ORG27569 (Stornaiuolo et al., 2015). This was in complete contrast to the site(s) identified by the other group of researchers which suggested more extracellular sites of binding. Mutational analysis identified three mutations $C^{1.55}Y$, $H^{2.41}L$ and $F^{4.46}L$ (P2 in the intracellular regions of TM1,2 and 4), that demonstrated no loss of T1117 binding upon incubation with ORG27569, suggesting these residues to be important for binding of ORG27569. The mass-spectrometry data identified two serines, $S^{2.45}$ and $S^{3.42}$ to be important for the binding of ORG27569. The mass-spectrometry data did not report the residues found important from mutagenesis to be involved in cross-linking although the residues belong to the same region. The

authors negated two other extracellular pockets (P3 in the transmembrane regions of TM3 and 4; and P4 in the extracellular regions in TM3 , 6 and 7) identified from modeling based on one mutant tested from each region. Also, another pocket identified by computational analysis in the intracellular surface of TM 1, 7 and 8 was evaluated by two mutants, $I^{7.51}V$ and $F^{8.54}A$. The $I^{7.51}V$ demonstrated no loss in T1117 binding in the presence of ORG27569, suggesting this residue to be important for ORG27569 binding.. However, this mutant was not pursued further because $F^{8.54}A$ of the same pocket in exhibited loss in T1117 binding in the presence of ORG27569.

Thus, overall, different researchers have identified very different sites of binding of ORG27569 and none agree with each other (Fay et al., 2012; Shore et al., 2013; Stornaiuolo et al., 2015). Also, no investigations into the binding site for PSNCBAM-1 have been reported.

To identify the regions of the CB_1 receptor important for ORG27569 and PSNCBAM-1 binding, we chose a chimera construction approach. CB_1 and CB_2 have a high degree of conservation in the transmembrane regions (Shire et al., 1996). As a result, most of the orthosteric ligands such as CP55,940, WIN55,212-2 are not subtype-specific and bind both CB_1 and CB_2. However, most of the allosteric modulators of the CB_1 receptor known so far such as ORG27569, PSNCBAM-1 show undetectable binding to the CB_2 receptor (Ahn et al., 2012; Horsewill et al., 2010). We took advantage of this subtype selectivity and constructed chimeras of CB_1 and CB_2, where no -binding sequences of CB_2 replaced the corresponding pieces of high affinity sequence in CB_1 to evaluate loss of binding affinity of allosteric modulators to identify the CB_1 allosteric site(s). Two pharmacophorically different allosteric modulators, ORG27569 and PSNCBAM-1 (Figure 4.1) were chosen to identify whether multiple binding sites or the sane site exists on CB_1 receptor for these allosteric modulators.

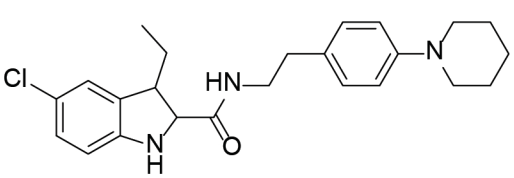

ORG27569

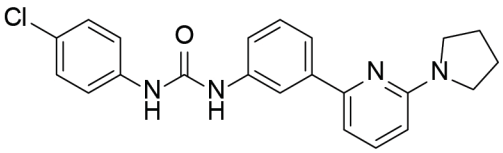

PSNCBAM-1

Figure 4.1 Structures of some allosteric modulators of the CB_1 receptor.

4.3 Materials and Methods

Construction of chimeric receptors and site-directed mutagenesis. For the construction of chimeric receptors, sequences recognized by AgeI (ACCGGT) and NotI (GCGGCCGC) enzymes were introduced in CB_1 and CB_2 vectors at the beginning and end of the regions which were to be exchanged. The two vectors were digested and run on an agarose gel to separate the sliced regions. The regions of interest of CB_1 and CB_2 were cut out of the agarose gel and the DNA was extracted. The two regions were ligated by DNA ligase and the sequences for AgeI and NotI were deleted by site-directed mutagenesis to form the chimeric constructs. For some of the chimeras which had small inserts such as those of the EC3, EC2, IC1 and IC2 loops, sequential site-directed mutageneis was performed (QuikChange, Stratagene, La Jolla, CA) to construct the chimeras using the human CB_1 cDNA cloned into pcDNA3.1 as a template, following the manufacturer's protocol. Nomenclature used for chimeric receptors is: CB_1/CB_2 (region replaced) as previously described (Shire et al., 1996). All the chimeric mutations were confirmed by DNA sequencing.

Expression of constructs and membrane preparation. Wild type-CB_1 or the CB_1/CB_2 constructs were expressed in HEK293 cells and membrane prepared as described previously (Ahn et al., 2012). Briefly, HEK293 cells were seeded at 1,00,000 cells in 100 mm dishes. The

cDNA encoding CB_1 or the newly generated constructs was transiently transfected using calcium-phosphate precipitation method. 24h post-transfection, the cells were harvested and washed with phosphate-buffered saline (PBS) and resuspended in PBS containing mammalian protease inhibitor cocktail ((4-2-aminoethyl) benzene-sulfonyl fluoride, pepstatin A, E-64, bestatin, leupeptin, and aprotinin) (Sigma-Aldrich, St. Louis, MO). The cells were lysed by nitrogen cavitation and the lysate collected. The lysate was spun at 500 *g* for 10 min to remove nuclei and cell debris, followed by centrifugation of the supernatant at 100,000 g for 45 min at 4°C. The pelleted membrane is then resuspended in TME buffer (25 mM Tris-HCl, 5 mM $MgCl_2$, and 1 mM EDTA, pH 7.4) containing 7% w/v sucrose.

Radioligand binding assays. To assess proper folding and expression of the chimeric receptors and that the chimeras do not impact the orthosteric site, the chimeric receptors were evaluated for their CP55,940 binding. Membrane preparations of the chimeric constructs were incubated with at least nine different concentrations of CP55,940 (ranging from 100 pM to 1 μM) in the presence of a fixed concentration of [^{3}H]CP55,940 (141.2 Ci/mmol, PerkinElmer Life Sciences (Boston, MA)), typically at its K_D as previously described (Antona et al., 2006).

For determining the allosteric parameters K_B and α, the receptor preparations were incubated with nine different concentrations of ORG27569 or PSNCBAM-1 (ranging from 100 pM to 100 μM) in the presence of a fixed concentration of [^{3}H]CP55,940 as previously described (Ahn et al., 2012).

For both the assays described above, TME containing 0.2% fatty acid-free BSA was used as a reaction buffer to make a final volume of 200 μL. Unlabeled CP55,940 (1 μM) was incubated with membrane preparations to determine the non-specific binding. The reaction was incubated

at 30°C for an hour and the reaction was adding 300 µL of TME containing 5% BSA followed by filtration through Whatman GF/C filter paper using a Brandel cell harvester. The filter paper was washed with ice-cold TME buffer to reduce non-specific binding and radioactivity of the collected samples was measured.

Data analysis. Each data point in the radioligand binding assays was performed in duplicate and each curve is generated from at least three independent assays. Data are presented as a mean with the corresponding 95% confidence limits. Data was analysed using nonlinear regression using Prism 6.0 (Graph pad Software Inc., San Diego, CA) as described previously (Ahn et al., 2012). The K_B values of wild-type CB_1 were compared with the mutants using analysis of variance (ANOVA) followed by Dunnett's test. $P<0.05$ was considered statistically significant.

4.4 Results and discussion

In our efforts to identify the allosteric binding site(s), chimeric constructs of CB_1/CB_2 were made (as shown in Figure 4.2) based on two hypotheses. CB_1/CB_2 chimeras previously published to be functional and properly folded will also be used to guide chimera construction (Shire et al., 1996). Following were the two hypothesis:

1. Most of the positive allosteric modulators of CB_1 including ORG27569, PSNCBAM-1 decrease G-protein coupling suggesting that this allosteric modulator binding site(s) may overlap with the G-protein coupling site and physically preclude G-protein coupling. Modeling and mutational analysis of the CB_1 receptor have demonstrated that the intracellular loop especially IC3 and C-terminus tail are regions where the G-protein may couple to (Shim et al., 2016). Thus, chimeric constructs of IC loops and the C-terminal tail were constructed.

2. The allosteric modulators of CB_1 are highly subtype specific and do not bind to CB_2, suggesting that there is a high sequence divergence at the allosteric binding site(s). The transmembrane regions show a high sequence homology of 70% in the transmembrane regions. However, the EC and IC loops have high sequence divergence. An allosteric binding site in the EC loops has been reported for some GPCRs such as mAChRs where mutation of an acidic sequence called EDGE in the M_2 subtype to the corresponding neutral sequence LAGQ of M_1 subtype resulted in reduced affinity of the allosteric modulator, Gallamine for M_2 receptor subtype (Gnagey et al., 1999). Thus, chimeric mutants of the EC loops were constructed.

To evaluate proper folding and expression of the receptor and to ensure that these mutations do not impact the orthosteric binding site, competition assays with [^{3}H]CP55,940 were performed for the chimeric receptors. As seen in Table 1, none of the chimeric mutants except IC2 showed alterations in K_i values for CP55,940 compared to wild type CB_1, suggesting that these mutations do not impact the orthosteric ligand binding site. This was not surprising since CP55,940 binds to both CB_1 and CB_2 with similar affinities and no TM regions were mutated. The chimeric mutants were further evaluated for their impact on the allosteric binding parameters, K_B and α. Two pharmacophorically different allosteric modulators, ORG27569 and PSNCBAM-1 (Figure 4.1) were used and their allosteric parameters were evaluated. Statistical analysis of the allosteric parameters was performed versus wild type CB_1 bound to the allosteric ligand under the same conditions.

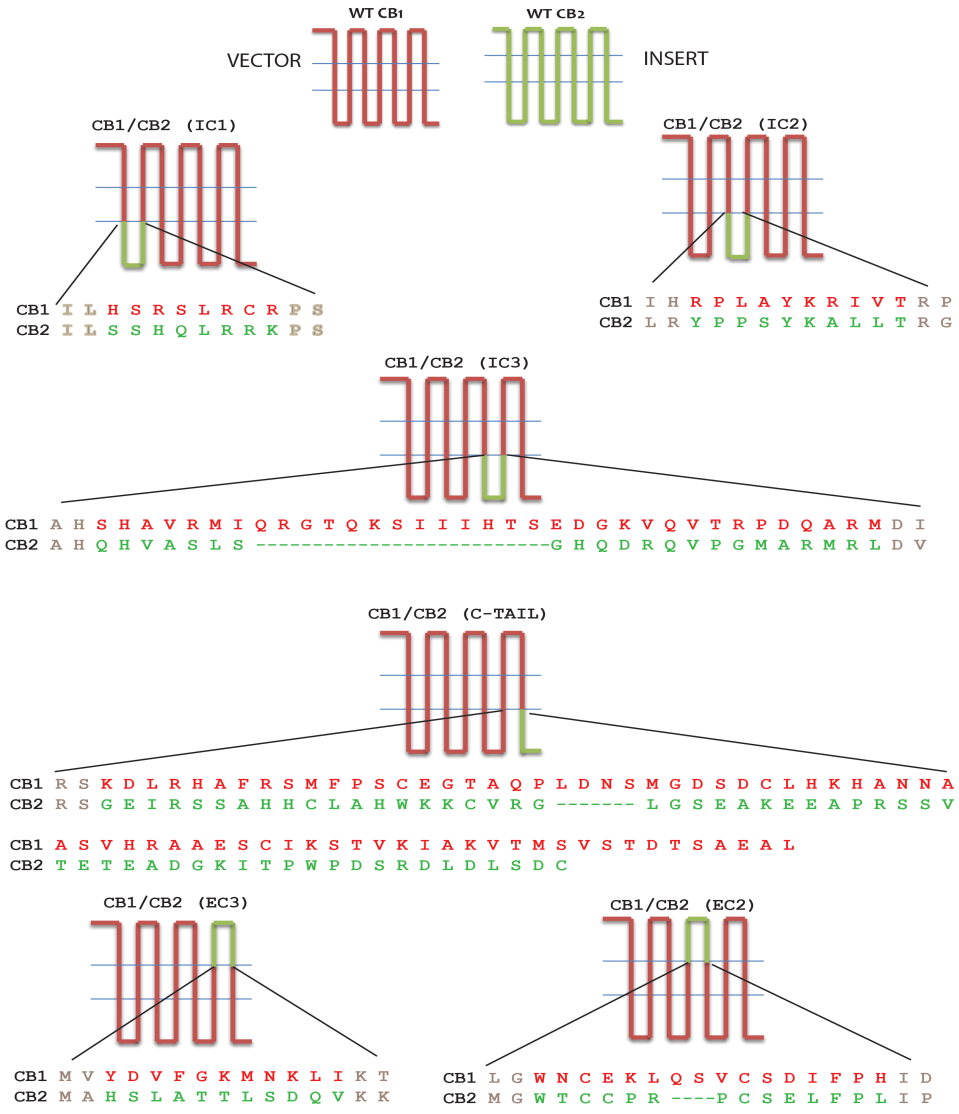

Figure 4.2 Schematic representations of the amino acid sequences of CB_1, CB_2 and the CB_1/CB_2 chimeras. Amino acid sequences of the regions of CB_1 that was replaced are shown in red and the regions of CB_2 that were inserted are shown in green for the different chimeric mutants. The residues of the putative transmembrane regions which flank the points of digestion are shown in grey.

As shown in the Table 4.1, none of the chimeric mutants demonstrated any change in the allosteric parameters for PSNCBAM-1, suggesting that these regions do not play a key role in the binding of PSNCBAM-1.

Interestingly, for ORG27569, some of the chimeric mutants showed a decrease in the binding affinity as reflected by high K_B values as shown in Figure 4.3 and Table 1. In particular, the CB_1/CB_2 (EC2) chimera showed a statistically significant decrease in the binding affinity of ORG2756, thus suggesting the importance of this loop in the binding affinity of ORG27569. The difference in the impact of these mutants on ORG27569 versus PSNCBAM-1 suggests that these allosteric modulators may bind different sites on the CB_1 receptor. Further investigations of these motifs may help identify the key amino acids that cause the preferential binding of ORG27569 to CB_1 as compared to CB_2.

Receptor	CP55,940 Binding	ORG27569 Binding[a]		PSNCBAM-1 Binding[a]	
	K_i (nM)	K_B (nM)	α	K_B (nM)	α
Wild Type	1.7 (1.2-2.6)	380 (271.6-531.5)	5.2	54.3 (21.9-134.6)	7.3
CB_1/CB_2 (C-tail)	2.9 (1.2-7.6)	296.8 (115-766)	14	62.9 (17.9-221)	9.6
CB_1/CB_2 (IC1)	3.6 (1.7-5.5)[b]	1057 (738-1514)	6.7	138.3 (75.7-252)	4.5
CB_1/CB_2 (IC2)	NB	ND	ND	ND	ND
CB_1/CB_2 (IC3)	1.2 (0.7-2.0)	502.3 (277.3-909.9)	3.8	78.5 (44.8-138)	4.0
CB_1/CB_2 (EC2)	0.5 (0.1-1.9)	2265 (1486-3453)*	4.3	116.6 (36.5-373)	2.9
CB_1/CB_2 (EC3)	2.8 (0.7-12.1)	881.2 (566-1372)	4.9	109.9 (39.4- 306)	3.0

Table 4.1. Binding parameters for the different CB_1/CB_2 chimera mutants. The K_i values for [^{3}H]CP55,940 binding to the wild-type and the CB_1/CB_2 chimera mutants is shown. For the allosteric modulators, ORG27569 and PSNCBAM-1, the parameters, K_B and α are shown in the table. Data are presented as a median and the corresponding 95% confidence limits, from atleast three independent assays that were performed in duplicate. Asterisks depict the statistically significant differences between the parameters of chimeric mutants compared with the wild-type receptor using analysis of variance followed by Dunnett's test. *, $P < 0.05$, **, $P < 0.01$, ***, $P < 0.001$. NB: no detectable binding for [3H]CP55,940 was seen upto 32 μM. ND: not determined for ORG27569 and PSNCBAM-1 binding due to loss of [3H]CP55,940 binding. [a]: using [^{3}H]CP55,940 as the orthosteric ligand. [b] data represents K_D values for the chimera.

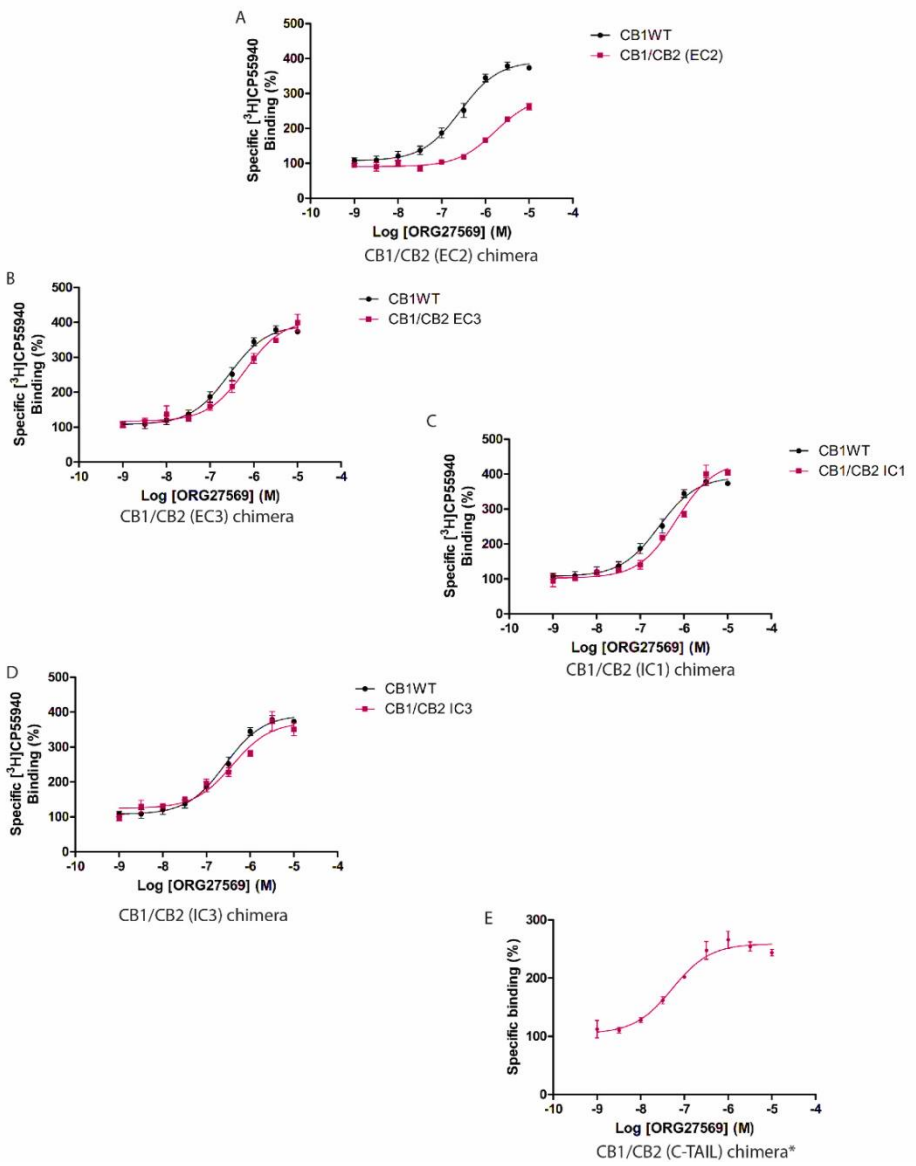

Figure 4.3 Binding curves of ORG27569 binding to CB_1 wild-type and the different CB_1/CB_2 chimeric mutants. The curves show comparison of modulation of [^{3}H]CP55,940 binding by different concentrations of ORG27569 to the wild-type CB_1 receptor and (A) CB_1/CB_2 (EC2) chimera, (B) CB_1/CB_2 (EC3) chimera, (C) CB_1/CB_2 (IC1) chimera, (D) CB_1/CB_2 (IC3) chimera and (E) CB_1/CB_2 (C-tail) chimera. *the CB_1WT curve is not shown because different concentration of [^{3}H]CP55,940 was used for determining the K_B values.

4.5 Conclusions and Future Directions

This project helps to identify the key motifs that are involved in the identification of the allosteric site on the CB_1 receptor. Interestingly, we found that the extracellular loop EC2 significantly altered the affinity parameter, K_B for ORG27569. However, none of the tested mutants impacted the binding of PSNCBAM-1. This suggests that multiple allosteric sites may exist on the CB_1 receptor. A reasonable argument for the extracellular loops to be involved in the allosteric binding site may be that it is because the allosteric site is extracellular in nature that CP55,940, which binds in the transmembrane region, is blocked from dissociating from the receptor due to an allosteric ligand residing above it, which increases the binding of CP55,490. Interestingly, the two extracellular loops show a high sequence divergence as shown in Figure 4.2. Further investigations of the amino acid residues can help identify the individual amino acids that may be responsible for the binding of ORG27569. Many charged amino acids in the CB_1 receptor in the EC2 loop are replaced by uncharged residues in the CB_2 receptor and vice-versa, which could explain the loss of charged interactions of ORG27569 upon binding to the CB_2 receptor. Some of these residues include:

1. Positively charged E258, which is replaced by an uncharged cysteine in the CB_2 receptor.
2. Positively charged K259, which is replaced by an uncharged proline in the CB_2 receptor.
3. Uncharged L260, which is replaced by a positively charged arginine in the CB_2 receptor.
4. Positively charged H270, which is replaced by an uncharged leucine in the CB_2 receptor.

Binding assays using point mutations replacing the CB_1 residue for the corresponding CB_2 residues will help to identify key interactions which stabilize ORG27569 binding to the CB_1 receptor.

Once the amino acids that play a key role in the binding of these allosteric modulators are identified, further evaluation on how these residues affect G-protein coupling would help identify the mechanisms which cause a decrease in G-protein coupling efficacy with these modulators. Evaluation of these motifs for their impact on β-arrestin coupling efficacy is another area of interest that can be investigated.

Identification of the allosteric binding sites at the CB1 receptor will provide a better understanding of the molecular mechanisms that govern allostery at the CB1 receptor. It will also aid in screening of additional compounds using virtual libraries that may provide improved properties like higher affinity and improved cooperativity with the receptors. These studies will pave the way for a structure-based drug design for allosteric modulators of CB_1 where the key amino acids in the allosteric pocket can be targeted to improve allostery at the CB_1 receptor.

Chapter 5
Conclusions and Future Directions

In this thesis project, we aimed to improve our understanding of allosteric modulation of the CB_1 receptor by focusing on two important scaffolds that demonstrate allosterism. First, the indole-2-carboxamide, which is the scaffold of ORG27569, was evaluated to identify the key chemical functionalities that are important for exhibiting allostery at the CB_1 receptor. We identified that a critical length of the alkyl group on the indole ring is important for maintaining the allosteric parameters, K_B and α. While a n-propyl chain improves the α value for orthosteric ligand binding, a n-hexyl chain improves the binding affinity (K_B) of the allosteric modulator. We also identified that a dimethylamino substitution at the piperidinyl ring improves both the $\mathbf{K_B}$ and α values. We also demonstrated that the linker length between the indole ring and the piperidinyl moiety, when shortened or extended resulted in loss of allostery. The importance of a EWG at the C5 position of the indole-ring was also demonstrated and that change in position of substituent results in a loss of binding affinity of the allosteric modulators. A SAR study was also done with a pyrimidinyl biphenylurea scaffold, which was a modified scaffold of the compound PSNCBAM-1. The SAR study identified that a cyanide moiety at the para position of the aromatic ring A demonstrated an improved K_B value for both the regioisomers of this scaffold. We also identified that a diethylamino group substitution on the pyrimidine ring showed allosteric parameters similar to PSNCBAM-1.

For both the scaffolds, it was further demonstrated that these positive allosteric modulators of the CB_1 receptor were pathway-biased. They decreased G-protein coupling pathways of the CB_1

receptor. Interestingly, they function via β-arrestin 1 mediated pathways as was demonstrated by ERK1/2 phosphorylation by these allosteric modulators.

This project helps to demonstrate and appreciate that signaling via GPCRs is not linear. It has a pluridimensional nature and different conformations generated by different ligands cause manipulation of different signaling pathways. Thus, the same GPCR can exhibit signaling via different G-proteins or other signaling proteins such as β-arrestins. Taking advantage of this, a GPCR can be directed to trigger different translational responses depending upon the ligand bound to the GPCR. Future work on this project may include using the best allosteric modulators identified here for translational evaluation in mice models. Since the ORG27569 has shown promise for the treatment of addiction (Jie et al., 2014), evaluation of the robust allosteric modulators identified in this project may be done to evaluate the efficacy of these compounds for the treatment of addiction. Also, evaluation of pyrimidinyl biphenylurea derivatives in mice models for the treatment of obesity may be pursued as PSNCBAM-1 has shown promise as an anti-obesity drug previously (Horsewill et al., 2010).

Another goal of this thesis was the identification of allosteric site(s) on the CB_1 receptor. We identified the EC2 loop as likely to play a critical role in the binding of the allosteric modulator, ORG27569 but not PSNCBAM-1. This suggests that the motifs that were evaluated for ORG27569 are not part of the binding site of PSNCBAM-1. This opens up the possibilities that more than one allosteric site may exist on the CB_1 receptor. Moreover, the conformations induced by ORG27569 and its derivatives versus that induced by PSNCBAM-1 and its derivatives are likely different. Further, identifying which of the residues impact G-protein coupling inhibition by these allosteric modulators may be evaluated to understand the

mechanisms governing the contradictory impact of these allosteric modulators on orthosteric ligand binding and G-protein coupling.

Further evaluation of the EC2 loop by single-site mutations will allow identification of the key amino acid residues that are important for binding of ORG27569. This project will add to the computational modeling of the allosteric site(s) on the CB_1 receptor. This will further help in the strategic design of small molecules for lead identification and optimization, which is currently hindered by the paucity of reliable models of the CB_1 receptor.

Future directions of this project may include identifying differences in conformations of the CB_1 receptor upon binding to differentially biased ligands. For the CB_1 receptor, three ligands with different functional selectivity may be utilized:

1. Unbiased ligands such as 2-AG, which have been demonstrated to exhibit both G-protein dependent and β-arrestin dependent signaling (albeit with different kinetics).
2. G-protein biased ligands such as CP55,940 which is a G_i- biased ligand.
3. β-arrestin biased ligands such as the allosteric modulators ORG27569 and PSNCBAM-1 identified in this project.

Many FRET techniques such as FlAsh-based FRET are available that can be utilized to examine conformations (Hoffmann et al., 2005). For FlAsh-based FRET, specific tetracysteine sequence can be inserted in the intracellular loops of the CB_1 receptor that are identified by small, membrane-permeant derivative of fluorescein, FlAsh (fluorescent arsenical hairpin binder). By transiently transfecting CFP-tagged G_i-fusion protein or β-arrestin protein, and treating the CB_1 receptor with the different ligands mentioned above, changes in conformations of the receptor

upon binding to the different ligands may be identified. This will add to the wealth of information available for the dynamic changes in GPCRs with differently signaling ligands.

The current project identified modulation of one of the key kinases of the MAPK family, the ERK1/2. However, many other important downstream kinases other than ERK1/2 such as c-Jun, FAK, beta-catenin, CREB are present in cells, which may be differently impacted by treatment with the differentially-biased ligands. Future work on this project may include identifying how the biased ligands impact these downstream kinases. These future studies will help us to better understand the complex signaling pathways generated by different conformations of a receptor and their outcome. Finally, we need to learn how these impact animal models of diseases that can be treated via targeting CB_1. Moreover, new biomarkers that are modified by these compounds can be identified by examining the RNA expression.

References

Abadji, V.; Lucas-Lenard, J.M.; Chin, C.; Kendall, D.A. Involvement of the carboxyl terminus of the third intracellular loop of the cannabinoid CB1 receptor in constitutive activation of Gs. *J. Neurochem*. **1999**, 72, 2032–2038.

Ahn K.H.; Mahmoud, M.M.; Samala, S.; Lu, D.; Kendall, D.A.. Profiling two indole-2-carboxamides for allosteric modulation of the CB1 receptor. *J. Neurochem.* **2013**, 124, 584-589.

Ahn, K. H.; Mahmoud, M. M.; Kendall, D. A. Allosteric modulator ORG27569 induces CB1 cannabinoid receptor high affinity agonist binding state, receptor internalization, and Gi protein-independent ERK1/2 kinase activation. *J. Biol. Chem.* **2012**, 287, 12070-12082.

Ahn, K. H.; Mahmoud, M. M.; Shim, J. Y.; Kendall, D. A. Distinct roles of beta-arrestin 1 and beta-arrestin 2 in ORG27569-induced biased signaling and internalization of the cannabinoid receptor 1 (CB1). *J. Biol. Chem.* **2013**, 288, 9790-9800.

Ahn, K.H.; Bertalovitz, A.C.; Mierke, D.F.; Kendall, D.A. Dual role of the second extracellular loop of the cannabinoid receptor 1: ligand binding and receptor localization. *Mol. Pharmacol*. **2009**, 76, 833-842.

Ameri, A. The effects of cannabinoids on the brain. *Prog. Neurobiol*. **1999**, 58, 315-348.

D'Antona A.M.; Ahn, K.H.; Kendall, D.A. Mutations of CB1 T210 produce active and inactive receptor forms: correlations with ligand affinity, receptor stability, and cellular localization. *Biochemistry.* **2006**, 45, 5606-5617.

Atwood, B.K.; Mackie, K. CB_2: a cannabinoid receptor with an identity crisis. *Br. J. Pharmacol.* **2010**, 160, 467-479.

Baillie, G. L.; Horswill, J. G.; Anavi-Goffer, S.; Reggio, P. H.; Bolognini, D.; Abood, M. E.; McAllister, S.; Strange, P. G.; Stephens, G. J.; Pertwee, R. G.; Ross, R. A. CB(1) receptor allosteric modulators display both agonist and signaling pathway specificity. *Mol. Pharmacol.* **2013**, 83, 322-338.

Ballesteros, J.; Kitanovic, S.; Guarnieri, F.; Davies, P.; Fromme, B.J.; Konvicka, K.; Chi, L.; Millar, R.P.; Davidson, J.S.; Weinstein, H.; Sealfon, S.C. Functional microdomains in G-protein-coupled receptors — the conserved arginine-cage motif in the gonadotropin-releasing hormone receptor. *J. Biol. Chem*., **1998**, 273, 10445–10453.

Bauer, M.; Chicca, A.; Tamborrini, M.; Eisen, D.; Lerner, R.; Lutz, B.; Poetz, O.; Pluschke, G.; Gertsch, J. Identification and quantification of a new family of peptide endocannabinoids (Pepcans) showing negative allosteric modulation at CB1 receptors. *Journal of Biological Chemistry* **2012,** 287, 36944-36967.

Beltramo, M.; Bernardini, N.; Bertorelli, R.; Campanella, M.; Nicolussi, E.; Fredduzzi, S. CB_2 receptor-mediated antihyperalgesia: possible direct involvement of neural mechanisms. *Eur. J. Neurosci*. **2006**, 23, 1530–1538.

Bisogno, T.; Howell, F.; Williams, G.; Minassi, A.; Cascio, M.G.; Ligresti, A. Cloning of the first sn1-DAG lipases points to the spatial and temporal regulation of endocannabinoid signaling in the brain. *J. Cell Biol*. **2003**, 163, 463‑468.

Black, S.C. Cannabinoid receptor antagonists and obesity. *Curr. Opin. Investig. Drugs*. **2004**, 5, 389-394.

Blankman, J.L.; Simon, G.M.; Cravatt, B.F. A comprehensive profile of brain enzymes that hydrolyze the endocannabinoid 2-arachidonoylglycerol. *Chem. Biol*. **2007**, 1347‑1356.

Bockaert, J.; Pin, J.P. Molecular tinkering of G-protein coupled receptors: an evolutionary success. *EMBO J*. **1999**, 18, 1723-1729.

Bonnamour, J.; Bolm, C. Iron (II) Triflate as a catalyst for the Synthesis of Indole by Intramolecular C-H animation. *Org. Lett.* **2011**, 13, 2012-2014.

Bosier, B.; Muccioli, G.G.; Hermans, E.; Lambert, D.M. Functionally selective cannabinoid receptor signalling: Therapeutic implications and opportunities. *Biochem. Pharmacol*., **2010**, 80, 1-12.

Bradford, M.M. A rapid and sensitive method for the quantification of microgram quantitites of protein utilizing the principle of protein-dye binding. *Anal. Biochem*. **1976**, 72, 248-254.

Bridges, T. M.; Lindsley, C. W. G-protein-coupled receptors: from classical modes of modulation to allosteric mechanisms. *ACS chemical biology* **2008,** 3, 530-541.

Brown, D. J. *The Chemistry of Heterocyclic Compounds, The Pyrimidines*. John Wiley & Sons: 2009; Vol. 52.

Brown, S.P.; Safo, P.K.; Regehr, W.G. Endocannabinoids inhibit transmission at granule cell to Purkinje cell synapses by modulating three types of presynaptic calcium channels. *J. Neurosci.* **2004**, 24, 5623–5631.

Bruno, A.;, Lembo, F.; Novellino, E.; Stornaiuolo, M.; Marinelli, L. Beyond radio-displacement techniques for identification of CB1 ligands: the first application of a fluorescence-quenching Assay. *Scientific Reports,* **2014**, 4, 3757.

Burford, N. T.; Clark, M. J.; Wehrman, T. S.; Gerritz, S. W.; Banks, M.; O'Connell, J.; Traynor, J. R.; Alt, A. Discovery of positive allosteric modulators and silent allosteric modulators of the μ-opioid receptor. *Proceedings of the National Academy of Sciences* **2013,** 110, 10830-10835.

Burford, N.T.; Watson, J.; Bertekap, R.; Alt, A. Strategies for the identification of allosteric modulators of G-protein-coupled receptors. *Biochem. Pharmacol.* **2011**, 81, 691-702.

Calandra, B.; Portier, M.; Kerneis, A.; Delpech, M.; Carillon, C.; Le Fur, G.; Ferrara, P.; Shire, D. Dual intracellular signaling pathways mediated by the human cannabinoid CB1 receptor. *Eur. J. Pharmacol*. **1999**, 374, 445–455.

Caltabiano, G.; Gonzalez, A.; Cordomi, A.; Mercedes, C.; Pardo, L. The role of hydrophobic amino acids in the structure and function of the rhodopsin family of G protein-coupled receptors. *Methods Enzymol.* **2013**, 520, 99-115.

Carmona, M.R.; Barth, F.; Heaulme, M.; Shire, D.; Calandra, B.; Congy, C.; Martinez, S.; Maruani, J.; Neliat, G.; Caput, D.; Ferrara, P.; Soubrie, P.; Breliere, J.C.; Fur, G.L. SR141716A, a potent and selective antagonist of the brain cannabinoid receptor. *Febs Lett*. **1994**, 350, 240-244.

Carpenter, E.P.; Beis, K.; Cameron, A.D.; Iwata, S. Overcoming the challenges of membrane protein crystallography. *Curr Opin Struct Biol.* **2008**, 18, 581–586.

Chen, C.; Okayama, H. High-efficiency transformation of mammalian cells by plasmid DNA. *Mol. Cell. Biol.* **1987**, 7, 2745-2752.

Cherezov, V.; Rosenbaum, D.M.; Hanson, M.A.; Rasmussen, S.G.; Thian, F.S.; Kobilka, T.S.; Choi, H.J.; Kuhn, P.; Weis, W.I.; Kobilka, B.K.; Stevens, R.C. High-resolution crystal structure of an engineered human beta2-adrenergic G protein-coupled receptor. *Science*. **2007**, 318, 1258-1265.

Chin, C.N.; Lucas-Lenard, J.; Abadji, V.; Kendall, D.A. Ligand binding and modulation of cyclic AMP levels depend on the chemical nature of residue 192 of the human cannabinoid receptor 1. *J. Neurochem.* **1998**, 70, 366-373.

Chin, C.N.; Murphy, J.W.; Huffman, J.W.; Kendall, D.A. The third transmembrane helix of the cannabinoid receptor plays a role in the selectivity of aminoalkylindoles for CB2, peripheral cannabinoid receptor. *J. Pharmacol. Exp. Ther*. **1999**, 291, 837-844.

Choe, H.W.; Kim, Y.J.; Park, J.H.; Morizumi, T.; Pai, E.F.; Krauss, N. Crystal structure of metarhodopsin II. *Nature*. **2011**, 471, 651–655.

Christopoulos, A. Allosteric binding sites on cell-surface receptors: novel targets for drug discovery. *Nature Reviews Drug Discovery* **2002,** 1, 198-210.

Christopoulos, A.; Kenakin, T. G protein-coupled receptor allosterism and complexing. *Pharmacol. Rev.* **2002**, 54, 323-374.

Christopoulos, A.; May, L. T.; Avlani, V. A.; Sexton, P. M. G-protein-coupled receptor allosterism: the promise and the problem(s). *Biochem. Soc. Trans.* **2004**, 32, 873-877.

Christopoulos, A.; Sorman, J. L.; Mitchelson, F.; El-Fakahany, E. E. Characterization of the subtype selectivity of the allosteric modulator heptane-1,7-bis-(dimethyl-3'-phthalimidopropyl) ammonium bromide (C7/3-phth) at cloned muscarinic acetylcholine receptors. *Biochem. Pharmacol.* **1999**, 57, 171-179.

Cismowski, M.J.; Lanier, S.M. Activation of heterotrimeric G-proteins independent of a G-protein coupled receptor and the implications for signal processing. *Rev. Physiol. Biochem. Pharmacol.* **2005**, 155, 57-80.

Claing, A.; Laporte, S.A.; Caron, M.G.; Lefkowitz, R.J. Endocytosis of G protein-coupled receptors: roles of G protein-coupled receptor kinases and beta-arrestin proteins. *Prog. Neurobiol.* **2002**, 66, 61-79.

Clark, A.J. General Pharmacology, in Handbook of Experimental Pharmacology. **1937**, vol 35. 625.

Comer, J.; Tam, K. *Pharmacokinetic optimization in drug research: Biological, physicochemical, and computational strategies*. 2001.

Condie, G. C.; Channon, M. F.; Ivory, A. I.; Kumar, N.; Black, D. S. Regioselective reactivity of some 5,7-dimethoxylindoles. *Tetrahedron* **2005**, 61, 4989-5004.

Conn, P.J.; Christopoulos, A.; Lindsley, C.W. Allosteric modulators of GPCRs: a novel approach for the treatment of CNS disorders. *Nat. Rev. Drug. Discov.* **2009**, 8, 41-54.

Console-Bram, L., Marcu, J., Abood, M.E. Cannabinoid Receptors: nomenclature and pharmacological principles. *Prog. Neuropsychopharmacol. Biol. Pyschiatry.* **2012**, 38, 4-15.

Cooper, Z.D.; Haney, M. Actions of delta-9-tetrahydrocannabinol in cannabis: relation to use, abuse, dependence. *Int. Rev. Psychiatry*, **2009**, 21, 104–112.

Cota, D.; Marscicano, G.; Tschop, M.; Grubler, Y.; Flachskamm, C. The endogenous cannabinoid system affects energy balance via central orexigenic drive and peripheral lipogenesis. *J. Clin. Invest.* **2003**, 112, 423-431.

Cridge, B. J.; Rosengren, R. J. Critical appraisal of the potential use of cannabinoids in cancer management. *Cancer Manag Res* **2013,** 5, 301-313.

Croci, T.; Manara, L.; Aureggi, G.; Guagnini, F.; Rinaldi-Carmona, M.; Maffrand, J.P. In vitro functional evidence of neuronal cannabinoid CB1 receptor in human ileum. *Bri. J. Pharmacol.* **1998**, 125, 1393-1395.

De Lean, A.; Stadel, J.M.; Lefkowitz, R.J. A ternary complex model explains the agonist-specific binding properties of the adenylate cyclase-coupled β-adrenergic receptor. *J. Biol. Chem*. **1980**, 255, 7108–7117.

Derkinderen, P.; Ledent, C.; Parmentier, M.; Girault, J.A. Cannabinoids activate p38 mitogen-activated protein kinases through CB1 receptors in hippocampus. *J. Neurochem*. **2001**, 77, 957–960.

Derocq, J.M.; Segui, M.; Marchand, J.; Le Fur, G.; Casellas, P. Cannabinoids enhance human B-cell growth at low nanomolar concentrations. *FEBS Lett*. **1995**, 369, 177–182.

Deutsch, D.G.; Chin, S.A. Enzymatic synthesis and degradation of anandamide, a cannabinoid receptor agonist. *Biochem. Pharmacol*. **1993**, 46, 791–796.

Devane, W.A.; Dysarz, F.A.3rd; Johnson, M.R.; Melvin, L.S.; Howlett, A.C. Determination and characterization of a cannabinoid receptor in rat brain. *Mol. Pharmacol*. **1988**, 34, 605-613.

Devane, W.A.; Hanus, L.; Breuer, A.; Pertweem R.G.; Stevenson, L.A.; Griffin, G.; Gibson, D.; Mandelnaum, A.; Etinger, A.; Mechoulam, R. Isolation and structure of a brain constituent that binds to the cannabinoid receptor. *Science*, **1992**, 258, 1946–1949.

DeWire, S. M.; Violin, J. D. Biased ligands for better cardiovascular drugs dissecting G-protein-coupled receptor pharmacology. *Circulation research* **2011,** 109, 205-216.

Di Marzo, V.; De Petrocellis, L.; Bisogno, T.; Meick, D. Metabolism of anadamide and 2-arachidonoylglycerol: an historical overview and some recent developments. *Lipids*, **1999**, 34, S319–S325.

Dittel, B.N. Direct suppression of autoreactive lymphocytes in the central nervous system via the CB2 receptor. *Br. J. Pharmacol*. *2008*;153, 271–276.

Drake, M.T.; Shenoy, S.K.; Lefkowitz, R.J. Trafficking of G protein coupled receptors. *Circ. Res.* **2006**, 99, 570-582.

Ellgard, L.; Helenius, A. Quality control in the endoplasmic reticulum. *Nat. Rev. Mol. Cell*. Biol., **2003**, 181-191.

Enna, S. Pharmacology of G protein coupled receptors. *Elsevier,* **2011**, 350-354.

Fagan, S.G.; Campbell, V.A. The influence of cannabinoids on generic traits of neurodegeneration. *Br. J. Pharmacol.* **2014**, 171, 1347–1360.

Fay, J.F., Dunham, T.D., Farrens, D.L. Cysteine residues in the human cannabinoid receptor: only C257 and C264 are required for a functional receptor, and steric bulk at C386 impairs antagonist SR141716A binding. *Biochemistry*. **2005**, 44, 8757-8769.

Filizola, M.; Visiers, I.; Skrabanek, L.; Campagne, F.; Weinstei, H. Functional mechanism of GPCRs in a structural context. *Mol. Neuropharmacol*. **2003**, 235–266.

Fleming, F. F.; Yao, L.; Ravikumar, P.; Funk, L.; Shook, B. C. Nitrile-containing pharmaceuticals: efficacious roles of the nitrile pharmacophore. *Journal of medicinal chemistry* **2010,** 53, 7902-7917.

Flower, D.R**.** Modelling G-protein-coupled receptors for drug design. *Biochim. Biophys. Acta.***1999**, 1422, 207-234.

Fredriksson, R.; Lagerstrom, M.C.; Lundin, L.G.; Schioth, H. B. The G-protein-coupled receptors in the human genome form five main families. phylogenetic analysis, paralogon groups, and fingerprints. *Mol. Pharmacol*. **2003**, 63, 1256-1272.

Freire, E. Statistical thermodynamic linkage between conformational and binding equilibria. *Adv. Protein Chem*. **1998**, 51, 255–79.

Galiegue, S.; Mary, S.; Marchand, J.; Dussossoy, D.; Carriere, D.; Carayon, P.; Bouaboula, M.; Shire, D.; Le Fur, G.; Casellas, P. Expression of central and peripheral cannabinoid receptors in human immune tissues and leukocyte subpopulations. *Eur. J. Biochem.* **1995**, 232, 54-61.

Gao, Z. G.; Jacobson, K. A. Allosteric modulation and functional selectivity of G protein-coupled receptors. *Drug Discov. Today Technol.* **2013**, 10, e237-e243.

Gazi, L.; Nickolls, S.A.; Strange, P.G. Functional coupling of the human dopamine D2 receptor with Gi1, Gi2, Gi3 and Go G proteins: evidence for agonist regulation of G protein selectivity. *Br. J. Pharmacol.*, **2003**, 138, 775–786.

Gebremedhin, D.; Lange, A.R.; Campbell, W.B.; Hillard, C.J.; Harder, D.R. Cannabinoid CB1 receptor of cat cerebral arterial muscle functions to inhibit L-type Ca^{2+} channel current. Am. J. Physiol. **1999**, 276, H2085–H2093.

Gerard, C. M.; Mollereau, C.; Vassart, G.; Parmentier, M. Molecular cloning of a human cannabinoid receptor which is also expressed in testis. *Biochem. J.* **1991**, 279, 129-134.

German, N.; Decker, A. M.; Gilmour, B. P.; Gay, E. A.; Wiley, J. L.; Thomas, B. F.; Zhang, Y. Diarylureas as Allosteric Modulators of the Cannabinoid CB1 Receptor: Structure–Activity Relationship Studies on 1-(4-Chlorophenyl)-3-{3-[6-(pyrrolidin-1-yl) pyridin-2-yl] phenyl} urea (PSNCBAM-1). *Journal of medicinal chemistry* **2014,** 57, 7758-7769.

Glass, M.; Faull, R.L.; Dragunow, M. Loss of cannabinoid receptors in the substantia nigra in Huntington's disease. *Neuroscience*, 1993, 523-527.

Glass, M.; Felder, C. C. Concurrent stimulation of cannabinoid CB1 and dopamine D2 receptors augments cAMP accumulation in striatal neurons: evidence for a Gs linkage to the CB1 receptor. *J. Neurosci.* **1997**, 17, 5327-5333.

Goblysos, A.; Ijzerman, A.P. Allosteric modulation of adenosine receptors. *Biochim. et Biophy. Acta.* **2011**, 1808, 1309-1318.

Graham, E.S.; Ball, N.; Scotter, E.L.; Narayan, P.; Dragunow, M.; Glass, M. Induction of Krox-24 by endogenous cannabinoid type 1 receptors in Neuro2A cells is mediated by the MEK–ERK MAPK pathway and is suppressed by the phosphatidylinositol 3-kinase pathway. *J. Biol. Chem*. **2006**, 281, 29085–29095.

Grimaldi, P.; Orlando, P.; Di Siena, S.; Lolicato, F.; Petrosino, S.; Bisogno, T. The endocannabinoid system and pivotal role of the CB2 receptor in mouse spermatogenesis. *Proc. Natl. Acad. Sci. U S A*. **2009**, 106, 11131–11136.

Guindon, J.; Hohmann, A.G. The endocannabinoid system and pain. *CNS Neurol. Disorders Drug Targets,* **2009**, 8, 403–421.

Hague, C.; Uberti, M.A.; Chen, Z.; Hall, R.A.; Minneman, K.P. Cell surface expression of alpha1D-adrenergic receptors is controlled by heterodimerizarion with alpha1B-adrenergic receptors. *J. Biol. Chem*. 2004, 279, 15541-15549.

Hanyaloglu, A.C.; Von-Zastrow, M. Regulation of GPCRs by endocytotic membrane trafficking and its potential implications. *Annu. Rev. Pharmacol. Toxicol*. **2008**, 48, 537-568.

He, F.; Song, Z.H. Molecular and cellular changes induced by the activation of CB2 cannabinoid receptors in trabecular meshwork cells. *Mol. Vis*. **2007**, 13, 1348–1356.

Heimann, A.S.; Gomes, I.; Dale, C.S.; Pagano, R.L.; Gupta, A.; de Souza, L.L.; Luchessi, A.D.; Castro, L.M.; Giorgi, R.; Rioli, V.; Ferro, E.S.; Devi, L.A. Hemopressin is an inverse agonist of CB1 cannabinoid receptors. *Proc. Natl. Acad.Sci. U.S.A.* **2007**, 104, 20588-20593.

Hemetsberger, H. K., D. Synthese und Thermolyse von α-Azidoacrylestern. *Monatsh. Chem.* **1972**, 103, 194-204.

Hemetsberger, H.; Knittel, D.; Weldmann, H. Synthese von α-Azidozimtsaureestern. *Monatsh. Chem.* **1969**, 100, 1599-1603.

Henness, S.; Robinson, D.M.; Lyseng-Williamson, K.A. Rimonabant. *Drugs*, **2006**, 66, 2109-2119.

Herkenham, M.; Lynn, A.B.; de Costa, B.R.; Richfield, E.K. Neuronal localization of cannabinoid receptors in basal ganglia of the rat. *Brain Res.* **1991**, 547, 267-274.

Herkenham, M.; Lynn, A.B.; Little, M.D.; Johnson, M.R.; Melvin, L.S.; de Costa, B.R. Cannabinoid receptor localization in brain. *Proc. Natl. Acad. Sci. USA*. **1990**, 87, 1932-1936.

Hoffmann, C.; Gaietta, G.; Bunemann, M.; Adams, S.R.; Oberdorff-Maass, S.; Behr, B.; Vilardaga, J.P., Tsein, R.Y., Ellisman, M.H., Lohse, M.J. A FlAsH-based FRET approach to determine G protein-coupled receptor activation in living cells. *Nat. Methods*, **2005**, 2, 171-176.

Horswill, J. G.; Bali, U.; Shaaban, S.; Keily, J. F.; Jeevaratnam, P.; Babbs, A. J.; Reynet, C.; Wong Kai In, P. PSNCBAM-1, a novel allosteric antagonist at cannabinoid CB1 receptors with hypophagic effects in rats. *Br. J. Pharmacol.* **2007**, 152, 805-814.

Howlett, A. C. Cannabinoid receptor signaling. *Handb. Exp. Pharmacol.* **2005**, 53-79.

Howlett, A. C.; Blume, L. C.; Dalton, G. D. CB(1) cannabinoid receptors and their associated proteins. *Curr. Med. Chem.* **2010**, 17, 1382-1393.

Howlett, A. C.; Breivogel, C. S.; Childers, S. R.; Deadwyler, S. A.; Hampson, R. E.; Porrino, L. J. Cannabinoid physiology and pharmacology: 30 years of progress. *Neuropharmacology* **2004**, 47 (Suppl 1), 345-358.

Howlett, A.C. Cannabinoid receptor signaling. *Handbook of experimental pharmacology*. **2005**, 168, 53-79.

Howlett, A.C.; Qualy, J.M.; Khachatrian, L.L. Involvement of Gi in the inhibition of adenylate cyclase by cannabimimetic drugs. *Mol. Pharmacol*. **1986,** 29, 307-313.

Hubbard, R.; Kropf, A. The action of light on rhodopsin. *Proc. Natl. Acad. Sci. U.S.A.* **1958**, 44, 130–139.

Huffman, J.W.; Dai, D.; Martin, B.R. Design, synthesis and pharmacology of cannabimimetic indoles. *Bioorg. Med. Chem. Lett*. **1994**, 4, 563-566.

Hughes, C.A.; Robinson, L.; Tseng, A.; MacArthur, R.D. New antiretroviral drugs: a review of the efficacy, safety, pharmacokinetics and resistance profiles of tipranavir, darunavir, etravirine, rilpivirine, maraviroc and raltegravir. *Expert Opin. Pharmacother.* **2009**, 10, 2445-2466.

Hurst, D.P.; Lynch, D.L.; Barnett-Norris, J.; Hyatt, S.M.; Seltzman, H.H.; Zhong, M.; Song, Z.H.; Nie, J.; Lewis, D.; Reggio, P.H. N-(piperidin-1-yl)-5-(4-chlorophenyl)-1-(2,4-dichlorophenyl)-4-methyl-1H-pyrazole-3-carboxamide (SR141716A) interaction with LYS 3.28(192) is crucial for its inverse agonism at the cannabinoid CB1 receptor. *Mol. Pharmacol.* **2002**, 62, 1274-87.

Ignatowska-Jankowska, B. M.; Baillie, G. L.; Kinsey, S.; Crowe, M.; Ghosh, S.; Owens, R. A.; Damaj, I. M.; Poklis, J.; Wiley, J. L.; Zanda, M. A cannabinoid CB1 receptor-positive allosteric modulator reduces neuropathic pain in the mouse with no psychoactive effects. *Neuropsychopharmacology* **2015,** 40, 2948-2959.

Jing, L.; Qiu, Y.; Zhang, Y.; Li, J.-X. Effects of the cannabinoid CB 1 receptor allosteric modulator ORG 27569 on reinstatement of cocaine-and methamphetamine-seeking behavior in rats. *Drug and alcohol dependence* **2014,** 143, 251-256.

Julien, B.; Grenard, P.; Teixeira-Clerc, F.; Van Nhieu, J.T.; Li, L.; Karsak, M. Antifibrogenic role of the cannabinoid receptor CB2 in the liver. *Gastroenterology*, **2005**, 128, 742–755.

Justinova, Z.; Tanda, G.; Redhi, G.H.; Goldberg, S.R. Self-administration of delta9-tetrahydrocannabinol (THC) by drug naive squirrel monkeys. *Psychopharmacology,* **2003**, 169, 135–140.

Kapur, A.; Hurst, D.P.; Fleischer, D.; Whitnell, R.; Thakur, G.A.; Makriyannis, A.; Reggio, P.H.; Abood, M.E. Mutation studies of Ser7.39 and Ser2.60 in the human CB1 cannabinoid receptor: evidence for a serine-induced bend in CB1 transmembrane helix 7. *Mol. Pharmacol*. **2007**, 71, 1512-1524.

Katona, I.; Sperlagh, B.; Sik, A.; Kafalvi, A.; Vizi, E.S.; Mackie, K.; Freund, T.F. Presynaptically located CB1 cannabinoid receptors regulate GABA release from axon terminals of specific hippocampal interneurons. *J. Neurosci*. **1999**, 19, 4544‑4558.

Kearn, C.S.; Blake-Palmer, K.; Daniel, E.; Mackie, K.; Glass, M. Concurrent stimulation of cannabinoid CB1 and dopamine D2 receptors enhances heterodimer formation: a mechanism for receptor cross-talk? *Mol. Pharmacol*. **2005**, 67, 1697–1704.

Kenakin, T. Efficacy at g-protein-coupled receptors*. Nat. Rev. Drug Disc*. **2002**, 1, 103-110.

Kenakin, T. New concepts in drug discovery: collateral efficacy and permissive antagonism. *Nat. Rev.: Drug Disc.* **2005**, 4, 919-927.

Kenakin, T. P. Biased signalling and allosteric machines: new vistas and challenges for drug discovery. *British journal of pharmacology* **2012,** 165, 1659-1669.

Kenakin, T.; Miller, L. J. Seven transmembrane receptors as shapeshifting proteins: the impact of allosteric modulation and functional selectivity on new drug discovery. *Pharmacological reviews* **2010**, 62, 265-304.

Keov, P.; Sexton, P.M.; Christopoulos, A. Allosteric modulation of G protein-coupled receptors: A pharmacological perspective. *Neuropharmacol.***2011**, 60, 24-35.

Kirilly, E.; Gonda, X.; Bagdy, G. CB1 receptor antagonists: new discoveries leading to new perspectives. *Acta. Physiol. (Oxf)*. **2012**, 205, 41-60.

Knudsen, L.B.; Kiel, D.; Teng, M.; Behrens, C.; Bhumralkar, D.; Kodra, J.T. Small-molecule agonists for the glucagon-like peptide 1 receptor. *Proc. Natl. Acad. Sci. USA.* **2007**, 104, 937-942.

Kobilka, B.K.; Deupi, X. Conformational complexity of G-protein-coupled receptors. *Trends Pharmacol. Sci.* **2007**, 28, 397-406.

Kohout, T.A.; Lin, F.S.; Perry, S.J.; Conner, D.A.; Lefkowitz, R.J. β-arrestin 1 and 2 differentially regulate heptahelical receptor signaling and trafficking. *Proc. Natd. Acad. Sci. USA.* **2001**, 98, 1601-1606.

Komatsu, H. Novel therapeutic GPCRs for psychiatric disorders. *Int. J.Mol.Sci*. **2015**, 16, 14109-14121.

Kurrasch-Orbaugh, D.M.; Watts, V.J.; Barker, E.L.; Nichols, DE. Serotonin 5-hydroxytryptamine2A receptor-coupled phospholipase C and phospholipase A2 signaling pathways have different receptor reserves. *J. Pharmacol. Exp. Ther.* **2003**, 304, 229 –237.

Lander, E.S.; Linton, L.M.; Birren, B.; Nusbaum, C.; Zody, M.C.; Baldwin, J.; Devon, K.; Dewar, K.; Doyle, M.; FitzHugh, W. The international human genome sequencing consortium. initial sequencing and analysis of the human genome. *Nature*. **2001**, 409, 860–921.

Lauckner, J. E.; Hille, B.; Mackie, K. The cannabinoid agonist WIN55,212-2 increases intracellular calcium via CB1 receptor coupling to Gq/11 G proteins. *Proc. Natl. Acad. Sci. USA* **2005**, 102, 19144-19149.

Leach, K.; Loiacono, R.E.; Felder, C.C.; Mckinzie, D.L.; Mogg, A.; Shaw, D.B.; Sexton, P.M.; Christopoulos, A. Molecular mechanisms of action and invivo validation of a M_4 muscarinic acetylcholine receptor allosteric modulator with potential antipsychotic properties. *Neuropsychopharmacol.* **2010**, 35, 855-869.

Leff, P. The two-state model of receptor activation. *Trends Pharmacol*. *Sci*. **1995**, 16, 89–97.

Lehmanna, F.; Holma, M.; Laufer, S. Rapid and easy access to indoles via microwave-assisted Hemetsberger–Knittel synthesis. *Tetrahedron Lett.* **2009**, 50, 1708–1709.

Leung, D.; Saghatelian, A.; Simon, G.M.; Cravatt, B.F. Inactivation of N-acyl phosphatidylethanolamine phospholipase D reveals multiple mechanisms for the biosynthesis of endocannabinoids. *Biochem*. **2006**, 45, 4720-4726.

Levinson, N. M.; Boxer, S. G. A conserved water-mediated hydrogen bond network defines bosutinib's kinase selectivity. *Nature chemical biology* **2014,** 10, 127-132.

Li, J.; Edwards, P.C.; Burghammer, M.; Villa, C.; Schertler, G.F. Structure of bovine rhodopsin in a trigonal crystal form. *J. Mol. Biol*. **2004**, 343, 1409-1438.

Lindsley, C.W.; Wiscnoski, D.D.; Leister, W.H.; O'Brien, J.A.; Lemaire, W.; Williams, D.L.; Burno, M.; Sur, C.; Kinney, G.G.; Doug, J.P.; Tiller, P.R.; Smith, S.; Duggan, M.E.; Hartman, G.D.; Conn, P.J.; Huff, J.R. Discovery of positive allosteric modulators for the metabotropic glutamate receptor subtype 5 from a series of N-(1,3-diphenyl-1H-pyrazol-5-yl)benzamides that potentiate receptor function in vivo. *J.Med.Chem.* **2004**, 47, 5825-5828.

Liu, J.; Wang, L.; Harvey-White, J.; Huang, B.X.; Kim, H.Y.; Luquet, S.; Palmiter, R.D.; Krystal, G.; Rai, R.; Mahadevan, A.; Razdan, R.K; Kunos, G. Multiple pathways involved in the biosynthesis of anandamide. *Neuropharmacol.* **2008**, 54, 1-7.

Mackie, K. Cannabinoid receptors as therapeutic targets. *Annu. Rev. Pharmacol. Tox.* **2006**, 46, 101-122.

Mackie, K. Cannabinoid receptors: where they are and what they do. *J. Neuroendocrinol.* **2008**, 20 (Suppl 1), 10-14.

Mackie, K. Signaling via CNS cannabinoid receptors. *Mol. Cell Endocrinol.* **2008**, 286, S60-S65.

Mackie, K.; Hille, B. Cannabinoids inhibit N-type calcium channels in neuroblastoma-glioma cells. *Proceedings of the National Academy of Sciences* **1992,** 89, 3825-3829.

Mackie, K.; Lai, Y.; Westenbroek, R.; Mitchell, R. Cannabinoids activate an inwardly rectifying potassium conductance and inhibit Q-type calcium currents in AtT20 cells transfected with rat brain cannabinoid receptor. *J. Neurosci*. **1995**, 15, 6552–6561.

Mahmoud, M. M.; Ali, H. I.; Ahn, K. H.; Damaraju, A.; Samala, S.; Pulipati, V. K.; Kolluru, S.; Kendall, D. A.; Lu, D. Structure-Activity relationship study of indole-2-carboxamides identifies a potent allosteric modulator for the cannabinoid Receptor 1 (CB1). *J. Med. Chem.* **2013**, 56, 7965-7975.

Maldonado, R.; Valverde, O.; Berrendero, F. Involvement of the endocannabinoid system in drug addiction. *Trends Neurosci*. **2006**, 29, 225-232.

Manzanares, J..;Julian, M.; Carrascosa, A. Role of the cannabinoid system in pain control and therapeutic implications for the management of acute and chronic pain episodes. *Curr. Neuropharmacol*., **2006**, 4, 239–257.

Maresz, K.; Pryce, G.; Ponomarev, E.D.; Marsicano, G.; Croxford, J.L.; Shriver, L.P. Direct suppression of CNS autoimmune inflammation via the cannabinoid receptor CB1 on neurons and CB2 on autoreactive T cells. *Nat. Med*. **2007**, 13, 492–497.

Marlo, J.E.; Niswender, C.M.; Days, E.L.; Bridges, T.M.; Xiang, Y.; Rodriguez, A.L.; Shirey, J.K.; Brady, A.E.; Nalywajko, T.; Luo, Q.; Austin, C.A.; Williams, M.B.; Kim, K.; Williams, R.; Orton, D.; Brown, H.A.; Lindsley, C.W.; Weaver, C.D.; Conn, P.J. Discovery and characterization of novel allosteric potentiators of M_1 muscarinic receptors reveals multiple modes of activity. *Mol. Pharmacol.***2009**, 75, 577-588.

Marsicano, G.; Lutz, B. Expression of the cannabinoid receptor CB1 in distinct neuronal subpopulations in the adult mouse forebrain. *Eur. J. Neurosci.* **1999**, 11, 4213.

Martin, B.; Stevenson, L.A.; Pertwee, R.G.; Breivogel, C.S.; Williams, W.; Mahadevan, A.; Razdan, R.K. Agonists and silent antagonists in a series of cannabinoid sulfonamides. Symposium on the Cannabinoids, *International Cannabinoid Res. Soc* .**2002**.

Martini, L.; Waldhoer, M.; Pusch, M.; Kharazia, V.; Fong, J.; Lee, J.H. Ligand-induced down-regulation of the cannabinoid 1 receptor is mediated by the G-protein-coupled receptor-associated sorting protein GASP1. *FASEB J.* **2007**, 21, 802–811.

Marzo, V.D. The endocannabinoid system: Its general strategy of action, tools for its pharmacological manipulation and potential therapeutic exploitation. *Pharmacol. Res*. **2009**, 60, 77-84.

Mathiesen, M.; Ulven, T.; Martini, L.; Gerlach, L.O.; Heinemann, A.; Kostenis, E. Identification of indole derivatives exclusively interfering with the G protein-independent signaling pathway of the prostaglandin D2 receptor CRTH2. *Mol. Pharmacol.* **2005**, 68, 393-402.

May, L.T.; Lin, Y.; Sexton, P. M.; Christopoulos, A. Regulation of M2 muscarinic acetylcholine receptor expression and signaling by prolonged exposure to allosteric modulators. *J. Pharmacol. Exp. Ther.* **2005**, 312, 382-390.

May, L.T.; Leach, K.; Sexton, P.M.; Christopoulos, A. Allosteric modulators of G-protein coupled receptors. *Annu. Rev. Pharmacol. Toxicol.* **2007**, 47, 1-51.

McAllister, S.D.; Rizvi, G.; Anavi-Goffer, S.; Hurst, D.P.; Barnett-Norris, J.; Lynch, D.L.; Reggio, P.H.; Abood, M.E. An aromatic microdomain at the cannabinoid CB(1) receptor constitutes an agonist/inverse agonist binding region. *J. Med. Chem*. **2003**, 46, 5139-5152.

McAllister, S.D.; Tao, Q.; Barnett-Norris, J.; Buehner, K.; Hurst, D.P.; Guarnieri, F.; Reggio, P.H.; Nowell Harmon, K.W.; Cabral, G.A.; Abood, M.E. A critical role for a tyrosine residue in the cannabinoid receptors for ligand recognition. *Biochem Pharmacol*. **2002**, 63, 2121-2136.

McCudden, C.R; Hains, M.D.; Kimple, R.J.; Siderovski, D.P.; Willard, F.S. G-protein signaling: back to the future. *Cell. Mol. Life Sci*. **2005**, 62, 551-577.

Messa, P.; Alfieri, C.; Brezzi, B. Cinacalcet: pharmacological and clinical aspects. *Expert Opin. Drug Metab. Toxicol.* **2008**, 4, 1551-1560.

Miedlich, S.U.; Gama, L.; Seuwen, K.; Wolf, R.M.; Breitwieser, G.E. Homology modeling of the transmembrane domain of the human calcium sensing receptor and localization of an allosteric binding site. *J. Biol. Chem.* **2004**, 279, 7254-7263.

Moriera, I.S. Structural features of the G-protein/GPCR interactions. *Biochim. et Biophys. Acta.* **2014**, 1840, 116–133.

Moukhametzianov, R.; Warne, T.; Edwards, P.C.; Serrano-Vega, M.J.; Leslie, A.G.; Tate, C.G.; Schertler, G.F. Two distinct conformations of helix 6 observed in antagonist-bound structures of a beta1-adrenergic receptor. *Proc. Natl. Acad. Sci. U.S.A*. **2011**, 108, 8228-8232.

Mu, J.; Zhuang, S.-y.; Kirby, M. T.; Hampson, R. E.; Deadwyler, S. A. Cannabinoid receptors differentially modulate potassium A and D currents in hippocampal neurons in culture. *Journal of Pharmacology and Experimental Therapeutics* **1999,** 291, 893-902.

Munk, C.; Isberg, V.; Mordalski, S.; Harpsoe, K.; Rataj, K.; Hauser, A. S.; Kolb, P.; Bojarski, A. J.; Vriend, G.; Gloriam, D. E. GPCRdb: the G protein-coupled receptor database – an introduction. *Br. J. Pharmacol.* **2016**.

Munro, S.; Thomas, K.L.; Abu-Shaar, M. Molecular characterization of a peripheral receptor for cannabinoids. *Nature*. **1993**, 365, 61-65.

Murakami, Y.; Watanabe, T.; Suzuki, H.; Kotake, N.; Takahashi, T.; Toyonari, K.; Ohno, M.; Takase, K.; Suzuki, T.; Kondo, K. New Findings on the Hemetsberger-Knittel Reaction (Synthetic Studies on Indoles and Related Compounds. XLIII) *Chem. Pharm. Bull.* **1997**, 45, 1739-1744.

Navarro, H. A.; Howard, J. L.; Pollard, G. T.; Carroll, F. I. Positive allosteric modulation of the human cannabinoid (CB) receptor by RTI-371, a selective inhibitor of the dopamine transporter. *Br. J. Pharmacol.* **2009**, 156, 1178-1184.

O'Brien, A. G.; Lévesque, F.; Seeberger, P. H. Continuous flow thermolysis of azidoacrylates for the synthesis of heterocycles and pharmaceutical intermediates. *Chem. Commun.* **2011**, 47, 2688-2690.

Ofek, O.; Karsak, M.; Leclerc, N.; Fogel, M.; Frenkel, B.; Wright, K. Peripheral cannabinoid receptor, CB2, regulates bone mass. *Proc. Natl. Acad. Sci U S A*. **2006**, 103, 696–701.

Ohno, H.; Stewart, J.; Fournier, M.C.; Bosshart, H.; Rhee, I.; Miyatake, S.; Saito, T.; Gallusser, A.; Kirchhausen, T.; Bonifacino, J.S. Interaction of tyrosine-based sorting signals with clathrin-associated proteins. *Science* **1995**, 269, 1872-1875.

Okada, T.; Fujiyoshi, Y.; Silow, M.; Navarro, J.; Landau, E.M.; Shichida,Y. Functional role of internal water molecules in rhodopsin revealed by X-ray crystallography. *Proc. Natl. Acad. Sci.* **2002**, 99, 5982-5987.

Okada, T.; Sugihara, M.; Bondar, A.N.; Elstner, M.; Entel, P.; Buss, V. The retinal conformation and its environment in rhodopsin in light of a new 2.2 Å crystal structure. *J. Mol. Biol.,* **2004**, 342, 571–83.

Osei-Hyiaman, D.; Depetrillo, M.; Pacher, P.; Liu, J.; Radaeva, S.; Endocannabinoid action at hepatic CB1 receptors regulates fatty acid synthesis: role in diet-induced obesity. *J. Clin. Invest.* **2005**, 115, 1298-1305.

Otrubova, K.; Ezzili, C.; Boger, D.L. The discovery and development of inhibitors of fatty acid amide hydrolase (FAAH). *Bioorg. Med. Chem. Lett*. **2011**, 21, 4674–4685.

Overington, J.P.; Al-Lazikani, B.; Hopkins, A.L. How many drug targets are there? *Nat. Rev. Drug Discov.* **2006**, 5, 993-996.

Pacher, P.; Bátkai, S.; Kunos, G. The endocannabinoid system as an emerging target of pharmacotherapy. *Pharmacological reviews* **2006,** 58, 389-462.

Palczewski, K.; Kumasaka, T.; Hori, T.; Behnke, C.A.; Motoshima, H.; Fox, B.A.; Trong, I.L.; Teller, D.C.; Okada, T.; Stenkamp, R.E.; Yamamoto, M.; Miyano, M. Crystal Structure of Rhodopsin: A G Protein-Coupled Receptor. *Science,* **2000**, 289, 739-745.

Pamplona, F. A.; Ferreira, J.; Menezes de Lima, O., Jr.; Duarte, F. S.; Bento, A. F.; Forner, S.; Villarinho, J. G.; Bellochio, L.; Wotjak, C. T.; Lerner, R.; Monory, K.; Lutz, B.; Canetti, C.; Matias, I.; Calixto, J. B.; Marsicano, G.; Guimaraes, M. Z.; Takahashi, R. N. Anti-inflammatory lipoxin A4 is an endogenous allosteric enhancer of CB1 cannabinoid receptor. *Proc. Natl. Acad. Sci. USA* **2012**, 109, 21134-21139.

Park, J.H.; Scheerer, P.; Hofmann, K.P.; Choe, H.W.; Ernst, O.P. Crystal structure of the ligand-free G-protein-coupled receptor opsin. *Nature.* **2008**, 454, 183–187.

Park, P.S.; Lodowski, D.T. Activation of G protein–coupled receptors: Beyond two-state models and tertiary conformational changes. *Annu. Rev. Pharmacol. Toxicol*. **2008**, 48, 107–141.

Patel, P.N.; Pathak, R. Rimonabant: a novel selective cannabinoid-1 receptor antagonist for treatment of obesity. *Am. J. Health Syst. Pharm.* **2007**, 64, 481-489.

Perez, D.M.; Karnik, S.S. Multiple Signaling States of G-Protein-Coupled Receptors. *Pharmacol. Rev.* **2005**, 57, 147-161.

Pertwee, R. G. Cannabinoid pharmacology: the first 66 years. *Br. J. .Pharmacol.* **2006**, 147 (Suppl 1), S163-S171.

Pertwee, R. G. The pharmacology of cannabinoid receptors and their ligands: an overview. *Int. J. Obes. (Lond)* **2006**, 30 (Suppl 1), S13-S18.

Pertwee, R.G. Inverse agonism and neutral antagonism at cannabinoid CB1 receptors. *Life Sci*., **2005**, 76, 1307-1324.

Pertwee, R.G. Pharmacological actions of cannabinoids. *Handb. Exp. Pharmacol*. **2005**, 168, 1-51.

Pertwee, R.G. Pharmacology of cannabinoid CB1 and CB2 receptors. *Pharmacol. Ther*., **1997**, 74, 129–180.

Pertwee, R.G. The diverse CB1 and CB2 receptor pharmacology of three plant cannabinoids: Δ9-tetrahydrocannabinol, cannabidiol and Δ9-tetrahydrocannabivarin. *Br. J. Pharmacol*., **2008**, 153, 199–215.

Pertwee, R.G. Pharmacology of cannabinoid receptor ligands. *Curr. Med. Chem*. **1999**, 6, 635–664.

Petrocellis, L.D.; Cascio, M.G.; Marzo, V.D. Mini review: The endocannabinoid system: a general view and latest additions. *Bri. J. Pharmacol*. **2004**, 141, 765–774.

Picone, R.P.; Khanolkar, A.D.; Xu,W.; Ayotte, L.A.; Thakur, G.A.; Hurst, D.P.; Abood, M.E.; Reggio, P.H.; Fournier, D.J.; Makriyannis, A. (-)-7'-Isothiocyanato-11-hydroxy-1',1'-dimethylheptylhexahydrocannabinol (AM841), a high-affinity electrophilic ligand, interacts covalently with a cysteine in helix six and activates the CB1 cannabinoid receptor. *Mol. Pharmacol*. **2005**, 68, 1623-1635.

Piscitelli, F.; Ligresti, A.; La Regina, G.; Coluccia, A.; Morera, L.; Allara, M.; Novellino, E.; Di Marzo, V.; Silvestri, R. Indole-2-carboxamides as allosteric modulators of the cannabinoid CB(1) receptor. *J. Med. Chem.* **2012**, 55, 5627-5631.

Price, M. R.; Baillie, G. L.; Thomas, A.; Stevenson, L. A.; Easson, M.; Goodwin, R.; McLean, A.; McIntosh, L.; Goodwin, G.; Walker, G.; Westwood, P.; Marrs, J.; Thomson, F.; Cowley, P.; Christopoulos, A.; Pertwee, R. G.; Ross, R.A. Allosteric modulation of the cannabinoid CB1 receptor. *Mol. Pharmacol*. **2005**, 68, 1484−1495.

Pryce, G.; Baker, D. Potential control of multiple sclerosis by cannabis and the endocannabinoid system. *CNS Neurol Disord Drug Targets*, **2012**, 11, 624–641.

Ranasinghe, N.; Jones, G. B. Extending the versatility of the Hemetsberger-Knittel indole synthesis through microwave and flow chemistry. *Bioorg. Med. Chem. Lett.* **2013**, 23, 1740-1742.

Reggio, P.H. The cannabinoid receptors. *Humana press.* **2008**, pp 3-11.

Reuda, D.; Galve-Roperh, I.; Haro, A.; Guzman, M. The CB(1) cannabinoid receptor is coupled to the activation of c-Jun N-terminal kinase. *Mol. Pharmacol*. **2000**, 58, 814–820.

Robinson, M.S. Adaptable adaptors for coated vesicles. *Trends Cell. Biol*. **2004**, 14, 167-174.

Robinson, M.S. The role of clathrin, adaptors and dynamin in endocytosis. *Curr. Opi. Cell Biol***. 1994**, 6, 538-544.

Roche, R.; Hoareau, L.; Bes-Houtmann, S.; Gonthier, M.P.; Laborde, C.; Baron, J.F. Presence of the cannabinoid receptors, CB1 and CB2, in human omental and subcutaneous adipocytes. *Histochem. Cell Biol.* 2006, 126, 177–187.

Rosenbaum, D.M.; Rasmussen, S.G.; Kobilka, B.K. The structure and function of G-protein-coupled receptors. *Nature*. **2009**, 459, 356–363.

Rosenbaum, D.M.; Zhang, C.; Lyons, J.A.; Holl, R.; Aragao, D.; Arlow, D.H.; Rasmussen, S.G.; Choi, H.J.; Devree, B.T.; Sunahara, R.K.; Chae, P.S.; Gellman, S.H.; Dror, R.O.; Shaw, D.E.;

Weis, W.I.; Caffrey, M.; Gmeiner, P.; Kobilka, B.K. Structure and function of an irreversible agonist-β(2) adrenoceptor complex. *Nature*. **2011**, 469, 236-240.

Rosenbaum, D.M.; Cherezov, V.; Hanson, M.A.; Rasmussen, S.G.; Thian, F.S.; Kobilka, T.S.; Choi, H.J.; Yao, X.J.; Weis, W.I.; Stevens, R.C.; Kobilka, B.K. GPCR engineering yields high-resolution structural insights into beta2-adrenergic receptor function. *Science.* **2007**, 318, 1266-7123.

Rozenfeld, R.; Devi, L.A. Regulation of CB1 cannabinoid receptor trafficking by the adaptor protein AP-3. *FASEB J.* **2008**, 22, 2311-2322.

Ruiu, S.; Pinna, G.A.; Marchese, G.; Mussinu, J.M.; Saba, P.; Tambaro, S.; Casti, P.; Vargiu, R.; Pani, L. Synthesis and characterization of NESS0327: a novel putative antagonist of the CB1 cannabinoid receptor. *J. Pharmacol. Exp. Ther*., **2003**, 306, 363-370.

Ryberg, E.; Larsson, N.; Sjogren, S.; Hjorth, S.; Hermansson, N.O.; Leonova, J.; Elebring, T.; Nilsson, K.; Drmota, T.; Greasley, P.J. The orphan receptor GPR55 is a novel cannabinoid receptor. *Bri. J. Pharmacol*. **2007**, 152, 1092-1101.

Salahpour, A.; Angers, S.; Mercier, J.F.; Lagace, M.; Marullo, S.; Bouvier, M. Homodimerization of the beta2-adrenergic receptor as a prerequisite for cell surface targeting. *J. Biol. Chem.* **2004**, 279, 33390-33397.

Salom, D.; Lodowski, D.T.; Stenkamp, R.E.; Le Trong, I.; Golczak, M.; Jastrzebska, B. Crystal structure of a photoactivated deprotonated intermediate of rhodopsin. *Proc. Natl. Acad. Sci. U.S.A.* **2006**, 103, 16123–16128.

Samama, P.; Cotecchia, S.; Costa, T.; Lefkowitz, R.J. A mutation-induced activated state of the β2-adrenergic receptor. extending the ternary complex model. *J. Biol. Chem*. **1993**, 268, 4625–4636.

Sanchez, C.; Reuda, D.; Segui, B.; Galve-Roperh, I.; Levade, T.; Guzman, M. The CB(1) cannabinoid receptor of astrocytes is coupled to sphingomyelin hydrolysis through the adaptor protein fan. *Mol. Pharmacol*. **2001**, 59, 955-959.

Sanudo-Pena, M.C.; Patrick, S.L.; Khen, S.; Patrick, R.L.; Tsou, K.; Walker, J.M. Cannabinoid effects in basal ganglia in a rat model of Parkinson's disease. *Neurosci. Lett*. **1998**, 248, 171-174.

Schatz, A.R.; Lee, M.; Condie, R.B.; Pulaski, J.T.; Kaminski, N.E. Cannabinoid receptors CB_1 and CB2: a characterization of expression and adenylate cyclase modulation within the immune system. *Toxicol. Appl. Pharmacol*. **1997,** 142, 278-287.

Scheerer, P.; Park, J.H.; Hildebrand, P.W.; Kim, Y.J.; Krauss, N.; Choe, H.W. Crystal structure of opsin in its G-protein-interacting conformation. *Nature.* **2008**, 455, 497- 502.

Schertler, G.F.; Claudio, V.; Henderson, R. Projection structure of rhodopsin. *Nature*, **1993**, 362, 770-772.

Schioth, H.B.; Fredriksson, R. The GRAFS classification system of G-protein coupled receptors in comparative perspective. *Gen. Comp. Endocr*. **2005**, 142, 94-101.

Schmid, S.L. Clathrin-coated vesicle formation and protein sorting: An integrated process. *Annu. Rev. Biochem.* **1997**, 66, 511-548.

Shenoy, S.K.; Lefkowitz, R.J. Trafficking patterns of β-arrestin and G protein-coupled receptors determined by the kinetics of β-Arrestin deubiquitination. *J. Bio. Chem*. **2003**, 278, 14498-14506.

Shim, J. Understanding functional residues of the cannabinoid CB1 receptor for drug discovery. *Curr. Top. Med. Chem*. **2010**, 10, 779–798.

Shim, J.Y. Transmembrane helical domain of the cannabinoid CB1 receptor. *Biophys. J*. **2009**, 96, 3251-3262.

Shire, D.; Calandra, B.; Delpech, M.; Dumont, X.; Kaghad, M.; Le Fur, G.; Caput, D.; Ferrara, P. Structural features of the central cannabinoid CB1 receptor involved in the binding of the specific CB1 antagonist SR 141716A. *J. Bio. Chem*. **1996**, 271, 6941-6946.

Shmist, Y.A.; Goncharov, I.; Eichler, M.; Shneyvays, V.; Isaac, A.; Vogel, Z. Delta-9-tetrahydrocannabinol protects cardiac cells from hypoxia via CB2 receptor activation and nitric oxide production. *Mol Cell. Biochem*. **2006**, 283, 75–83.

Shonberg, J.; Kling, R.C.; Gmeiner, P.; Lober, S. GPCR crystal structures: medicinal chemistry in the pocket. *Bioorg. Med. Chem*. **2015**, 23, 3880-3906.

Smith, T. H.; Sim-Selley, L. J.; Selley, D. E. Cannabinoid CB1 receptor-interacting proteins: novel targets for central nervous system drug discovery? *Br. J. Pharmacol.* **2010**, 160, 454-466.

Solinas, M.; Panlilio, L.V.; Antoniou, K.; Pappas, L.A.; Goldberg, S.R. The cannabinoid CB1 antagonist N-piperidinyl-5-(4-chlorophenyl)-1-(2,4-dichlorophenyl)-4-methylpyrazole-3-carboxamide(SR-141716A) differentially alters the reinforcing effects of heroin under continuous reinforcement, fixed ratio, and progressive ratio schedules of drug self-administration in rats. *J. Pharmacol. Exp. Ther*. **2003**, 306, 93–102.

Song, Z.H.; Bonner, T.I. A lysine residue of the cannabinoid receptor is critical for receptor recognition by several agonists but not WIN55212-2. *Mol. Pharmacol*. **1996**, 49, 891-896.

Song, Z.H.; Slowey, C.A.; Hurst, D.P.; Reggio, P.H. The difference between the CB(1) and CB(2) cannabinoid receptors at position 5.46 is crucial for the selectivity of WIN55212-2 for CB(2). *Mol. Pharmacol*. **1999**, 56, 834-840.

Sorkin, A. Cargo recognition during clathrin-mediated endocytosis: a team effort. *Curr. Opin. Cell. Biol.* **2004**, 16, 392-399.

Standfuss, J.; Edwards, P.C.; D'Antona, A.; Fransen, M.; Xie, G.; Oprian, D.D. The structural basis of agonist-induced activation in constitutively active rhodopsin. *Nature*. **2011**, 471, 656–660.

Standfuss, J.; Xie, G.; Edwards, P.C.; Burghammer, M.; Oprian, D.D.; Schertler, G.F. Crystal structure of a thermally stable rhodopsin mutant. *J. Mol. Biol*. **2007**,372, 1179-1188.

Stevens, R.C.; Cherezov, V.; Katritch, V.; Abagyan, R.; Kuhn, P.; Rosen, H.; Wuthrich, K. The GPCR Network: a large-scale collaboration to determine human GPCR structure and function. *Nat. Rev. Drug Disc.* **2013**, 12, 25-34.

Stokes, B. J.; Dong, H.; Leslie, B. E.; Pumphrey, A. L.; Driver, T. G. Intramolecular C-H amination reactions: exploitation of the Rh(2)(II)-catalyzed decomposition of azidoacrylates. *J. Am. Chem. Soc.* **2007**, 129, 7500-7501.

Straiker, A. J.; Maguire, G.; Mackie, K.; Lindsey, J. Localization of cannabinoid CB1 receptors in the human anterior eye and retina. *Invest. Ophthalmol. Vis. Sci.* **1999**, 40, 2442-2448.

Sugiura, T.; Kodaka, T.; Kondo, S.; Tonegawa, T.; Nakane, S.; Kishimoto, S.; Yamashita, A.; Waku, K. 2-Arachidonoylglycerol, a putative endogenous cannabinoid receptor ligand, induces rapid, transient elevation of intracellular free Ca^{2+} in neuroblastoma×glioma hybrid NG108-15 cells. *Biochem. Biophys. Res. Commun*. **1996**, 229, 58–64.

Sugiura, T.; Kondo, S.; Sukagawa, A.; Nakane, S.; Shinoda, A.; Itoh, K.; Yamashita, A.; Waku, K. 2-Arachidonoylglycerol: a possible endogenous cannabinoid receptor ligand in brain. *Biochem. Biophys. Res. Commun*., **1995**, 215, 89–97.

Svizenska, I.; Dubovy, P.; Sulcova, **A.** Cannabinoid receptors 1 and 2 (CB1 and CB2), their distribution, ligands and functional involvement in nervous system structures- a short review. *Pharmacol. Biochem. Behav.* **2008**, 90, 501-511.

Szabo, B.; Nordheim, U.; Niederhoffer, N. Effects of cannabinoids on sympathetic and parasympathetic neuroeffector transmission in the rabbit heart. *J. Pharmacol. Exp. Ther*. **2001**, 297, 819-826.

Tan, C.M.; Brady, A.E.; Nickols, H.H.; Wang, Q.; Limbird, L.E. Membrane trafficking of G protein-coupled receptors. *Annu. Rev. Pharmacol. Toxicol*. **2004**, 44, 559-609.

Tao, Q.; Abood, M.E. Mutation of a highly conserved aspartate residue in the second transmembrane domain of the cannabinoid receptors, CB1 and CB2, disrupts G-protein coupling. *J. Pharmacol. Exp. Ther*. **1998**, 285, 651-658.

Terrillon, S.; Durroux, T.; Mouillac, B.; Briet, A.; Ayoub, M.A.; Taulan, M.; Jockers, R.; Barberis, C.; Bouvier, M. Oxytocin and vasopression VIa and V2 receptors form constitutive homo- and heterodimers during biosynthesis. *Mol. Endocrinol*. **2003**, 17, 677-691.

Thakur, G. A.; Nikas, S.P.; Makriyannis, A. CB1 Cannabinoid Receptor Ligands. *Mini-Rev. Med. Chem*. **2005**, 5, 631-640.

Trzaskowski, B.; Latek, D.; Yuan, S.; Ghoshdastider, U.; Debinski, A.; Filipek, S. Action of Molecular Switches in GPCRs - Theoretical and Experimental Studies. *Curr. Med. Chem*. **2012** 19, 1090–1109.

Tsou, K.; Mackie, K.; Sanudo-Pena, M.C.; Walker, J.M. Cannabinoid CB1 receptors are localized primarily on cholecystokinin-containing GABAergic interneurons in the rat hippocampal formation. *Neurosci*ence, **1999**, 93, 969.

Turu, G.; Hunyady, L. Signal transduction of the CB1 cannabinoid receptor. *J. Mol. Endocrinol.* **2010**, 44, 75-85.

Urban, J.D.; Clarke, W.P.; Zastrow, M.V.; Nichols, D.E.; Kobilka, B.; Weinstein, H.; Javitch, J.A.; Roth, B.L.; Christopoulos, A.; Sexton, P.M.; Miller, K.J.; Spedding, M.; Mailman, R.B. Functional selectivity and classical concepts of quantitative pharmacology. *J. Pharmacol. Exp. Ther.* **2007**, 320, 1-13.

Vassilatis, D.K.; Hohmann, J.G.; Zeng, H.; Li, F.; Ranchalis, J.E.; Mortrud, M.T.; Brown, A.; Rodriguez, S.S.; Weller, J.R.; Wright, A.C.; Bergmann, J.E.; Gaitanaris, G.A. The G protein-coupled receptor repertoires of human and mouse. *Proc. Natl. Acad. Sci. USA.* **2003**, 100, 4903-4908.

Venter, J.C.; Adams, M.D.; Myers, E.W.; Li, P.W.; Mural, R.J.; Sutton, G.G.; Smith, H.O.; Yandell, M.; Evans, C.A.; Holt, R.A. The sequence of the human genome. *Science.* **2001**, 291, 1304–1351.

Vermeulen, E. S.; van Smeden, M.; Schmidt, A. W.; Sprouse, J. S.; Wikstrom, H. V.; Grol, C. J. Novel 5-HT7 receptor inverse agonists. Synthesis and molecular modeling of arylpiperazine- and 1,2,3,4-tetrahydroisoquinoline-based arylsulfonamides. *J. Med. Chem.* **2004**, 47, 5451-5466.

Vieira, T. O.; Meaney, L. A.; Shi, Y. L.; Alper, H. Tandem palladium-catalyzed N,C-coupling/carbonylation sequence for the synthesis of 2-carboxyindoles. *Org. Lett.* **2008**, 10, 4899-4901.

Visiers, I.; Ballesteros, J.A.; Weinstein, H. Three-dimensional representations of G protein-coupled receptor structures and mechanisms of G protein pathways. *Receptors.* **2002**, 343, 329–371.

Von-Zastrow, M.; Kobilka, B.K. Antagonist-dependent and –independent steps in the mechanism of adrenergic receptor internalization. *J. Biol. Chem*. **1994**, 269, 18848-18452.

Wang, C. I.; Lewis, R. J. Emerging opportunities for allosteric modulation of G-protein coupled receptors. *Biochem. Pharmacol.* **2013**, 85, 153-162.

Wang, X.; Horsewill, J.G.; Whalley, B.J.; Stephens, G.J. Effects of the allosteric antagonist 1-(4-Chlorophenyl)-3-[3-(6-pyrrolidin-1-ylpyridin-2-yl)phenyl]urea (PSNCBAM-1) on CB1 receptor modulation in the cerebellum. *Mol. Pharmacol*. **2010**, 79, 758-767.

Warne, T.; Serrano-Vega, M.J.; Baker, J.G.; Moukhametzianov, R.; Edwards, P.C.; Henderson, R.; Leslie, A.G.; Tate, C.G.; Schertler, G.F. Structure of a beta1-adrenergic G-protein-coupled receptor. *Nature.* **2008**, 454, 486-491.

Warne, T.; Moukhametzianov, R.; Baker, J.G.; Nehme, R.; Edwards, P.C.; Leslie, A.G.; Schertler, G.F.; Tate, C.G. The structural basis for agonist and partial agonist action on a β(1)-adrenergic receptor. *Nature.* **2011**,469, 241-244.

Weiss, J.M.; Morgan, P.H.; Lutz, M.W.; Kenakin, T.P. The cubic ternary complex receptor-occupancy model. I. Model description. *J. Theor. Biol.* **1996**, 178**,** 151-167.

Wild, C.; Cunningham, K.A.; Zhou, J. Allosteric modulation of G protein-coupled receptors: an emerging approach of drug discovery. *Austin J. Pharmacol. Ther.* **2013**, 2, 1.

Wisler, J. W.; DeWire, S. M.; Whalen, E. J.; Violin, J. D.; Drake, M. T.; Ahn, S.; Shenoy, S. K.; Lefkowitz, R. J. A unique mechanism of β-blocker action: carvedilol stimulates β-arrestin signaling. *Proceedings of the National Academy of Sciences* **2007,** 104, 16657-16662.

Wootten, D.; Christopoulos, A.; Sexton, P. M. Emerging paradigms in GPCR allostery: implications for drug discovery. *Nat. Rev. Drug Discov.* **2013**, 12, 630-644.

Wootten, D.; Christopoulos, A.; Sexton, P.M. Emerging paradigms in GPCR allostery: implications for drug discovery. *Nat. Rev. Drug Disc*. **2013**, 12, 630-644.

Xiang, Y.; Devic, E.; Kobilka, B. The PDZ binding motif of the beta 1 adrenergic receptor modulates receptor trafficking and signaling in cardiac myocytes. *J. Biol. Chem*. **2002**, 277, 33783–33790.

Yamazaki, K.; Nakamura, Y.; Kondo, Y. Solid Phase Synthesis of Indolecarboxylate Using palladium-Catalyzed Reactions. *J. Org. Chem.* **2003**, 68, 6011-6019.
Zezula, J.; Freissmuth, M. The A(2A)-adenosine receptor: a GPCR with unique features? *Br. J. Pharmacol*. **2008**, 153, S184-190.

Zhou, X.E.; Melcher, K.; Xu, H.E. Structure and activation of rhodopsin. *Acta Pharmacol Sin.* **2012**, 33, 291–299.

Appendix

Darla Henderson

August 29, 2016 at 7:39 PM

To: Leepakshi Khurana Cc: Kendall, Debra

Inbox - Google

DH

RE: need permission to include some manuscript data in PhD thesis

New contact info found in this email: Darla Henderson d_henderson@acs.org add...

Dear Leepakshi,

Thank you for your inquiry. I confirm you have permission to reuse the article you published here http://pubs.acs.org/doi/full/10.1021/jm5000112 in the thesis you are writing to complete the degree-granting requirements of the University of Connecticut. ACS asks that you:

- Cite the Journal of Medicinal Chemistry article as the source;
- Note modifications (if any) from the original article; and
- Include a direct link from your thesis to the ACS article, direct link here http://pubs.acs.org/doi/full/10.1021/jm5000112

Lastly, I wish you the best of luck as you complete your degree and start your career in chemistry!

Kind regards,
Darla

Darla Henderson, PhD.
Assistant Director, Open Access Programs
Publications Division
American Chemical Society
1155 16th Street NW
Washington, D.C. 20036
V 828.245.3702

The ACS Vision: *Improving people's lives through the transforming power of chemistry*

ACS Chemistry for Life
American Chemical Society

See More from Leepakshi Khurana

Copyright Clearance Center September 19, 2016 at 4:14 PM

To: Leepakshi Khurana

Reply-To: Copyright Clearance Center

Thank you for your RightsLink / Nature Publishing Group transaction

To view this email as a web page, go here.

Do Not Reply Directly to This Email

To ensure that you continue to receive our emails,
please add rightslink@marketing.copyright.com to your address book.

RightsLink

Copyright Clearance Center

Thank You For Your Order!

Dear Ms. Leepakshi Khurana,

Thank you for placing your order through Copyright Clearance Center's RightsLink service. Nature Publishing Group has partnered with RightsLink to license its content. This notice is a confirmation that your order was successful.

Your order details and publisher terms and conditions are available by clicking the link below:
http://s100.copyright.com/CustomerAdmin/PLF.jsp?ref=07a5535b-59d3-4bce-9848-b998273539c2

Order Details
Licensee: Leepakshi Khurana
License Date: Sep 19, 2016
License Number: 3952670360670
Publication: Nature Reviews Drug Discovery
Title: Efficacy at g-protein-coupled receptors
Type Of Use: reuse in a dissertation / thesis
Total: 0.00 USD

To access your account, please visit https://myaccount.copyright.com.

Please note: Online payments are charged immediately after order confirmation; invoices are issued daily and are payable immediately upon receipt.

To ensure that we are continuously improving our services, please take a moment to complete our customer satisfaction survey.

B.1:v4.2